Did crocodiles become secondarily ectothermic ? : a paleohistological approach

Lucas Legendre

Université Pierre et Marie Curie

École doctorale 398 : Géosciences, ressources naturelles et environnement

Institut des Sciences de la Terre de Paris (ISTeP) - UMR 7193

Équipe Biominéralisation et environnements sédimentaires

Les crocodiles sont-ils devenus secondairement ectothermes ?

Étude paléohistologique

Par Lucas LEGENDRE

Thèse de doctorat de Paléontologie

Dirigée par Jorge CUBO

Présentée et soutenue publiquement le 23/09/2014

Devant un jury composé de :

Kevin PADIAN	Professeur UCMP, Berkeley	Rapporteur
Philippe JANVIER	Directeur de recherche CNRS, Paris	Rapporteur
Francisco ORTEGA	Professeur associé UNED, Madrid	Examinateur
Romain AMIOT	Chargé de recherche CNRS, Lyon	Examinateur
Alexandra HOUSSAYE	Chargée de recherche CNRS, Paris	Examinatrice
Yves DESDEVISES	Professeur UPMC, Banyuls-sur-Mer	Examinateur
Damien GERMAIN	Maître de conférences MNHN, Paris	Invité
Jorge CUBO	Professeur UPMC, Paris	Directeur de la thèse

A toi, lecteur aventureux en quête de savoir, qui peut-être un jour tombera sur ces pages jaunies par le temps.

Puisses-tu y trouver quelque réconfort !

‘Palaeohistology now stands as a powerful tool to reconstruct fossil vertebrates as living organisms, and accordingly, it is becoming a more and more popular approach for the more palaeobiologically-oriented students of vertebrate evolution.’

Armand de Ricqlès

‘It is paradoxical, yet true, to say, that the more we know, the more ignorant we become in the absolute sense, for it is only through enlightenment that we become conscious of our limitations. Precisely one of the most gratifying results of intellectual evolution is the continuous opening up of new and greater prospects.’

Nikola Tesla

Remerciements

En premier lieu, merci à mon directeur de thèse, Jorge Cubo. Depuis déjà plus de trois ans que nous partageons les joies et les peines de l'étude de toutes ces coupes histologiques et autres méthodes statistiques, et ç'a été un vrai plaisir. Tu es l'une des personnes les plus patientes, dévouées et passionnées que j'ai pu rencontrer dans ma vie. Encore merci pour tout.

Merci à toute l'équipe des irréductibles histologistes de Paris VI, en particulier Armand de Ricqlès, dont la réputation de légende vivante (devrais-je dire grand maître Jedi ?) de l'histologie osseuse est encore bien en dessous de la réalité ; Hayat Lamrous, pour sa disponibilité et son expertise technique irréprochable ; et Laetitia Montes, pour m'avoir permis d'accéder à son incroyable échantillonnage. Alexandra, Louise, nous n'avons pas eu l'opportunité de travailler ensemble, mais qui sait, ce n'est peut-être que partie remise !

Merci à Marc de Rafélis, à Loïc Segalen et à l'ensemble de l'équipe Biominéralisations. Bien que n'ayant qu'un lien scientifique très indirect avec vos travaux, j'ai pu constater le professionnalisme et la bonne ambiance qui règnent dans l'équipe au cours de mon séjour « chez les géologues ». Marc, c'est aussi à toi que je dois la suggestion de faire de l'enseignement, je ne te remercierai jamais assez de l'avoir faite.

Un grand merci à Élodie Boucheron-Dubuisson et Sidney Delgado ainsi qu'à toute l'équipe du LV102, qui m'auront permis de faire mes preuves en tant que chargé de TD et de TP face à des hordes d'étudiants à peine plus jeunes que moi (et c'est un euphémisme). Ce fut une sacrée aventure, et je regrette qu'elle se soit terminée de façon aussi abrupte. Un jour, je l'espère, la biologie des organismes et l'étude de l'évolution seront de nouveau reconnues comme les disciplines indispensables qu'elles devraient encore être en licence de biologie dans la plus grande université française. *Your move, mister president!*

Merci aussi à Julien Gasparini et à l'ensemble de l'équipe du LV373 pour avoir accueilli en catastrophe un pauvre paléontologue privé d'enseignement et l'avoir converti, tant bien que mal, à l'écologie évolutive. Cette UE est vraiment bien construite, et je suis content d'avoir pu en faire partie pour cette courte année 2014.

Merci à Michel Laurin et à Yves Desdevises ; le premier pour m'avoir « offert » ma première publication avec beaucoup de courtoisie, le second pour ses précieux conseils en matière de méthodes phylogénétiques comparatives, et tous deux pour un comité de thèse complètement improvisé qui s'est avéré aussi intéressant que haut en couleurs (et tant mieux si Pénélope a bien aimé les dinosaures).

Merci à Guillaume Guénard pour son aide (le mot est faible) sur la construction de mes modèles prédictifs – quelle connaissance de R ! – et à Pierre Legendre (aucun lien de parenté !) pour nous avoir mis en contact. Au plaisir de collaborer de nouveau sur un autre projet !

Un grand merci à Jennifer Botha-Brink pour ses échantillons d'archosauromorphes fossiles et pour nos longs échanges sur la taille de notre échantillonnage. Là aussi, ce n'est peut-être que le début d'une plus grande aventure…

En vrac pour ne pas trop m'étendre, merci à : Holly Woodward et l'ensemble du comité d'organisation de l'ISPH 2013, pour ce merveilleux congrès au fin fond du Montana ; Cary Woodruff et toute la bande de fouilleurs passionnés avec qui j'ai passé dix jours de folie

à déterrer des sauropodes au milieu du désert ; Jérôme Sueur et tous ceux qui m'ont aidé dans ma longue découverte de R ; Gaëlle Boutin, la meilleure secrétaire de toute l'UPMC, et le personnel de la défunte école doctorale Diversité du Vivant (ah, Roscoff…) ; Estelle Bourdon, grande prétresse de l'ornithologie et co-auteur particulièrement prolifique ; René Zaragüeta i Bagils, Santiago Aragon et toute la « bande des espagnols », pour nos passionnantes discussions sur tout et n'importe quoi ; Eli Amson et toute l'équipe du BDEM, pour m'avoir invité à faire une présentation à leur congrès ; Kevin Padian et Damien Germain, pour s'être spontanément proposés pour être membres de mon jury de thèse, ainsi que Alexandra Houssaye, Francisco Ortega, Philippe Janvier et Romain Amiot pour avoir accepté d'en faire partie ; Régine Vignes-Lebbe, Pascal Tassy, Véronique Barriel et toute l'équipe pédagogique du Master SEP, qui m'a tant appris aussi bien sur le plan scientifique qu'humain, et sans qui je ne serai jamais arrivé jusqu'à la thèse.

Merci à mes parents et à ma sœur, qui bien que ne comprenant pas toujours en quoi consiste exactement mon travail au quotidien m'ont toujours encouragé et soutenu durant toutes ces années. Je ne suis pas toujours très expansif sur le sujet, mais à votre façon vous m'avez énormément aidé.

Merci à tous les membres (ils sont désormais trop nombreux pour tous les citer) de la plus si secrète Confrérie des Francs-Taxons, qui en aura surpris et intrigué beaucoup, mais qui malgré son caractère humoristique initial a fait beaucoup plus pour la communication entre étudiants passionnés de systématique et d'évolution que n'importe qui ne l'aurait imaginé au départ. Déjà cinq ans maintenant que les quatre étudiants un peu dingues et idéalistes que nous étions avons fondé ce projet délirant, et je n'ai jamais eu à le regretter. Vous êtes tous des gens géniaux, et vous m'avez apporté tellement que j'ai du mal à réaliser la chance que j'ai de tous vous connaître. Cladistique, VAVE, 3IA !

Et enfin, merci à Houda, qui m'a accompagné durant tout ce temps sans jamais rien demander en retour. Il ne doit pas être facile de vivre avec un doctorant, donc, plus que jamais, merci d'avoir supporté toutes les hésitations sur mon travail et tout le reste. Rendez-vous après la soutenance, et, promis, on pourra enfin se reposer un peu.

Sommaire

Introduction

Les archosaures

Les archosaures sont un groupe de vertébrés comprenant les oiseaux et les crocodiliens, ainsi que les groupes fossiles qui leur sont plus prochement apparentés qu'ils ne le sont de n'importe quel autre groupe de vertébrés. Ces groupes fossiles incluent, entre autres, les ptérosaures et les dinosaures non aviens. Le terme « archosaure » fut à l'origine défini par Cope (1869) dans un sens beaucoup moins restrictif que celui qui lui est attribué de nos jours – il incluait notamment des organismes aujourd'hui rattachés aux lépidosauriens ou aux synapsides. Durant la seconde moitié du XXe siècle, le développement de la méthode cladistique permit de clarifier les relations de parenté entre tous les organismes jusqu'alors regroupés sous l'appellation « reptiles », et le groupe des archosaures fut redéfini en fonction de plusieurs caractères dérivés, tels la présence d'une fenêtre antéorbitaire ou le quatrième trochanter (Benton, 2004). Le groupe fut même régulièrement cité comme un exemple d'apport significatif de la cladistique à la paléontologie (Hennig, 1975), et le crown group des archosaures acquit sa définition actuelle en 1986. Le stem group incluant les archosaures et leurs groupes-frères plus proches d'eux que des lépidosauriens est désigné sous le terme « archosauromorphes » (Figure 1).

Avant même que la définition formelle des archosaures ne soit établie, un débat existait déjà sur le thermométabolisme des « reptiles » et sur leur évolution. Après que l'origine dinosaurienne des oiseaux actuels fut mise en évidence par Ostrom (1969, 1974) grâce aux descriptions d'*Archaeopteryx* et de *Deinonychus*, plusieurs interrogations furent soulevées par de nombreux paléontologues concernant l'origine du thermométabolisme des

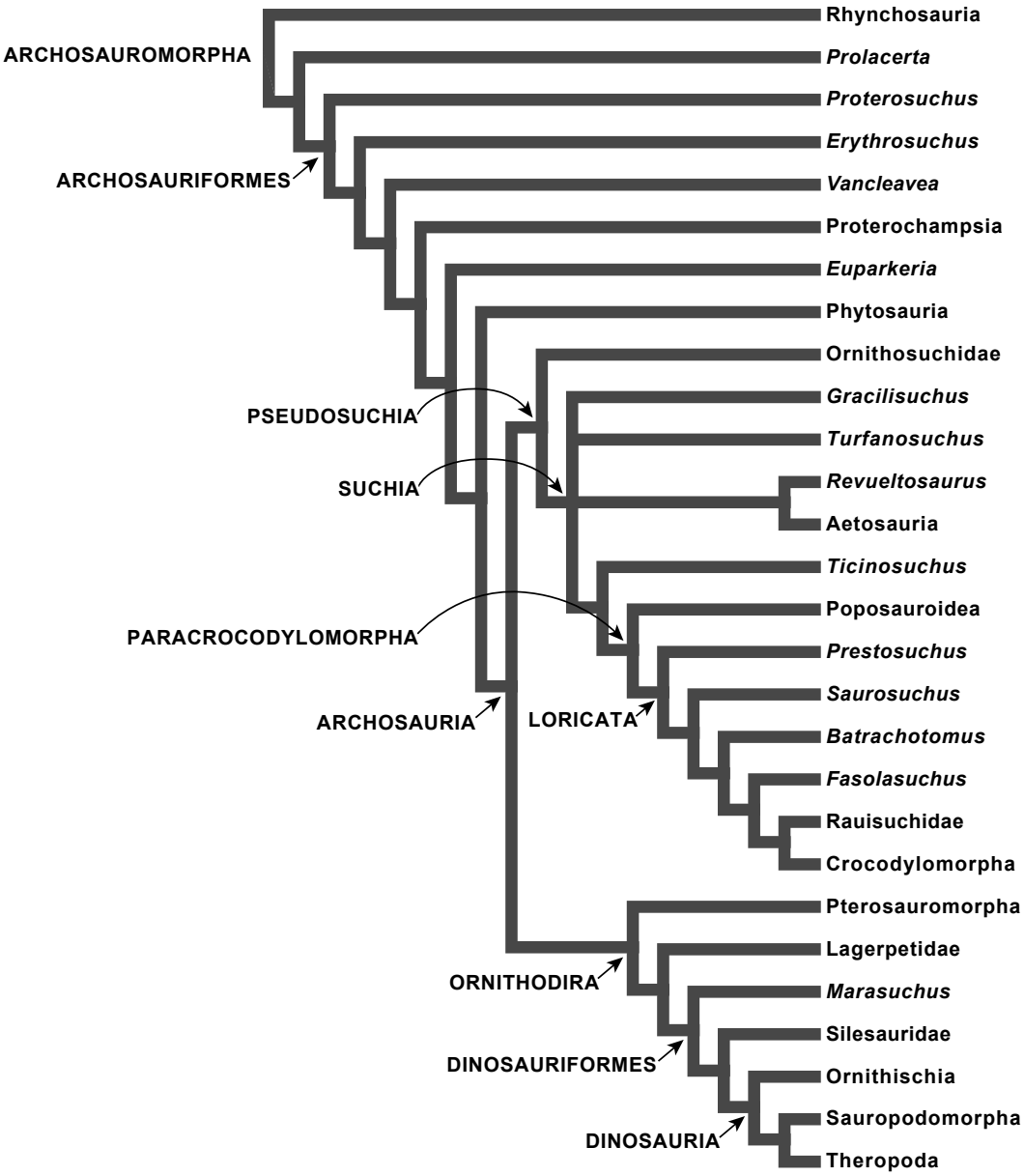

Figure 1. Arbre phylogénétique des archosauromorphes mettant en évidence les principaux groupes actuels et fossiles ; les crocodiliens actuels appartiennent au clade des Crocodylomorpha, les oiseaux actuels à celui des Theropoda (modifié d'après Nesbitt, 2011).

oiseaux. L'endothermie correspond à la capacité d'un organisme à produire sa propre chaleur corporelle au moyen d'une activité métabolique spécifiquement dédiée à cette tâche (Hulbert & Else, 2000). On considérait traditionnellement que deux groupes avaient acquis cette capacité au cours de l'évolution des vertébrés : les mammifères et les oiseaux. Ces derniers ayant été rattachés aux dinosaures, l'endothermie pouvait donc avoir été acquise à un niveau

plus inclusif de l'arbre et être une synapomorphie d'un groupe beaucoup plus large que le clade *Aves*. Au cours des années 1970, de nombreux articles furent consacrés à la potentielle endothermie des dinosaures – étonnamment, sans jamais aborder la question du thermométabolisme des autres archosaures. Les partisans d'une apparition de l'endothermie au nœud Dinosauria, tels Bakker (1972, 1974), se basaient principalement sur des assertions liées à des caractéristiques globales des organismes considérés, comme la taille du cerveau ou la posture droite. Selon cette hypothèse, des animaux tels que les dinosaures, dotés d'un cerveau de taille élevée comparé à celui d'un lépidosaurien, ainsi que de membres parasagittaux comme ceux des mammifères et des oiseaux, ne pouvaient être que des endothermes vrais.

Cependant, ces affirmations se heurtèrent à de nombreuses critiques (e.g. Feduccia, 1973, 1974) : en effet, ces caractères n'avaient pas été comparés de manière précise avec ceux des oiseaux, et la différence entre ectothermes et endothermes ne pouvait être perçue de manière évidente en se basant sur ces seuls critères de ressemblance globale. L'utilisation de méthodes phylogénétiques en paléontologie ne se généralisa qu'au début des années 1980 (Cracraft, 1981), ce qui peut expliquer l'absence de considérations phylogénétiques dans les articles de Bakker et de définition claire de l'endothermie en tant que caractère dérivé partagé. Dans une longue description des arguments pour et contre l'endothermie dinosaurienne, Benton (1979, p. 988) précise :

> *Different forms of endothermy have arisen independently several times. There is no clear dividing line between ectotherms and endotherms either today or presumably also in the past, and thus attempts to reclassify vertebrates on the basis of endothermy alone* […] *hardly seem justified.*

Benton montre également que les caractéristiques liées à l'endothermie selon Bakker (1974) peuvent être retrouvées chez des ectothermes homéothermes, c'est à dire capables de maintenir leur température corporelle à un niveau constant, et ne peuvent donc pas être interprétées comme des preuves directes d'une endothermie chez les dinosaures. Il va même jusqu'à affirmer à la fin de l'article que l'ectothermie des dinosaures aurait pu contribuer à leur extinction liée aux bouleversements climatiques de la fin du Crétacé, ce qui rendrait l'hypothèse de leur ectothermie plus probable. Cette hypothèse ne sera pas remise en question au cours des années 1980-1990, et le débat sur le thermométabolisme des dinosaures tombera dans un relatif oubli jusqu'au début des années 2000.

Les arguments histologiques

Plusieurs arguments utilisés par les défenseurs de l'hypothèse des dinosaures endothermes se basent sur la microstructure osseuse de ces derniers. L'histologie osseuse est une discipline connue depuis plusieurs siècles (Havers, 1691) ; l'étude de la microstructure des os des vertébrés fut l'un des principaux champs d'investigation liés au développement de la microscopie optique, et au cours du XIXe siècle plusieurs groupes de vertébrés firent l'objet d'études sur le sujet. Plusieurs de ces études définirent des caractères histologiques dans un cadre systématique en utilisant une nomenclature osseuse à usage taxonomique, notamment au sein des ostéichtyens (Agassiz, 1833-1844). Au cours du XXe siècle, cependant, l'histologie osseuse eut tendance à se focaliser sur des problématiques plus liées à l'étude de contraintes fonctionnelles ou d'interprétations paléobiologiques, sans chercher à replacer ces éléments dans un cadre taxonomique ou phylogénétique (pour une révision détaillée, voir Cubo & Laurin, 2011). Bien que la nomenclature des différents types de tissus osseux et de leurs modes de formation ait connu un développement important (Francillon-Vieillot *et al.*, 1990 ; de Ricqlès *et al.*, 1991), tous les grands types de tissus osseux (os à

fibres parallèles, complexe fibrolamellaire…) ont été retrouvés chez l'ensemble des grands groupes de vertébrés ; de fait, les caractères liés à l'histologie osseuse furent progressivement considérés comme trop homoplasiques et trop liés à des contraintes d'ordre fonctionnel pour être utilisés dans une approche évolutionniste.

Pourtant, c'est l'histologie osseuse qui fut à l'origine d'une nouvelle hypothèse concernant l'évolution du thermométabolisme chez les archosaures : Gross (1934), dans une étude sur la microstructure osseuse des organismes alors encore regroupés sous le nom de reptiles, décrit celle d'un spécimen fossile d'Afrique du Sud, *Erythrosuchus africanus*, plus tard identifié comme un archosauromorphe non archosaure. Ce spécimen présente un os compact avec un complexe fibrolamellaire très dense, caractéristique d'une croissance osseuse extrêmement rapide sur une durée prolongée. Ce type d'os, connu uniquement chez des organismes présentant une activité métabolique très élevée, semble indiquer un métabolisme très probablement endotherme chez cet animal. Dès les années 1970, de Ricqlès (1975, 1976, 1977a, b) décrira l'histologie osseuse de nombreux tétrapodes, associera de manière précise un type de tissu osseux à des modalités de croissance osseuse, et inscrira ces descriptions dans une perspective évolutionniste, ouvrant la voie à de nouvelles pistes de réflexions concernant l'évolution du taux de croissance osseuse et du thermométabolisme au sein des vertébrés.

Dès les années 2000, plusieurs éléments issus de nombreux domaines différents de la biologie feront naître l'hypothèse d'une endothermie primitivement acquise par les premiers archosauromorphes, et non par les seuls oiseaux actuels. Cette hypothèse implique donc que les crocodiliens actuels soient devenus secondairement ectothermes, probablement en réponse à leur retour au milieu aquatique, où l'ectothermie représente un net avantage en terme de

coût énergétique (Seymour *et al.*, 2004, et références y figurant). Les découvertes à l'origine de cette hypothèse ont été effectuées au niveau de l'histologie osseuse de crocodiliens actuels (Tumarkin-Deratzian, 2007), mais aussi de leur anatomie (Summers, 2005), ainsi que l'étude de leur physiologie cardiaque (Seymour *et al.*, 2004) et respiratoire (Farmer & Sanders, 2010). Par ailleurs, il existe de nombreuses descriptions histologiques d'archosauromorphes non archosaures présentant une structure osseuse de type endotherme comme celle d'*Erythrosuchus* (de Ricqlès *et al.*, 2008 ; Botha-Brink & Smith, 2011) qui confortent également cette hypothèse.

Les méthodes phylogénétiques comparatives

En parallèle de ces travaux s'est déroulé le développement considérable des méthodes phylogénétiques comparatives (souvent abrégées en PCMs en anglais) appliquées à l'histologie osseuse. Les PCMs, créées à l'origine pour éliminer l'influence de la composante phylogénétique des caractères quantitatifs dans une analyse statistique, trouvent leur origine dans les travaux de Felsenstein (1985) sur les contrastes phylogénétiques indépendants. Au cours des années 1990, avec le développement des premiers outils informatiques facilement utilisables par un large public, ces méthodes ont connu un engouement très important et ont rapidement fait l'objet d'une formalisation (Harvey & Pagel, 1991). Aujourd'hui, ces méthodes permettent une caractérisation extrêmement poussée de données quantitatives dans une perspective phylogénétique, et il existe un nombre très important de tests statistiques dédiés à la mesure de l'influence de la phylogénie sur un jeu de données, ainsi qu'à la modélisation prédictive de valeurs à partir d'un jeu de données dans un cadre phylogénétique (Paradis, 2012). De cette manière, on peut facilement mesurer le signal phylogénétique d'une variable quantitative. Le signal phylogénétique (*sensu* Blomberg & Garland, 2002) est défini comme la tendance qu'ont deux espèces proches phylogénétiquement à être plus proches

entre elles que de n'importe quelle autre espèce plus éloignée dans l'arbre, pour un caractère donné. Ainsi, on peut déterminer pour un caractère quantitatif quelle part de sa variation peut être expliquée par l'influence de contraintes phylogénétiques, fonctionnelles, structurales et leur chevauchement (Seilacher, 1970 ; Gould, 2002).

Cubo *et al.* (2005, 2008) ont montré l'importance de ce signal phylogénétique en histologie osseuse, et identifié plusieurs variables histologiques quantitatives présentant un signal statistiquement significatif. Montes *et al.* (2007, 2010) ont mis en évidence que ces variables histologiques sont significativement corrélées au taux de croissance osseuse des spécimens sur lesquelles elles avaient été mesurées, ainsi qu'à leur taux métabolique. Il est donc possible, en utilisant les PCMs pour construire un modèle statistique prédictif, d'estimer le taux de croissance osseuse et le taux métabolique de spécimens sur lesquels on a mesuré des variables histologiques quantitatives, tout en prenant en compte l'information phylogénétique présente chez ces spécimens (Cubo *et al.*, 2012).

Objectifs de la thèse

Le premier objectif de cette thèse consiste à construire un modèle prédictif permettant d'estimer le taux de croissance osseuse et le taux métabolique d'un organisme dans un cadre phylogénétique, à partir d'un échantillon de vertébrés actuels pour lesquels ces deux variables sont connues. Ce modèle sera ensuite utilisé pour prédire ces variables chez des archosauromorphes fossiles, ce qui permettra de connaître le taux de croissance osseuse et le taux métabolique dans l'ensemble des grands groupes d'archosaures. Ainsi, nous serons à même de pouvoir retracer l'évolution de ces deux variables au cours du temps, et ainsi de répondre à notre problématique initiale : les archosaures étaient-ils primitivement endothermes, et si oui, comment cette endothermie a-t-elle évolué ? Cela éclaircira également

d'autres points : à quel niveau de la phylogénie les pseudosuchiens ont-ils pu perdre cette endothermie ? Et comment a-t-elle évolué dans la lignée des ornithodiriens, dont font partie les dinosaures, sur lesquels se focalisait le débat au cours des années 1970 ?

Toutefois, avant de pouvoir modéliser ces variables et répondre à ces questions, il convient de se pencher sur un autre débat, beaucoup plus ancien : l'histologie osseuse renferme-t-elle vraiment un signal phylogénétique ? En effet, même si les travaux de Cubo *et al.* (2005) avaient permis d'identifier un signal significatif dans plusieurs caractères histologiques, l'échantillonnage utilisé se restreignait au clade des sauropsidés, et le nombre de spécimens et de variables pris en compte était encore très restreint. Pour cette raison, le débat sur la présence ou non d'une information phylogénétique significative dans l'histologie osseuse reste d'actualité. Dans la mesure où l'interprétation des résultats de notre modèle prédictif dépend en grande partie de la pertinence de nos caractères dans un cadre phylogénétique, nous avons consacré une première partie de cette thèse à tester la présence d'un signal phylogénétique dans la variation des caractères ostéohistologiques au sein d'un large échantillonnage de vertébrés, afin de mieux formaliser les prérequis de notre approche prédictive ultérieure. Il nous a également semblé crucial de mieux caractériser les méthodes à utiliser pour mesurer spécifiquement ce signal sur des caractères histologiques, en utilisant un bon modèle d'étude. Pour cela, nous avons choisi le groupe des paléognathes (*Aves*, Palaeognathae), en raison de sa grande diversité malgré un nombre d'espèces assez peu élevé.

Après cette première partie consacrée au signal phylogénétique, nous nous sommes focalisés sur la construction de modèles prédictifs au moyen des PCMs, et sur notre problématique initiale de l'évolution du thermométabolisme chez les archosaures. Nous avons tout d'abord effectué une première étude consacrée à la construction d'un modèle prédictif du

taux de croissance osseuse chez les amniotes. Cette variable est causalement liée au taux métabolique puisque un taux de croissance élevé comporte une grande consommation énergétique liée à un important turnover protéique (synthèse au niveau du périoste, destruction au niveau endostéal ; Montes *et al.*, 2007). Nous avons ensuite construit un modèle permettant d'estimer directement le taux métabolique chez l'ensemble des tétrapodes, appliqué à un échantillonnage fossile d'archosauromorphes.

Deux publications collatérales à la thèse ont également été incluses comme annexes à ce travail : une étude sur les caractères ostéologiques quantitatifs chez les ratites et le type de modèle d'évolution (gradualiste ou spéciationnel) auquel ils peuvent être associés, et une comparaison entre les contraintes énergétiques s'exerçant sur la vascularisation osseuse chez les oiseaux et chez les lépidosauriens.

PARTIE I

Le signal phylogénétique dans la variation des caractères ostéohistologiques

I – 1. Phylogenetic signal in bone histology of amniotes revisited

Lucas Legendre, Nathalie Le Roy, Cayetana Martinez-Maza, Laetitia Montes,

Michel Laurin et Jorge Cubo

Publication originale *in*: *Zoologica Scripta* **42**: 44–53 (Janvier 2013)

Résumé

Il existe actuellement un débat concernant la présence d'un signal phylogénétique dans les données relatives à l'histologie osseuse, mais peu d'études rigoureuses ont été menées pour tenter de répondre à cette problématique. Au cours de cette étude, nous avons effectué de nouvelles analyses utilisant un large jeu de données comprenant sept caractères histologiques mesurés sur 25 taxons (dont seize actuels et huit fossiles), à l'aide de trois méthodes : la régression de vecteurs propres phylogénétiques, la distribution de longueurs de branches et les régressions sur matrices de distances. Nos résultats montrent clairement que le signal phylogénétique dans notre échantillonnage de caractères ostéohistologiques est élevé, même après correction pour tests multiples. Une majorité de caractères présente un signal phylogénétique significatif pour au moins un de nos trois tests, la phylogénie expliquant entre 20 et 60% de la variation de ces caractères. En conclusion, les méthode phylogénétiques comparatives devraient être utilisées systématiquement dans les analyses interspécifiques de la diversité histologique de l'os, afin d'éviter les problèmes liés à la non-indépendance des observations.

Abstract

There is currently a debate about the presence of a phylogenetic signal in bone histological data, but very few rigorous tests have fuelled the discussions on this topic. Here, we performed new analyses using a larger set of seven histological traits and including 25 taxa (nine extinct and sixteen extant taxa), using three methods: the phylogenetic eigenvector regression, the tree length distribution and the regressions on distance matrices. Our results clearly show that the phylogenetic signal in our sample of bone histological characters is strong, even after correcting for multiple testing. Most characters exhibit a significant phylogenetic signal according to at least one of our three tests, with the phylogeny often explaining 20 – 60% of the variation in the histological characters. Thus, we conclude that phylogenetic comparative methods should be systematically used in interspecific analyses of bone histodiversity to avoid problems of non-independence among observations.

Introduction

The putative presence of a phylogenetic signal in bone histological data has played a prominent role in the development of paleohistology. Paleohistology was born during the early 19th century with the publication of the first observations of fossil samples (Agassiz, 1833-1844). The history of this discipline contains two well-delimited phases (Cubo & Laurin, 2011). During the second half of the 19th and the first half of the 20th centuries, paleohistologists were mainly interested in problems of taxon determination using fragments of bone tissue (e.g. Queckett, 1849a, b, 1855). All these studies assumed that osteohistological variation contains diagnostic information and a phylogenetic signal. In fact, a number of bone histological traits are synapomorphies at different nodes of the vertebrate phylogeny – for instance, the presence of endochondral bone tissue in Osteichthyes (Janvier, 1996) or the presence of acellular bone tissue in several teleosts (Meunier, 2011).

From the second half of the 20th century onwards, paleohistologists seemed no longer interested in utilizing bone tissue for systematics, and focused on paleobiology instead. These scientists used bone histological information to infer life history traits of extinct vertebrates, assuming that bone histodiversity is linked to functional parameters (e.g. Enlow & Brown, 1956, 1957, 1958; de Ricqlès, 1975, 1976, 1977a, b; Sander, 2000; Horner, Padian & de Ricqlès, 2001; Padian, de Ricqlès & Horner, 2001). This dichotomy between historicism and functionalism is unsatisfactory from a conceptual point of view because a given feature may simultaneously contain a phylogenetic signal (it may constitute a synapomorphy at a given node) and have a functional significance.

Desdevises *et al.* (2003) developed a statistical method allowing to partition the

variation of a trait into a phylogenetic component, a functional or ecological component, the covariation between these fractions, and finally an unexplained fraction. Cubo *et al.* (2005) applied this method to bone microstructural and histological traits and concluded that while phylogenetic signal was highly significant at the microstructural level of organization, it was significant for some histological traits, but not for others. This conclusion has been cited by many authors to argue that 'the histological level of organization by itself may reflect at best a weak signal' (de Ricqlès *et al*., 2008) and that bone histodiversity mainly reflects functional aspects (de Buffrénil, Houssaye & Böhme, 2008). The aim of this study is to test the presence of a phylogenetic signal in bone histodiversity of amniotes using a larger set of bone histological traits than previous studies and including extinct as well as extant taxa.

Material and methods

Material

We analyzed the histological data set published by Cubo *et al.* (2012). It includes information from humeri, femora and tibiae of a sample of 52 specimens belonging to 16 extant species of amniotes, plus the following samples of extinct archosaurs: *Postosuchus* UCMP 28353 (humerus), *Calyptosuchus* UCMP 25914 (femur), *Rutiodon* UCMP 25921 (femur) and *Typothorax* A269 25905 (femur) among Pseudosuchia, and *Lesothosaurus* QR 3076 (femur), *Maiasaura* MOR 005 (tibia), *Coelophysis* AMNH 27435 (tibia), *Allosaurus* UUVP 3694 (femur) and UUVP 154 (tibia), and *Troodon* MOR 748 (femur) among Ornithodira.

Methods

Phylogeny. A reference phylogeny is used in our analyses (Fig. 1). The divergence times are based mostly on fossil evidence. The topology for Testudines follows the established consensus according to which Cryptodira and Pleurodira are sister taxa, as was established long ago (Gaffney & Meylan, 1988). Our sample includes only three turtle terminal taxa, *Trachemys* (Emydidae), *Pelodiscus* (Trionychidae) and *Macrochelodina* (Pleurodira). For the squamates, the topology was compiled from Estes (1982), Estes, de Queiroz & Gauthier (1988), Rieppel (1988), and Caldwell (1999). The placement of Testudines is still controversial (Rieppel & Reisz, 1999; Zardoya & Meyer, 2001); therefore, we placed Testudines as the sister-group of Diapsida, as numerous paleontological studies have argued (Laurin & Reisz, 1995; Lee, 2001; Lyson *et al*., 2010).

Considering that the oldest known amniote (*Hylonomus lyelli*) comes from the late Bashkirian (Marjanović & Laurin, 2007), we used a divergence time between mammals and sauropsids (last common ancestor of Amniota) of 310 Ma. Divergence times between lepidosaurs and crocodylians (252 Ma) and between crocodiles and birds (last common ancestor of Archosauria, 243 Ma) were taken from Reisz & Müller (2004). The last two divergence times are reliable estimates because of the high quality of the fossil record before and after the first occurrence of these taxa (Reisz & Müller, 2004). Divergence time between Lacertidae and Varanidae (189 Ma) and the age of the last common ancestor of dinosaurs (230 Ma) were respectively taken from Evans (2003) and Langer *et al.* (2010), both obtained from the fossil record.

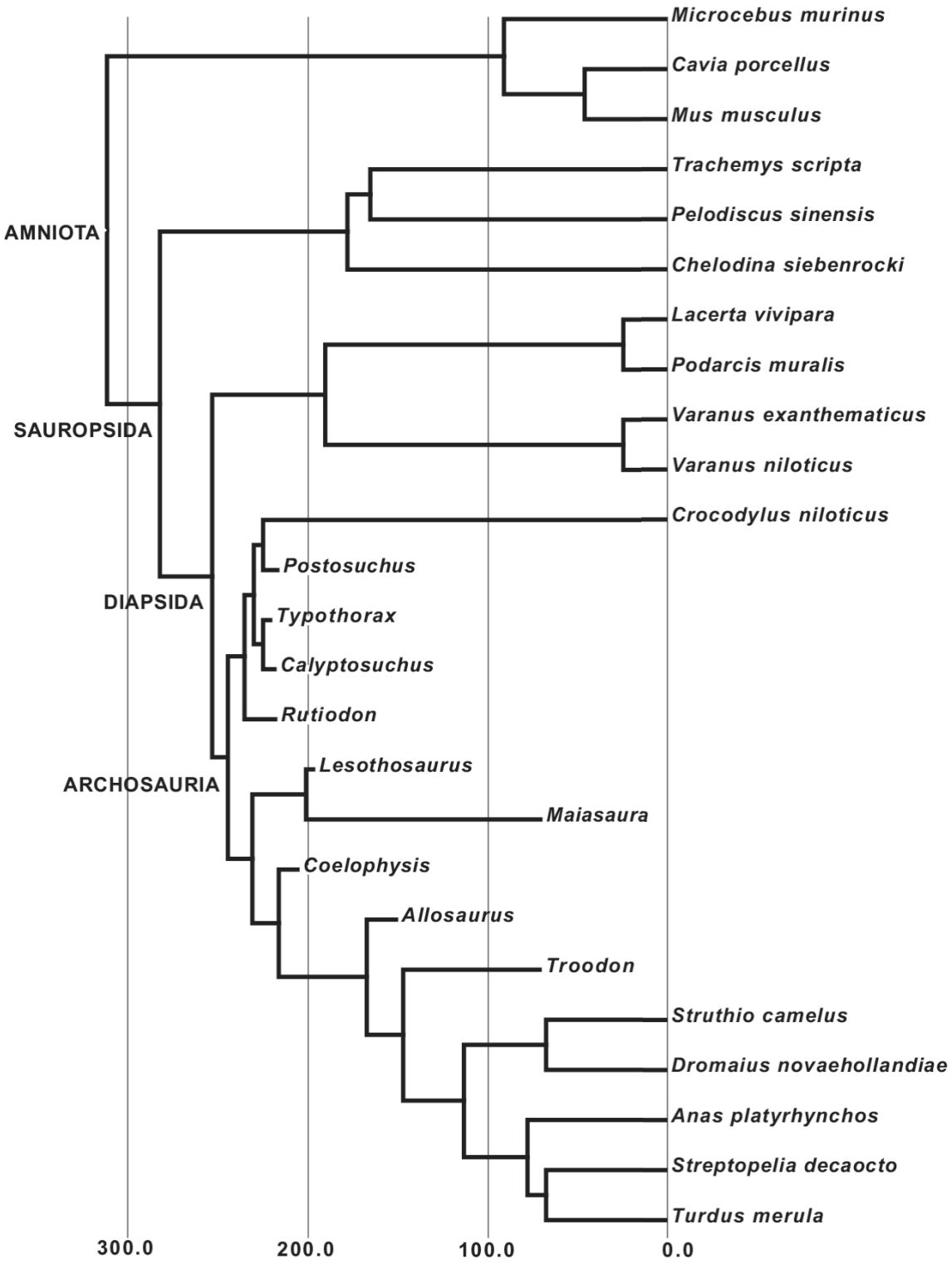

Figure 1. Phylogeny (topology and divergence dates) including the species of the sample (modified after Cubo *et al.*, 2012). The bottom edge contains a time calibration in Ma.

A few divergence times were taken from Pyron (2010), who used a molecular approach calibrated by the four well-constrained fossil dates obtained by Müller & Reisz

(2005). Dates taken from Pyron (2010) include divergence times between Paleognathae and Neognathae (last common ancestor of modern birds, 112 Ma) and between *Anas* and *Turdus* (last common ancestor of Neognathae, 77 Ma). These molecular clock estimates are congruent with vicariance biogeography and fossil evidence, respectively (Laurin *et al*., 2012).

All histological measures were performed on transverse bone sections 100 ± 10 μm thick, which were made across the diaphysis using a diamond-tip circular saw. Each thin section was ground and polished before being mounted on a side, and then observed using optical microscopy and digital imaging (Eclipse E600POL with DXM 1200 Digital Eclipse Camera System; Nikon, Japan). Vascular orientation and density were measured with a magnification of 40x, whereas cellular variables were measured with a 400x magnification.

Ontogenetic control. Considering that there is a marked ontogenetic variation of bone histological features mainly linked to bone growth rate, we standardized our data acquisition by measuring bone histological features in regions formed during the phase of sustained high growth rate. Whereas in our sample of extant species bone formed at sustained high growth rate is located at the bone periphery (specimens were actively growing when they were euthanized), in our samples from extinct taxa, this region is located in the deep cortex (*i.e.* fossil specimens were ontogenetically older than those belonging to extant species).

Variables

Vascular orientation. Blood vessels in the bones were lost during sample preparation in extant species, and during the fossilization process in the extinct taxa. Thus, this variable

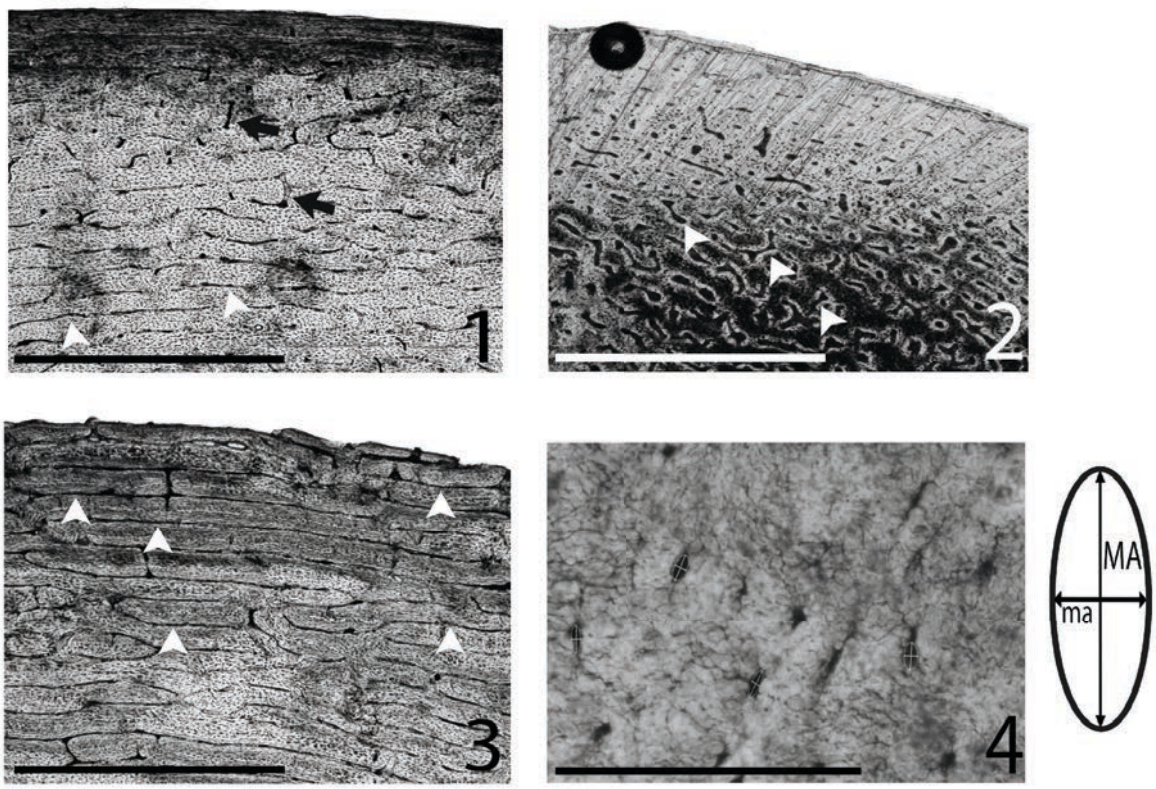

Figure 2. Cross sections in long bone diaphyses of archosaurs in ordinary light. —A. Two radial vascular canals (black arrows) in a mostly circular vascular pattern (white arrowheads), in *Dromaius* (femur). —B. Oblique vascular canals, in *Lesothosaurus* (femur). —C. Dense circular vascular pattern, in *Struthio* (femur). —D. Osteocytes of *Postosuchus* (humerus) with fitting ellipses, and major (MA) and minor (ma) axes figured to illustrate the measuring process of cell size (the ellipse area) and shape (the ma/MA ratio) in ImageJ. Scale bars: 1 mm in A, B, C; 0.05 mm in D.

measures the orientation of the cavities (called vascular canals) that contained the blood vessels and associated connective tissues (Fig. 2A, B). The orientation of each vascular cavity was determined using ImageJ. We inserted the largest ellipse that could fit into each vascular cavity. To improve repeatability, the orientation of each vascular cavity was measured using the radial index published by de Boef & Larsson (2007). The orientation of these cavities was computed as the angle between the major axis of each ellipse and a vector tangent to bone periphery. Thus, vascular canals running parallel to bone periphery have angles approaching 0°, and those running parallel to the radius of bone cross-section have angles approaching 90° (de Boef & Larsson, 2007). Vascular canal orientation is a continuously varying trait that we transformed into discrete orientation classes: circular canals (C), which run roughly parallel to

the bone periphery (0°+22.5°; 180°-22.5°); radial canals (R), which run roughly orthogonal to the bone periphery (90°± 22.5°); and oblique canals (O), that is, those canals excluded from the intervals corresponding to radial canals and to circular ones. These types of vascular orientation are illustrated in de Margerie (2002), de Margerie *et al.* (2004), and de Boef & Larsson (2007). We used three variables to describe the major vascular orientations found on each bone section: proportion of circular canals (C/[C+R+O]), proportion of radial canals (R/[C+R+O]), and proportion of oblique canals (O/[C+R+O]). In avascular bones, the proportions of circular, radial and oblique canals were considered as zero.

Vascular density. Vascular density was measured by Cubo *et al.* (2005) as the ratio of total vascular canal area to primary bone area (Fig. 2C). Here we measured the number of canals divided by mm^2 because the osteons are not yet filled in our sample of extant taxa (the individuals were still growing). Sections showing a single vascular canal were considered to be avascular because this single vascular canal most probably corresponds to a blood vessel running from the periosteum to the endosteum (a Volkmann canal oriented more or less radially).

Cellular variables. Cellular shape, size and density were carefully measured outside the osteons both in extant taxa (in which osteons are not yet filled because they are still growing) and in extinct taxa (in which osteons are already filled). Like vascular canals, osteocytes were lost during the preparation of bone samples in extant species and during the process of fossilization in extinct taxa (Fig. 2D). Thus, we measured the shape, size, and density of cavities (osteocyte lacunae) that contained bone cells (osteocytes). When possible in extant species (*i.e.* when the bone section contained enough osteocyte lacunae), we

measured 120 osteocyte lacunae for each bone section (*i.e.* 30 lacunae measured in four areas in each bone section – rostral, lateral, medial and caudal).

Cellular shape was quantified as the ratio between the minor and the major axes of these cavities ($0 < \text{shape} \leq 1$). The lacunae are perfectly circular in the plane of the section when the shape is equal to 1.

Cellular cross-sectional size was computed using the major and minor axes of osteocyte lacunae and assuming the geometry of an ellipse following the equation $\pi \times L/2 \times l/2$.

Cellular density was quantified as the number of lacunae divided by the surface of the bone section in mm^2.

All measurements were carried out using a microscope focused on a single layer of osteocyte lacunae. Thus, the measurements refer to a single layer of osteocyte lacunae whatever the thickness of the ground section. Cellular density was computed including all osteocyte lacunae of the selected single layer. Following Organ *et al.* (2007), only the largest osteocyte lacunae included in this layer were measured to compute cell size and shape, to ensure that cell lacunae were measured near the middle of their longitudinal axis.

Phylogenetic comparative methods

Three methods were used to test for phylogenetic signal. Obtained results were corrected for multiple testing.

Phylogenetic eigenvector regression. The phylogeny of our sample of amniotes (Fig. 1) was expressed in the form of principal coordinates (Diniz-Filho, de Sant'Ana & Bini,

1998) to be used as explanatory variables in tests of phylogenetic signal. Considering that we obtained as many principal coordinate axes as terminal taxa included in the analyses, a selection procedure was necessary. We retained and used the phylogenetic principal coordinate axes significantly related to the dependent variable as explanatory variables (Desdevises *et al.*, 2003).

Regressions on distance matrices. This method was described by Mantel (1967). Firstly we computed pairwise phylogenetic (patristic) distances using the consensus phylogeny (Fig. 1). For each pair of species, the histological dissimilarity was quantitatively assessed using the absolute value of the difference between the character values. Two distance matrices were constructed: the phylogenetic distance matrix (the sum of branch lengths connecting two taxa, in Ma) and the histological dissimilarity matrix. Afterwards, the histological dissimilarity (the dependent variable) was regressed on the phylogenetic distance (the independent variable). The significance of the regression coefficient could not be tested using a parametric test because the values of the phylogenetic distance matrices (the independent variables) are not normally distributed, and a normal distribution is a fundamental condition of parametric testing. In these cases, significance of statistics must be tested through randomization tests (Harvey & Pagel, 1991: 152–155). Therefore, the significance of the R^2 parameter was tested by a permutation test (Mantel, 1967) using Permute 3.4a9 (Casgrain, 2009), a software that can perform regressions on distance matrices as described by Legendre, Lapointe & Casgrain (1994). Each regression and its statistics were recomputed 9999 times by repeatedly randomizing the values of the histological dissimilarity matrix to obtain a null distribution against which to test the significance of the statistics of the regression on the original dataset.

Random squared tree length distribution. A phylogenetic signal can also be detected in a character by determining if the character requires fewer steps on the reference phylogeny than on most randomly generated trees, provided that the phylogeny has been produced using other characters. In the case of continuous characters, squared length (rather than number of steps) of the character over the tree can be used (Maddison, 1991). The squared length is the most appropriate statistic for a continuous character. It is the sum of the square of changes between each node or between nodes and terminal taxa. Squared change parsimony minimizes this statistic, and in the version that we used (weighted square-change parsimony, implemented in Mesquite), what is minimized is the sum over all branches of the squared change divided by branch length (Maddison, 1991). The probability that the character values are distributed randomly with respect to the phylogeny is simply the proportion of random trees in which squared length is equal or less than on the reference tree. These simulations were performed by the TreeFarm package of modules of Mesquite (Maddison & Maddison, 2011; Maddison, Maddison & Midford, 2011). The appropriate procedure is to randomly permute the taxa (along with their character values) on the tree while holding the topology as well as the branch lengths constant (Laurin, 2004). This procedure has the advantage of yielding random trees that have a branch length distribution identical to that of the reference tree. This is necessary because the squared length of a character over a tree depends on tree depth (Maddison, 1991).

All these tests were performed for our whole sample (Amniota), as well as for three nested sub-groups: Sauropsida, Diapsida, and Archosauria. We could not test other subsets of our sampled taxa because the sample size would have been insufficient, resulting in very low power and hence meaningless negative results.

Corrections for multiple testing. Given that we have seven characters, three bones, three tests, and four nested clades on which these tests were applied, we have performed 252 tests. Thus, corrections for multiple testing are required because at the customary 0.05 probability threshold, twelve or thirteen false positives are expected. For this purpose, we have used the False Discovery Rate (FDR) analysis, which is reasonably easy to use and powerful, as it retains more significant results than classical Bonferroni corrections (Benjamini & Hochbert, 1995; Curran-Everett, 2000). This is why it has been used in recent papers that included multiple tests (e.g. Laurin, Canoville & Quilhac, 2009).

Results

Most histological traits exhibit a significant phylogenetic signal according to at least one of our three tests (Table 1), at least for Amniota (15 bone by character combinations, out of 21, yielded significant results even after correction for multiple testing). For smaller, nested clades, the number of significant results was lower, presumably reflecting decreased power with a lower taxonomic sample size because the number of significant results is directly proportional to the number of included taxa (significant results for 12 bone by character combinations out of 21 for Sauropsida, but only 10 for Diapsida and four for Archosauria). Among these traits, only tibia cell shape yields non-significant results (with any of the three methods). The probabilities yielded by tree length distribution on tibia were higher than those obtained from phylogenetic eigenvector regression or regressions on distance matrices (Table 1). Of the 110 probabilities that were < 0.05 when taken in isolation, 77 remain significant after FDR analysis.

Bone histological variation explained by the phylogeny is in the order of 20 – 60%, as

shown by the phylogenetic eigenvector regression analysis (Table 2, first column). Variation explained by the phylogeny obtained using regressions on distance matrices are lower, as expected, because this method underestimates the real values, as Legendre (2000) showed using simulations. Here, the regression coefficients obtained using phylogenetic eigenvector regression are always much higher than those obtained using regressions on distance matrices (Table 2), which is congruent with the findings of Legendre (2000).

Discussion

Mayr (1961) separates evolutionary biology (concerning historical, or ultimate, causation) from functional biology (tackling immediate, or proximate, causation). The nature of the evidence is comparative in evolutionary biology, whilst it is typically experimental in functional biology. Within evolutionary biology, systematists and functional morphologists are interested in different patterns. For the former, interested in the reconstruction of phylogenetic patterns, the functional adaptation to current conditions (autapomorphies) may mask a pure phylogenetic signal (for example, the autapomorphic flightless condition of the Galapagos cormorant is associated with a whole array of morphological changes that may mask synapomorphies of more inclusive nodes, e.g. Phalacrocoracidae – Cubo & Casinos, 1997). For functional morphologists, phylogenetic patterns are factors that may explain why organisms do not appear to have reached optimal adaptation to current conditions. In 'The shadow of forgotten ancestors differently constrains the fate of Alligatoroidea and Crocodyloidea', Piras *et al.* (2009) suggest that the phylogenetic inheritance of a clade may determine its evolutionary fate. According to Seilacher (1970), a third set of factors (in addition to history and function) may contribute to explain evolutionary patterns: the properties inherent in the materials found in organs and their self-organization properties

Table 1. Probability that the observed covariation between the histological data and the phylogeny is random. This is obtained using phylogenetic eigenvector regression, tree length distribution, and regressions from distance matrices. Phylogenetic signal is considered as significant at a 0.05 threshold when taken in isolation. However, only the P-values marked with asterisks are still significant after correction for multiple testing (False Discovery Rate analysis). These data are available as Mesquite Nexus files in the supporting information (Data S1–S3).

Bone	Histological traits	*n*	Phylogenetic eigenvector regression	Tree length distribution	Regressions from distance matrices
Femur	Cell density				
	Amniota	22	-	0.023	0.607
	Sauropsida	19	0.0002*	0.020	0.373
	Diapsida	16	0.002*	0.023	0.033
	Archosauria	12	0.040	0.110	0.028
	Cell size				
	Amniota	22	0.020*	0.0009*	0.020*
	Sauropsida	19	-	0.0006*	0.442
	Diapsida	16	-	0.0006*	0.255
	Archosauria	12	0.011*	0.003*	0.024
	Cell shape				
	Amniota	22	0.012*	0.014*	0.945
	Sauropsida	19	0.026	0.019	0.379
	Diapsida	16	0.047	0.038	0.775
	Archosauria	12	-	0.056	0.678
	Vascular radial orientation				
	Amniota	22	0.015*	0.047	0.009*
	Sauropsida	19	0.004*	0.050	0.0005*
	Diapsida	16	0.003*	0.025	0.0001*
	Archosauria	12	-	0.897	0.613
	Vascular oblique orientation				
	Amniota	22	0.001*	0.085	0.022
	Sauropsida	19	-	0.255	0.165
	Diapsida	16	-	0.560	0.765
	Archosauria	12	0.007*	0.221	0.732
	Vascular circular orientation				
	Amniota	22	0.010*	<0.0001*	0.000*
	Sauropsida	19	0.0001*	0.0001*	0.0001*
	Diapsida	16	0.0001*	0.0008*	0.0001*
	Archosauria	12	-	0.578	0.927
	Vascular density				
	Amniota	22	0.001*	0.0002*	0.016*
	Sauropsida	19	0.0001*	0.0002*	0.0008*
	Diapsida	16	0.0002*	0.001*	0.0001*
	Archosauria	12	0.062	0.028	0.023
Humerus	Cell density				
	Amniota	17	-	0.154	0.600
	Sauropsida	14	0.002*	0.161	0.133
	Diapsida	11	0.014	0.165	0.016
	Archosauria	7	0.054	0.119	0.004*
	Cell size				
	Amniota	17	0.002*	0.140	0.089
	Sauropsida	14	0.010*	0.106	0.654
	Diapsida	11	0.037	0.084	0.805
	Archosauria	7	-	0.598	0.287
	Cell shape				
	Amniota	17	-	0.006*	0.027
	Sauropsida	14	0.0003*	0.004*	0.0005*
	Diapsida	11	0.0009*	0.004*	0.0001*

Table 1. Continued.

Bone	Histological traits	*n*	Phylogenetic eieigenvector regression	Tree length distribution	Regressions from distance matrices
Humerus	Archosauria		0.037	0.046	0.0008*
	Vascular radial orientation				
	Amniota	17	0.008*	0.870	0.738
	Sauropsida	14	-	0.818	0.898
	Diapsida	11	-	0.768	0.397
	Archosauria	7	-	0.897	0.613
	Vascular oblique orientation				
	Amniota	17	0.003*	0.043	0.040
	Sauropsida	14	-	0.070	0.217
	Diapsida	11	-	0.051	0.154
	Archosauria	7	0.050	0.942	0.259
	Vascular circular orientation				
	Amniota	17	-	0.005*	0.056
	Sauropsida	14	0.0003*	0.007*	0.019
	Diapsida	11	0.0002*	0.005*	0.0001*
	Archosauria	7	0.050	0.713	0.778
	Vascular density				
	Amniota	17	-	0.012*	0.533
	Sauropsida	14	0.001*	0.018	0.162
	Diapsida	11	0.009*	0.013*	0.006*
	Archosauria	7	-	0.248	0.449
Tibia	Cell density				
	Amniota	19	-	0.505	0.018*
	Sauropsida	16	-	0.480	0.343
	Diapsida	13	-	0.581	0.144
	Archosauria	9	-	0.834	0.801
	Cell size				
	Amniota	19	0.045	0.388	0.015*
	Sauropsida	16	-	0.472	0.036
	Diapsida	13	-	0.295	0.575
	Archosauria	9	-	0.205	0.442
	Cell shape				
	Amniota	19	0.073	0.283	0.133
	Sauropsida	16	-	0.298	0.342
	Diapsida	13	-	0.289	0.459
	Archosauria	9	-	0.138	0.823
	Vascular radial orientation				
	Amniota	19	-	0.839	0.117
	Sauropsida	16	-	0.860	0.633
	Diapsida	13	-	0.872	0.212
	Archosauria	9	-	0.483	0.529
	Vascular oblique orientation				
	Amniota	19	0.007*	0.396	0.017*
	Sauropsida	16	0.004*	0.463	0.008*
	Diapsida	13	0.042	0.624	0.021
	Archosauria	9	-	0.614	0.493
	Vascular circular orientation				
	Amniota	19	0.037	0.0007*	0.139
	Sauropsida	16	0.002*	0.0002*	0.005*
	Diapsida	13	0.001*	0.0005*	0.0001*
	Archosauria	9	-	0.393	0.721
	Vascular density				
	Amniota	19	-	0.803	0.000*
	Sauropsida	16	-	0.746	0.002*
	Diapsida	13	-	0.683	0.066
	Archosauria	9	-	0.933	0.148

Table 2. Covariation between bone histology and the phylogeny assessed as the R^2 values of histological variances explained by the tree, as obtained in tests of phylogenetic signal using phylogenetic eigenvetor regression and regressions on distance matrices. In phylogenetic eigenvector regression, we retained and used the phylogenetic principal coordinate axes significantly related to the dependent variable as explanatory variables. When no axes were retained, the analysis could not be performed. Note that the third phylogenetic signal test (tree length distribution) does not yield an explained variance, so it is not reported here.

Bone	Histological traits	*n*	Phylogenetic eigenvector regression	Regressions from distance matrices
Femur	Cell density			
	Amniota	22	-	0.001
	Sauropsida	19	0.666	0.005
	Diapsida	16	0.676	0.038
	Archosauria	12	0.327	0.073
	Cell size			
	Amniota	22	0.247	0.024
	Sauropsida	19	-	0.004
	Diapsida	16	-	0.011
	Archosauria	12	0.397	0.077
	Cell shape			
	Amniota	22	0.378	0.000
	Sauropsida	19	0.258	0.005
	Diapsida	16	0.252	0.0007
	Archosauria	12	-	0.003
	Vascular radial orientation			
	Amniota	22	0.247	0.028
	Sauropsida	19	0.834	0.071
	Diapsida	16	0.818	0.176
	Archosauria	12	-	0.004
	Vascular oblique orientation			
	Amniota	22	0.576	0.022
	Sauropsida	19	-	0.012
	Diapsida	16	-	0.0008
	Archosauria	12	0.536	0.002
	Vascular circular orientation			
	Amniota	22	0.286	0.117
	Sauropsida	19	0.908	0.250
	Diapsida	16	0.945	0.438
	Archosauria	12	-	0.0001
	Vascular density			
	Amniota	22	0.598	0.024
	Sauropsida	19	0.775	0.061
	Diapsida	16	0.811	0.438
	Archosauria	12	0.307	0.077
Humerus	Cell density			
	Amniota	17	-	0.002
	Sauropsida	14	0.767	0.025
	Diapsida	11	0.656	0.107
	Archosauria	7	0.527	0.355
	Cell size			
	Amniota	17	0.582	0.021
	Sauropsida	14	0.585	0.002
	Diapsida	11	0.408	0.001
	Archosauria	7	-	0.059
	Cell shape			
	Amniota	17	-	0.037
	Sauropsida	14	0.857	0.132
	Diapsida	11	0.813	0.370

Table 2. Continued.

Bone	Histological traits	*n*	Phylogenetic eieigenvector regression	Regressions from distance matrices
Humerus	Archosauria		0.609	0.431
	Vascular radial orientation			
	Amniota	17	0.482	0.001
	Sauropsida	14	-	0.0002
	Diapsida	11	-	0.014
	Archosauria	7	-	0.146
	Vascular oblique orientation			
	Amniota	17	0.57	0.031
	Sauropsida	14	-	0.017
	Diapsida	11	-	0.038
	Archosauria	7	0.798	0.067
	Vascular circular orientation			
	Amniota	17	-	0.027
	Sauropsida	14	0.764	0.061
	Diapsida	11	0.886	0.247
	Archosauria	7	0.608	0.004
	Vascular density			
	Amniota	17	-	0.003
	Sauropsida	14	0.613	0.021
	Diapsida	11	0.625	0.136
	Archosauria	7	-	0.031
Tibia	Cell density			
	Amniota	19	-	0.033
	Sauropsida	16	-	0.008
	Diapsida	13	-	0.029
	Archosauria	9	-	0.002
	Cell size			
	Amniota	19	0.215	0.033
	Sauropsida	16	-	0.038
	Diapsida	13	-	0.004
	Archosauria	9	-	0.017
	Cell shape			
	Amniota	19	0.179	0.013
	Sauropsida	16	-	0.008
	Diapsida	13	-	0.007
	Archosauria	9	-	0.002
	Vascular radial orientation			
	Amniota	19	-	0.014
	Sauropsida	16	-	0.002
	Diapsida	13	-	0.021
	Archosauria	9	-	0.011
	Vascular oblique orientation			
	Amniota	19	0.308	0.034
	Sauropsida	16	0.058	0.559
	Diapsida	13	0.295	0.072
	Archosauria	9	-	0.014
	Vascular circular orientation			
	Amniota	19	0.219	0.013
	Sauropsida	16	0.067	0.539
	Diapsida	13	0.676	0.234
	Archosauria	9	-	0.004
	Vascular density			
	Amniota	19	-	0.094
	Sauropsida	16	-	0.077
	Diapsida	13	-	0.043
	Archosauria	9	-	0.060

(with few genetic inputs). These three perspectives are not necessarily mutually exclusive.

In the field of bone biology, Cubo *et al.* (2005) found a significant phylogenetic signal at the microanatomical level of bone organization, but concluded that the histological level contained a lower signal. However, considering that Cubo *et al.* (2008, 2012) showed evidence for a significant phylogenetic signal in the variation of bone growth rate in amniotes, and that, according to Amprino's rule, bone histodiversity may reflect variation in bone growth rates (Amprino, 1947; Montes *et al.*, 2010), we expected that bone histological variation contained a significant phylogenetic signal. Here we expand upon the analyses initiated by Cubo *et al.* (2005) using a larger set of histological traits and including extinct taxa.

Our results clearly show that the phylogenetic signal in the bone histological characters that we studied is strong, with the phylogeny often explaining 20 – 60% of the variation in the histological characters. The proportion of significant results appears to depend rather strongly on taxonomic sample size, reflecting the common and expected increase power at larger sample sizes. Nevertheless, our results do not imply that functional factors are unimportant. In fact, some of the variation explained by the phylogeny may represent covariation with functional factors (rather than purely phylogenetic variation), although variation partition analyses would be required to determine this. These are beyond the scope of this study, as they would require additional data (such as growth rate, metabolic rate, *etc.*). However, some evidence suggests that part of this phylogenetic signal represents covariation with functional factors, at least for the femur. Cubo *et al.* (2012) constructed a paleobiological inference model using extant taxa for estimating bone growth rate of extinct taxa (a functional factor according to Amprino's rule) from bone histological data. The response variable (*i.e.*

the functional variable, bone growth rate) was significantly correlated with, and could be reliably inferred from, predictor variables (bone histological traits). These results are evidence of a significant functional effect on bone histological variation, and are complementary to the evidence presented in this study for a significant phylogenetic signal on the same traits.

We conclude that, in view of the results reported above, phylogenetic comparative methods should be used in any study dealing with interspecific variation of bone histology to avoid problems of non-independence among observations. This is unfortunately still not common practice. Some disciplines such as ecology and, to a lesser extent, vertebrate morphology incorporated phylogenetic comparative methods soon after the initial development of this approach in the middle of the 1980s (see a review in Harvey & Pagel, 1991). In contrast, the use of these methods is not yet generalized in other fields such as bone histology (e.g. de Buffrénil, Houssaye & Böhme, 2008), but we hope that this study will help motivate bone histologists to adopt these methods.

Acknowledgements

This study was funded by the grant CGL2011-23919 of the Spanish Government (to JC), the JAE-Doc program CSIC, cofunded by FSE (to CMM), and by the CNRS and the French ministry of research (operating grants of UMR 7207 for ML and 7193 for LL, LM, and JC). This draft was improved by comments from Tim Bromage and Hans Larsson.

I – 2. Bone histology, phylogeny, and palaeognathous birds (*Aves*, Palaeognathae)

Lucas J. Legendre, Estelle Bourdon, R. Paul Scofield, Alan J. D. Tennyson,

Hayat Lamrous, Armand de Ricqlès et Jorge Cubo

Publication originale *in*: *Biological Journal of the Linnean Society* (sous presse, 2014).

Résumé

La présence d'un signal phylogénétique dans la variation des traits ostéohistologiques a fait récemment l'objet d'un débat dans la littérature. Des études précédentes avaient identifié un signal significatif pour certains caractères, mais ces résultats avaient été obtenus sur un nombre peu élevé de caractères et avec un échantillonnage réduit. Nous effectuons ici une étude très complète au cours de laquelle nous quantifions le signal phylogénétique pour soixante-deux caractères ostéohistologiques au sein d'un échantillonnage exhaustif d'oiseaux paléognathes. Nous avons utilisé quatre estimateurs différents pour mesurer le signal phylogénétique – le λ de Pagel, le C_{mean} d'Abouheif, le K de Blomberg et les PVR de Diniz-Filho, ainsi que quatre topologies issues de la litérature. La taille de l'os et la densité vasculaire osseuse présentent un fort signal phylogénétique, tandis que tous les autres caractères, à l'exception de quatre – la taille des cellules pour les transects caudal et médial des fémurs, et la proportion de canaux vasculaires obliques pour les transects rostral et caudal des tibiotarses – présentent un signal plus faible. Nous avons également découvert que l'effet des topologies utilisées dans les analyses est très faible comparé à celui de la taille de l'échantillonnage. Pour conclure, l'analyse d'un échantillonnage exhaustif est indispensable pour obtenir des estimations fiables du signal phylogénétique.

Mots-clés : Histologie osseuse – signal phylogénétique – paléognathes – méthodes phylogénétiques comparatives

Abstract
The presence of a phylogenetic signal in the variation of osteohistological features has been recently debated in the literature. Previous studies have found a significant signal for some features, but these results were obtained on a small amount of characters and a reduced sample. Here we perform a comprehensive study in which we quantify the phylogenetic signal on sixty-two osteohistological features in an exhaustive sample of palaeognathous birds. We used four different estimators to measure phylogenetic signal – Pagel's λ, Abouheif's C_{mean}, Blomberg's K, and Diniz-Filho's PVR – and four topologies taken from the literature. Bone size and bone vascular density exhibit a strong phylogenetic signal, whereas all but four of the remaining features measured at the histological level – cellular size in caudal and medial transects of femora, and proportion of oblique vascular canals in rostral and caudal transects of tibiotarsi – exhibit a weaker signal. We also found that the impact of the topologies used in the analyses is very low compared to that of sample size. We conclude that the analysis of a comprehensive sample is crucial to obtain reliable quantifications of the phylogenetic signal.

Keywords: Bone histology – phylogenetic signal – palaeognaths – phylogenetic comparative methods

Introduction

Early palaeohistologists were interested in problems of taxon determination using small bone fragments, assuming that bone histological variation contains diagnostic information and thus, put in modern terms, a phylogenetic signal (e.g. Queckett, 1849a, b, 1855). In the second half of the 20th century, palaeohistologists (with some exceptions such as Houde (1988), who focused on identifying synapomorphies in the bone histology of palaeognathous birds) were mainly interested in problems of palaeobiology and used bone histological features to infer life history traits of extinct vertebrates (review in Cubo & Laurin, 2011; de Ricqlès, 2011).

The first decade of the 21st century has been marked by a renewed interest for the

study of phylogenetic signal in bone histological variation. On the one hand, some studies have found that a number of bone histological features are synapomorphies at different nodes in the vertebrate phylogeny. For instance, Rensberger & Watabe (2000) suggested that mammals and hadrosaurs may have retained the primitive condition among amniotes characterized by the presence of canaliculi aligned in parallel with the direction of growth – that is, in a radial direction toward either the outer, periosteal surfaces, the inner, endosteal surfaces, or the lumina of vascular canals – while coelurosaurs (e.g. ornithomimid dinosaurs and birds) may have acquired the derived condition characterized by the presence of canaliculi organized as extensively branching channels that diverge at large angles from each other. Padian, de Ricqlès & Horner (2001) suggested that the last common ancestor of archosaurs was characterized by the presence of parallel-fibered bone tissue, whereas dinosaurs may share the derived condition characterized by the presence of fibrolamellar bone tissue. A more recent work (de Ricqlès *et al*., 2008) places the origin of fibrolamellar bone tissue at the more inclusive archosauromorph node. More recently, Bourdon *et al.* (2009a) showed that bone growth marks may have been absent in the last common ancestor of ratites, and suggested they may have been acquired by the last common ancestor of the clade (Kiwi – Moa).

Other studies used modern statistical methods to test the presence of phylogenetic signal in bone histological variation. For instance, Cubo *et al.* (2005) concluded that phylogenetic signal was strong at the microanatomical level of organization, whereas at the histological level it was weak at best. This last result was probably the outcome of the small sample size (35 species of sauropsids over a total of almost 20,000 extant species), the small number of bone histological features analyzed (three variables) and the absence of fossils in the analyzed sample. Efforts were recently made by Legendre *et al.* (2013) and Houssaye,

Tafforeau & Herrel (in press) in amniotes, Dumont *et al.* (2013) and Marín-Moratalla *et al.* (in press) in mammals, and Houssaye *et al.* (2013) in squamates. However, in all these cases, sample size compared to clade size was still reduced.

This study aims to quantify the phylogenetic signal in the variation of bone histological features on an exhaustive sample using a statistical approach. The palaeognath clade was selected because it contains a reduced number of species (thus allowing an exhaustive sampling) and has a long geological history deep into the Cretaceous (Cracraft, 2001; Bourdon, de Ricqlès & Cubo, 2009b). This large sample is thus likely to improve our ability to detect phylogenetic signal in bone histological features. Those features showing a significant signal can be included in predictive models to infer various life history traits in fossil specimens using phylogenetic comparative methods (Revell, 2010; Legendre, Segalen & Cubo, 2013).

Material and methods

Material

This study was performed using a sample of 46 specimens belonging to 21 species, covering all extant ratite genera (*Apteryx*, *Casuarius*, *Dromaius*, *Rhea* and *Struthio*), three (over nine) tinamou genera (Tinamidae: *Eudromia*, *Nothura* and *Rhynchotus*), all New Zealand moa genera (Dinornithidae: *Anomalopteryx*, *Dinornis*, *Emeus*, *Euryapteryx*, *Megalapteryx* and *Pachyornis*) and one elephant-bird genus (Aepyornithidae: *Aepyornis)* from Madagascar. These specimens come from the collections of the Muséum National d'Histoire Naturelle (MNHN; Paris, France), the Naturhistorisches Museum Wien (NHMW;

Vienna, Austria), the National Museum of Natural History (NMNH; Washington, United States), the Natural History Museum of Los Angeles County (LACM; Los Angeles, United States), the Canterbury Museum (Christchurch, New Zealand) and the National Museum of New Zealand Te Papa Tongarewa (Wellington, New Zealand).

Ontogenetic control

All analyzed specimens are subadults or young adults: primary osteons are fully formed in the outer cortex and there are few (if any) secondary (haversian) osteons outside the inner cortex (Francillon-Vieillot *et al.,* 1990; de Ricqlès *et al.,* 1991). Osteohistological features were measured in the deep cortex of primary periosteal bone tissue, in order to analyse the bone tissue formed at the fastest recorded rate, following the procedure described in Cubo *et al.* (2012).

Osteohistological features

We prepared 100 ± 10 µm thick bone sections from femoral and tibiotarsal midshafts. These sections were photographed with a polarizing microscope (Nikon Eclipse E600POL). The pictures were then edited and analyzed using Photoshop 7.0 and ImageJ 1.44. We followed Cubo et al. (2012) and defined osteohistological features as follows (Table 1):

Vascular canal orientation.— Blood vessels in bones were lost during sample preparation in extant species, and during post-mortem mechanisms in moa and elephant-bird subfossils. Thus, this variable measures the orientation of the cavities (called vascular canals) that contained the blood vessels and associated connective tissues (Figure 1). We inserted the

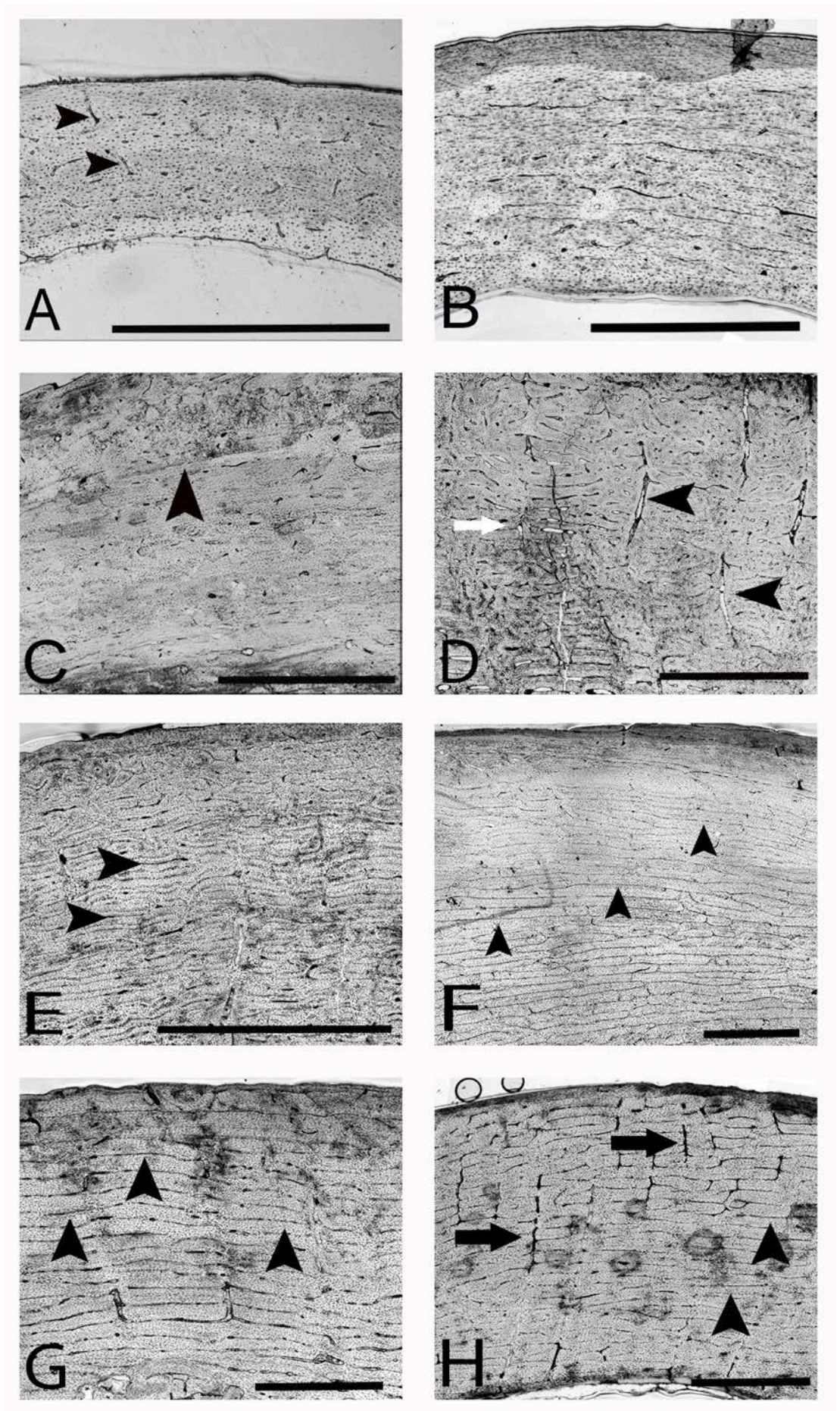
A
B
C
D
E
F
G
H

Figure 1. Cross-sections of long bones of palaeognaths in ordinary light. —A: Femur of a red-winged tinamou (*Rhynchotus rufescens*), showing oblique canals (arrowheads) isolated from each other. —B: Tibiotarsus of a southern brown kiwi (*Apteryx australis*); vascular canals are scattered and do not form a conspicuous pattern in the cortex. —C: Femur of a South Island giant moa (*Dinornis robustus*); the deep cortex lacks vascular pattern, and a line of arrested growth (LAG) is visible (arrowhead). —D: Femur of an elephant bird (*Aepyornis maximus*); the bone is seemingly fibrolamellar with a majority of circular canals (white arrow), connected with each other by large, radial anastomoses (black arrowheads). —E: Femur of a Darwin's rhea (*Rhea pennata*). —F: Tibiotarsus of an ostrich (*Struthio camelus*). —G: Femur of a southern cassowary (*Casuarius casuarius*). —H: Femur of an emu (*Dromaius novaehollandiae*). All bones in E, F, G and H present a dense pattern of circular canals (arrowheads), sometimes connected by radial canals formed by anastomosis (arrows in H). Scale bars equal 1 mm.

largest ellipse into each vascular cavity. To improve repeatability, the orientation of each vascular cavity was measured using the radial index published by de Boef & Larsson (2007). The orientation of these cavities was computed as the angle between the major axis of each ellipse and a vector tangent to bone periphery. Thus, vascular canals running parallel to bone periphery have angles approaching 0°, and those running parallel to the radius of bone cross-section have angles approaching 90° (de Boef & Larsson, 2007). Vascular canal orientation is a continuously varying trait that we transformed into discrete orientation classes using the following criteria: three types of standard vascular canal orientation were defined in our transverse sections (Figure 1) - circular canals (C), which run roughly parallel to the bone periphery (0°+22.5°; 180°-22.5°); radial canals (R), which run roughly orthogonal to the bone periphery (90°± 22.5°); and oblique canals (O), *i.e.* those canals excluded from the intervals corresponding to radial canals and circular ones. These types of vascular orientation are illustrated in de Margerie, Cubo & Castanet (2002), de Margerie *et al.* (2004), and de Boef & Larsson (2007). We used three variables to describe the major vascular orientations found on each bone section: proportion of circular canals: C/(C+R+O); proportion of radial canals: R/(C+R+O); and proportion of oblique canals: O/(C+R+O), in order to provide a reliable account of the variation of vascular orientation across each section.

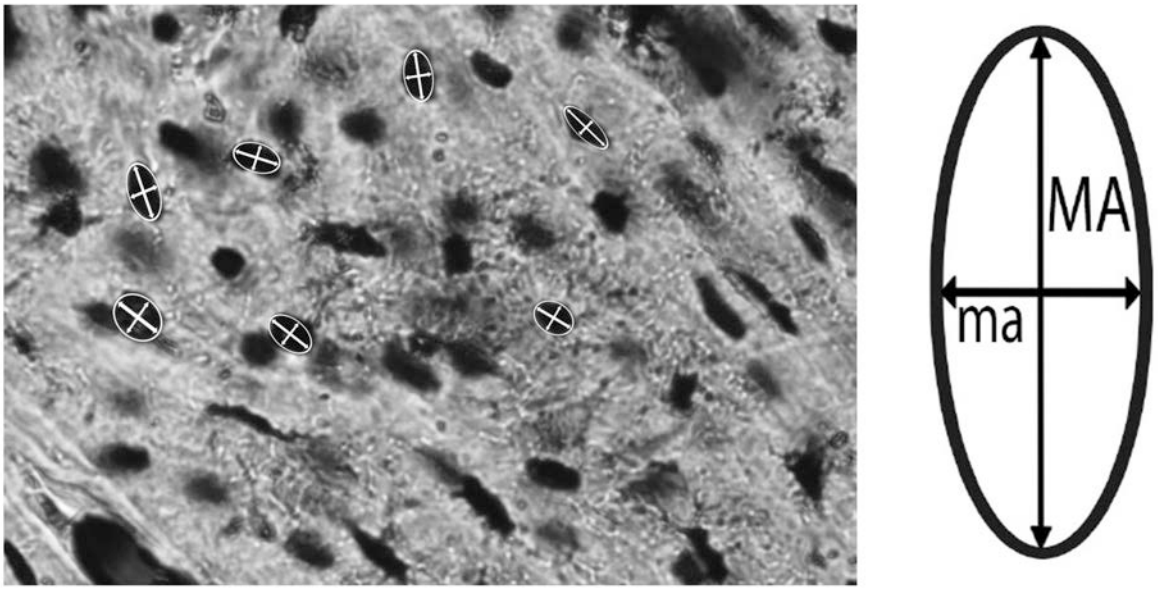

Figure 2. Schematic representation of the measures used to compute osteocyte size and shape: for each cell selected on the histological section – here on the femur of an emu (*Dromaius novaehollandiae*) observed at x400 magnification – we insert with ImageJ the biggest possible ellipse and measure the major axis (MA) and minor axis (ma) in this ellipse.

Vascular density.— Vascular density was measured as the number of canals divided by mm^2. We used this variable instead to the ratio vascular canal area / cortical bone area to minimize the bias caused by the ontogenetic status of specimens in our sample of extant taxa (some peripheral primary osteons still had residual centripetal apposition).

Cellular variables (Figure 2).— Cellular shape and size were carefully measured outside primary osteons. Like vascular canals, osteocytes were lost during the preparation of bone samples in extant species and during the post-mortem mechanisms in moa and elephant-bird subfossils. Thus, we measured the shape and size of cavities (osteocyte lacunae) that contained bone cells (the osteocytes).

Cellular shape was quantified as the ratio between the minor and the major axes of these cavities ($0 < \text{shape} \leq 1$). A value of 1 means that the lacunae are perfectly circular.

Cellular size was computed using the major and minor axes of osteocyte lacunae and assuming the geometry of an ellipse ($\pi \times L/2 \times l/2$).

All measurements were carried out using a microscope focused on a single layer of osteocyte lacunae. Thus, the measurements refer to a single layer of cells whatever the thickness of the ground section. Following Organ *et al.* (2011), only the largest osteocyte lacunae included in this layer were measured to compute cell size and shape, to ensure that cell lacunae were measured near the mid axis.

Bone size.— This variable was measured as bone cross-sectional area (bone surface encircled by the periosteum in mm^2).

All features (except bone size) were measured through four bone transects on each specimen, corresponding to the four main anatomical quadrants of the cortical bone (rostral, caudal, lateral and medial) on a bone section. These quadrants correspond to anatomical regions that can experience differences in appositional growth rate (cortical drift) or mechanical strains (e.g. tension or compression). By comparing the same topological regions within a given bone, we assumed to work in a strict frame of homology.

Unfortunately, several subfossil specimens used in this study do not present a whole bone section with the four intact quadrants, so that the number of measurements was not the same for all specimens/features. Moreover, sometimes it was impossible to orientate bone sections. To minimize the impact of this lack of information, we also computed mean values for each cross-section as additional variables. Each feature was measured 30 times and a mean was computed on each quadrant, and then for the whole section (4 x 30 measures, *i.e.* 120 measures when the whole section was available). For the fragmentary sections, the mean of the whole section included at least one transect, *i.e.* 30 measures.

Table 1. List of 62 osteohistological features measured for this study, with p-values for each estimator of phylogenetic signal we used (Pagel's λ, Blomberg's K, Diniz-Filho's PVR and Abouheif's C_{mean}), using the phylogeny taken from Haddrath & Baker (2012). Significant values (*i.e.* $p < 0.05$) are highlighted in **bold**. The complete dataset including specimen numbers is available as project 1133 in MorphoBank (http://www.morphobank.org/index.php). Abbreviations : C, caudal; L, lateral; M, medial; R, rostral transects.

	Variables	Pagel's λ	Blomberg's K	Diniz-Filho's PVR	Abouheif's C_{mean}
1	Femur size	**0,00172**	**0,00045**	**0,00532**	**0,02670**
2	Femur vascular density R	**0,00085**	**0,00070**	**0,00209**	**0,00310**
3	Femur vascular density C	**0,00729**	**0,00160**	**0,00118**	**0,00500**
4	Femur vascular density L	0,09104	0,07040	**0,00149**	**0,02720**
5	Femur vascular density M	**0,00311**	**0,00270**	**0,00078**	**0,00530**
6	Femur vascular density mean	**0,00146**	**0,00690**	0,07477	**0,00110**
7	Femur proportion of circular canals R	1,00000	0,98010	**0,00000**	0,90140
8	Femur proportion of circular canals C	1,00000	0,57950	0,07829	0,49420
9	Femur proportion of circular canals L	0,27198	0,13070	0,16050	0,35950
10	Femur proportion of circular canals M	0,23352	0,11970	**0,02580**	0,16680
11	Femur proportion of circular canals mean	0,24212	0,09550	0,17300	0,06590
12	Femur proportion of radial canals R	1,00000	0,95070	0,43610	0,89280
13	Femur proportion of radial canals C	1,00000	0,66035	0,24580	0,47880
14	Femur proportion of radial canals L	0,39112	0,35455	**0,00749**	0,05090
15	Femur proportion of radial canals M	0,57946	0,57520	**0,01699**	0,11060
16	Femur proportion of radial canals mean	**0,00246**	**0,00120**	**0,03608**	**0,00290**
17	Femur proportion of oblique canals R	0,92241	0,63095	0,08429	0,36170
18	Femur proportion of oblique canals C	1,00000	0,37890	**0,03563**	0,33880
19	Femur proportion of oblique canals L	0,48361	0,15865	0,57300	0,19330
20	Femur proportion of oblique canals M	1,00000	0,21775	0,11410	0,48110
21	Femur proportion of oblique canals mean	0,22129	0,05250	0,09429	0,13100
22	Femur osteocyte shape R	1,00000	0,44090	0,38900	0,45690
23	Femur osteocyte shape C	0,83003	0,13950	**0,01273**	0,73140
24	Femur osteocyte shape L	1,00000	0,42640	0,39770	0,74930
25	Femur osteocyte shape M	0,07663	**0,02650**	**0,03546**	0,06610
26	Femur osteocyte shape mean	**0,01327**	0,13030	**0,00005**	**0,00180**
27	Femur osteocyte size R	1,00000	0,06320	0,25030	0,41340
28	Femur osteocyte size C	**0,00504**	**0,03300**	**0,00389**	**0,04280**
29	Femur osteocyte size L	**0,02427**	0,07540	**0,03730**	0,11190
30	Femur osteocyte size M	**0,01258**	**0,03770**	**0,00194**	**0,03340**
31	Femur osteocyte size mean	1,00000	**0,04430**	**0,01758**	0,21850
32	Tibiotarsus size	**0,00115**	**0,00025**	**0,01659**	**0,03160**
33	Tibiotarsus vascular density R	0,05549	0,05735	**0,01059**	0,07710
34	Tibiotarsus vascular density C	0,07130	0,10970	0,43580	0,06300
35	Tibiotarsus vascular density L	0,09792	**0,03245**	**0,01220**	0,08060
36	Tibiotarsus vascular density M	0,23817	0,12840	**0,01368**	0,11450

37	Tibiotarsus vascular density mean	1,00000	0,32710	0,31070	0,20890
38	Tibiotarsus proportion of circular canals R	**0,01227**	**0,00810**	**0,02498**	0,07540
39	Tibiotarsus proportion of circular canals C	0,41427	0,45320	**0,00989**	0,05450
40	Tibiotarsus proportion of circular canals L	1,00000	0,98575	0,72310	0,95950
41	Tibiotarsus proportion of circular canals M	1,00000	0,60320	**0,01452**	0,98400
42	Tibiotarsus proportion of circular canals mean	0,49267	0,69500	0,12220	0,14950
43	Tibiotarsus proportion of radial canals R	1,00000	0,68105	0,37420	0,31260
44	Tibiotarsus proportion of radial canals C	1,00000	0,72555	0,31500	0,71460
45	Tibiotarsus proportion of radial canals L	0,49560	0,15120	0,60740	0,54630
46	Tibiotarsus proportion of radial canals M	1,00000	0,80290	0,37100	0,60300
47	Tibiotarsus proportion of radial canals mean	1,00000	0,73280	0,19990	0,62750
48	Tibiotarsus proportion of oblique canals R	**0,00958**	**0,00470**	**0,00004**	**0,00310**
49	Tibiotarsus proportion of oblique canals C	**0,01668**	**0,00405**	**0,00210**	**0,03290**
50	Tibiotarsus proportion of oblique canals L	1,00000	0,99820	0,51450	0,92870
51	Tibiotarsus proportion of oblique canals M	1,00000	0,28865	0,30270	0,88110
52	Tibiotarsus proportion of oblique canals mean	1,00000	0,97690	0,10580	0,45370
53	Tibiotarsus osteocyte shape R	0,45295	0,32145	0,15390	0,06790
54	Tibiotarsus osteocyte shape C	0,16205	0,14505	0,39990	**0,01300**
55	Tibiotarsus osteocyte shape L	0,85346	0,20495	0,21010	0,22990
56	Tibiotarsus osteocyte shape M	0,56820	0,52195	**0,03158**	0,08160
57	Tibiotarsus osteocyte shape mean	0,70686	0,18950	**0,03305**	0,09040
58	Tibiotarsus osteocyte size R	1,00000	0,69710	0,22620	0,73690
59	Tibiotarsus osteocyte size C	0,66471	0,15340	0,22600	0,37580
60	Tibiotarsus osteocyte size L	1,00000	0,33280	0,26300	0,64760
61	Tibiotarsus osteocyte size M	0,99349	0,62840	0,06275	0,26960
62	Tibiotarsus osteocyte size mean	1,00000	0,43370	**0,04715**	0,18280

Table 1. Continued.

When several individuals were available for a given species, we computed mean species values for each histological trait. We obtained a data matrix for 21 palaeognathous bird species and 62 histological features (see Table 1). The complete character matrix, as well as all the pictures used to measure those features, are archived as Project 1133 in MorphoBank (http://www.morphobank.org/index.php).

Measurement of phylogenetic signal

Quantification of phylogenetic signal using statistical approaches assumes that the phylogeny (topology and divergence times) is known. Monophyly and interrelationships of Palaeognathae are still hotly debated. With the exception of Johnston (2011), most morphoanatomical phylogenies of birds always identified flightless ratites as a monophyletic group distinct from flying tinamous (Livezey & Zusi, 2007, and references therein), but the relationships among ratites varied a lot from one study to another. Early molecular phylogenies also supported this dichotomy between tinamous and ratites (e.g. Sibley & Ahlquist, 1990; Van Tuinen, Sibley & Hedges, 2000; Paton, Haddrath & Baker, 2002; Harrison *et al.*, 2004; Slack *et al.*, 2006), but many recent molecular phylogenies found tinamous to be nested within ratites, thus supporting the hypothesis of multiple, independent losses of flight among palaeognaths (e.g. Hackett *et al.*, 2008; Harshman *et al.*, 2008; Phillips *et al.*, 2010; Haddrath & Baker, 2012; Smith *et al.*, 2013), but the topologies differ depending on the genes used.

We used four of the most recent phylogenies of palaeognathous birds as our reference topologies. Among these, the first two were built using 129 and 179 morphoanatomical characters, respectively (Bourdon *et al.*, 2009b; Worthy & Scofield, 2012). Both of them found ratite monophyly, with a kiwi-moa clade sister-group to a rhea-emu-ostrich clade (Figure 3A, B). The two other topologies were built using 27 nuclear genes and 27 retroposons (Haddrath & Baker, 2012; Figure 3D), and 40 nuclear genes (Smith, Brown & Kimball, 2013; Figure 3C), respectively. These two studies, like most phylogenetic analyses of palaeognaths based on molecular characters, provided evidence that ratites are paraphyletic, with tinamous as sister-group to either moa or emu-cassowary, and the ostrich

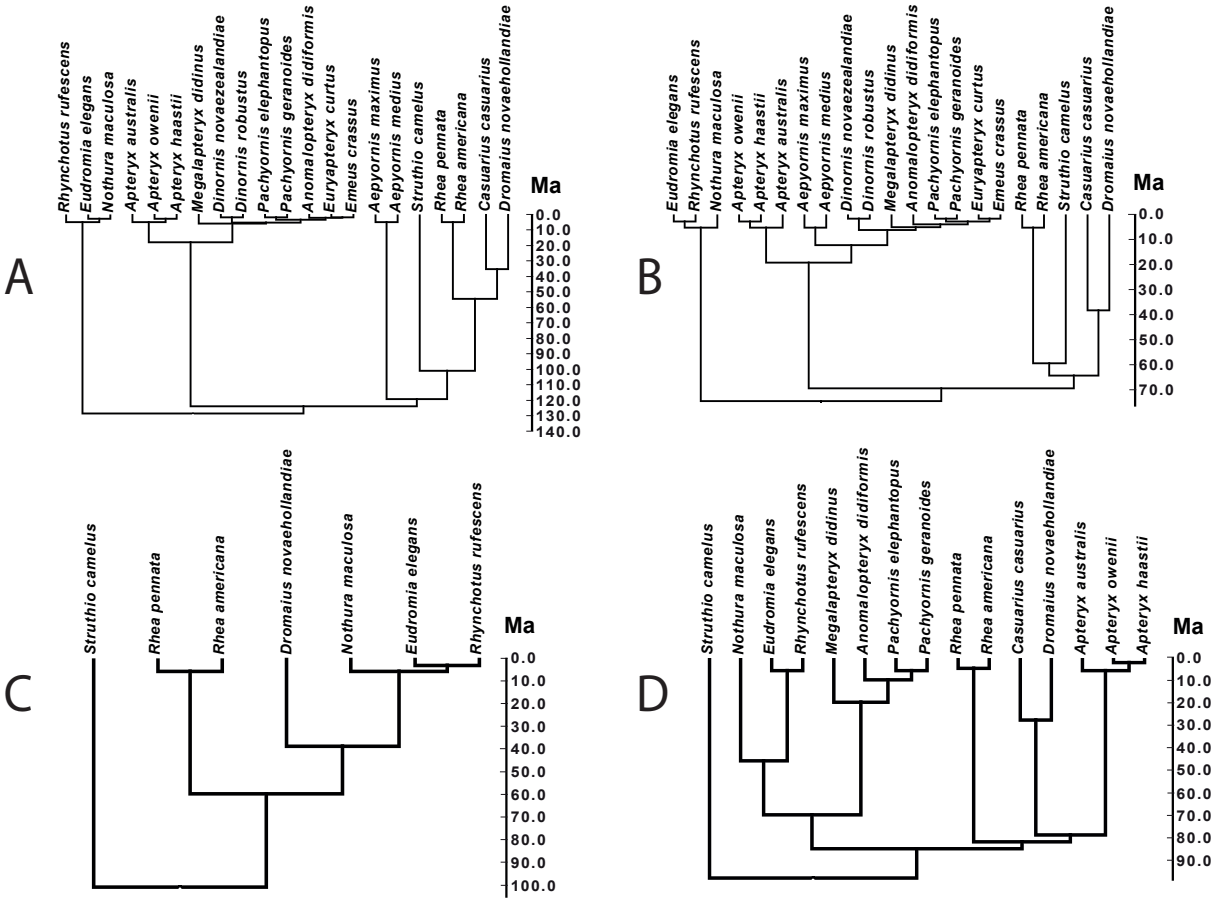

Figure 3. The four reference phylogenies used in this study, taken respectively from Bourdon *et al.*, 2009b (A), Worthy & Scofield, 2012 (B), Smith *et al.*, 2013 (C), and Haddrath & Baker, 2012 (D), figuring the species included in our taxonomic sample. For phylogenies shown in C and D, some species in our original sample were removed as they were not included in the analysis performed by the authors. Branch lengths on time scale at the right of the trees are expressed in million years (Ma).

as the most basal palaeognath. With the exception of Haddrath & Baker (2012), relationships to solve these inner nodes was compiled from Baker *et al.* (1995) and Bertelli, Giannini & Goloboff (2002).

Dating the reference phylogenies.— Our reference phylogenies were dated assuming that the minimum age for a node in the tree corresponds to the age of the oldest fossil included in it (Marjanović & Laurin, 2007). The divergence between the genera *Dromaius* and *Casuarius* has thus been dated at 38-35 Ma ago (Boles, 2001; Paton, Haddrath & Baker, 2002). The oldest known ratite, *Diogenornis*, has been referred to the Rheidae (Alvarenga,

1983; Mayr, 2009), which allowed us to estimate the divergence between Rheidae and their sister group to 59-56 Ma ago, in the Upper Palaeocene. Finally, moa remains and eggshells from the Lower Miocene (Worthy *et al.*, 2007; Tennyson *et al.*, 2010) indicate that the divergence of the moa clade from other palaeognaths is at least 19-16 Ma old.

The fossil record of other ratites groups is otherwise mostly incomplete: *Struthio coppensi*, the oldest known fossil in the genus *Struthio* (Mourer-Chauviré *et al.*, 1996), is dated from the Lower Miocene, and most fossil Apterygidae and Dinornithidae are found only in quaternary deposits (Worthy & Holdaway, 2002), although some Miocene kiwi fossils have recently been described (Worthy *et al.*, 2013). Oldest fossil tinamous are 17.5-16.5 Ma old (Bertelli & Chiappe, 2005). Some other palaeognath fossils, like *Palaeotis* (Houde & Haubold, 1987) or Lithornithidae (e.g. Houde, 1988; Leonard, Dyke & Van Tuinen, 2005), were not included in our study because of their controversial position among palaeognaths (e.g. Livezey & Zusi, 2007; Mayr, 2009; Johnston, 2011; Worthy & Scofield, 2012).

Topologies by Bourdon *et al.* (2009b) and Worthy & Scofield (2012) were dated using congruent informations taken from both the fossil record and vicariance biogeography (see Laurin *et al.*, 2012). The phylogenetic tree taken from Haddrath & Baker (2012) was already dated using a molecular clock calibrated with fossil anchor points which were used in this study, and the tree taken from Smith *et al.* (2013) was dated using the fossil record, except for the rooting that was dated using information taken from Haddrath & Baker (2012).

We could not find palaeontological or molecular data to reliably date terminal branches for some nodes. Thus, we enforced a minimal branch length of 5 Myr to both terminal branches within each ratite genus and internal branches stemming from nodes that

we were not able to date using either fossils or vicariance biogeography. This is analogous to the method proposed by Laurin, Canoville & Quilhac (2009) to deal with missing branch length data in comparative analyses.

Quantification of phylogenetic signal.— We chose four different measures commonly used to estimate phylogenetic signal in evolutionary biology and ecology – see Münkemüller *et al.* (2012) and references therein for a comprehensive review: Pagel's λ (Pagel, 1999), Abouheif's C_{mean} (Abouheif, 1999), Blomberg's K (Blomberg, Garland & Ives, 2003), and Diniz-Filho's phylogenetic eigenvector regressions (PVR; Diniz-Filho, de Sant'Ana & Bini, 1998).

The efficiency of PVR has been criticised in recent literature (Adams & Church, 2011; Freckleton, Cooper & Jetz, 2011). However, Diniz-Filho *et al.* (2012) found PVR to perform well with an appropriate phylogenetic eigenvector selection procedure, and suggested directly minimizing residual Moran's I as a powerful iterative approach; for this reason, we used this method for eigenvector selection. Although PVR was not included in the methodological review by Münkemüller *et al.* (2012), we decided to include it in this study because it was used by Cubo *et al.* (2005) and Legendre *et al.* (2013) for measuring the phylogenetic signal in osteohistological features. Including PVR in this work is thus essential to compare our estimations with the results of these previous studies.

Phylogenetic signal was estimated independently for each of the 62 histological characters, which were regressed on each of the four reference phylogenies using each of the four methods to measure signal, *i.e.* 992 estimations. All analyses were performed in R using the following functions: phylosig, from the package 'phytools' (Revell, 2012) for Pagel's λ;

phylosignal, from package ‘picante’ (Kembel *et al.*, 2010), for Blomberg’s K; abouheif.moran (method: oriAbouheif), from package ‘adephylo’ (Jombart, Balloux & Dray, 2010), for Abouheif’s C_{mean}; and PVR (method: moran), from package ‘PVR’ (Santos *et al.*, 2012), for Diniz-Filho’s PVR.

Results

An important amount of bone histological features – 27 to 32 characters out of 62, depending on the topology – do present a significant phylogenetic signal ($p < 0.05$) using at least one of the four methods (see Table 1). Among these, 5 to 16 (19 to 50%, depending on the topology) are selected by at least three of the four methods, suggesting the presence of a signal in these features.

All bone size features present a significant signal for every topology and at least three of the four methods (Table 2), which is also the case for most features related to vascular density (significant signal for at least 70% of the variables, with a congruence among estimators ≥ 50% except for the Smith *et al.* (2013) topology). These results are congruent with the findings of Cubo *et al.* (2005) and Legendre *et al.* (2013). Conversely, most features linked to osteocytes and relative proportions of vascular canals exhibit a much lower signal (≤ 60% characters selected by any method, and a congruence among estimators ≤ 40% except for cell size for both morphoanatomical topologies). Mean values, *i.e.* features created by compiling the mean of all four transects for a given section, share a much weaker signal than features measured on each individual transect (Table 2); with the exception of the Haddrath & Baker (2012) topology, the congruence among estimators for mean values is always less than half of the one observed for individual features.

	Number of variables	Number of variables presenting a significant signal for at least one phylogenetic comparative method			
		Bourdon *et al.*	Worthy & Scofield	Haddrath & Baker	Smith *et al.*
Bone size	2	2	2	2	2
Vascular density	10	8	9	8	7
Proportion of vascular canal types	30	14	12	11	12
Cell shape	10	6	5	6	3
Cell size	10	4	3	5	3
All characters, except mean values	50	27	24	26	27
All mean values	12	7	8	6	4
	Number of variables	**Number of features presenting a significant signal for at least three of the four phylogenetic comparative methods**			
		Bourdon *et al.*	Worthy & Scofield	Haddrath & Baker	Smith *et al.*
Bone size	2	2	2	2	2
Vascular density	10	5	7	4	0
Proportion of vascular canal types	30	5	4	4	3
Cell shape	10	0	1	1	0
Cell size	10	2	2	2	0
All characters, except mean values	50	13	14	10	5
All mean values	12	1	2	3	0

Table 2. Number of features considered as presenting a significant phylogenetic signal, for each category of features, plus for all characters measured on individual transects and all compiled mean values, independently (list on first column).

Overall, the amount of features selected as presenting a significant and congruent phylogenetic signal is very consistent through all four phylogenies. However, the amount of selected features is slightly weaker for the topology taken from Smith *et al.* (2013), which might be due to its reduced sample (only seven species) compared to other phylogenies that incorporate kiwi and moa species. This is particularly obvious in the case of Abouheif's C_{mean}, for which there are twice as many characters with a high signal when regressed on the two morphoanatomical topologies – the ones with the largest sample – as when regressed on the Smith *et al.* (2013) one, since Abouheif's C_{mean} is known to be strongly dependent on the structure and size of the phylogeny (Münkemüller *et al.*, 2012). Concerning methods for measuring phylogenetic signal, the number of features with a high signal is consistent through all four estimators for a given topology, with the exception of PVR, which identifies many more variables with a high signal for the two molecular phylogenies.

Finally, we identified four variables that are neither measures of bone size nor vascular density, but that nonetheless show a significant phylogenetic signal for every topology and almost every method. These variables include the cellular size measured in the caudal and medial transects of femora, and the proportion of oblique vascular canals measured in the rostral and caudal transects of tibiotarsi (Table 1).

Discussion

Phylogenetic signal in palaeognaths

We quantified phylogenetic signal in osteohistological features measured on a comprehensive palaeognath sample using various topologies and methods, in order to test the presence of a significant signal in these features, and the congruence between different topologies or different methods. Our results are congruent with previous ones (Cubo *et al.*, 2005) and show that two categories of features (*i.e.* bone size and vascular density) tend to be identified by most methods and for most phylogenies as those showing the highest phylogenetic signal. This supports the hypothesis of a high congruence between methods and, surprisingly, a relative independence between the presence of a strong signal in a feature and the topology used for the analysis. In contrast, sample size seems to have a strong influence on the identification of a character as presenting a high phylogenetic signal: topologies by Haddrath & Baker (2012) and Smith *et al.* (2013) are very similar, but the later identifies much less characters as having a significant signal than the former because of a much smaller sample size.

‘Traditional’ bone histology has mostly focused on the influence of functional constraints rather than historical constraints on the variation of qualitative histological characters over the last decades (reviews in Cubo & Laurin, 2011; Legendre *et al.*, 2013). All studies that intended to measure phylogenetic signal on osteohistological characters always found significantly better results for characters measured at the microanatomical level than at the histological one (e.g. Laurin, Girondot & Loth, 2004; Cubo *et al.*, 2005; Montes, Castanet & Cubo, 2010). Hence, even if the presence of a phylogenetic component in histological variability has been acknowledged by palaeohistologists, it is generally accepted that quantitative features measured on vascular canals and osteocytes also vary following a functional constraint. The strongest signal identified in this study was found at the macrostructural (bone size) and mesostructural (vascular density) level (*sensu* Huttenlocker, Woodward & Hall, 2013). The other four characters (proportion of oblique vascular canals in caudal and medial transects and size of osteocyte lacunae in rostral and caudal transects) with a significant and highly congruent phylogenetic signal were measured at the histological scale. The fact that mean features do present a weaker signal than features measured along transects (*i.e.* rostral, lateral, medial and caudal) indicates a potential bias in these type of variables for analysing phylogenetic signal. Hence, compiling measures from a whole histological section without distinguishing the different transects may result in the ‘mixing’ of different characters altogether by breaking the strict frame of secondary homology (*sensu* de Pinna, 1991), thus preventing the detection of a potentially high phylogenetic signal. For this reason, the procedure described in this paper for the measurement and organization of quantitative histological features is probably better than previous attempts to measure phylogenetic signal in histological characters, and should be applied to more taxa at a more inclusive level within vertebrates.

The phylogenetic comparative method in palaeohistology

The link between bone histology and phylogeny has long been a matter of controversy among palaeohistologists. Originally thought to be of great interest in the field of systematics (Queckett, 1849a, 1855), osteohistological characters have progressively become mostly used, at least among tetrapods, to study biomechanical and other functional constraints, relegating the phylogenetic information they potentially contain to a 'secondary' signal.

Studies on the bone histology of vertebrates in a phylogenetic perspective have been in constant increase over the last decade (e.g. Padian *et al.*, 2001; Padian, Horner & de Ricqlès, 2004; de Ricqlès, Castanet & Francillon-Vieillot, 2004; Cubo *et al.*, 2005, 2008, 2012; Montes *et al.*, 2007, 2010; Dumont *et al.*, 2013; Houssaye *et al.*, 2013; Houssaye, Tafforeau & Herrel, in press; Marín-Moratalla *et al.*, in press), and the dichotomy between phylogenetic and functional signals for histological features has been described as misleading (since these explanatory factors are not mutually exclusive and any feature can significantly exhibit both of them). Yet, most incursions of palaeohistologists in the field of phylogeny have consisted in optimizing these descriptive characters on phylogenies taken from the literature without further investigation on a potentially informative signal. De Ricqlès *et al.* (2008: 73), while acknowledging the presence of a significant phylogenetic signal in the bone histology of archosaurs at the microanatomical level, considered features measured at the histological level as reflecting "mostly […] autapomorphic signals" (citing the results obtained by Cubo *et al.*, 2005), and considered themselves "agnostic about whether the histological character-states that [they] tentatively used really depict apomorphic or plesiomorphic (or homoplastic) conditions at the nodes involved". In a recently published book, Padian (2013: 4) identifies the "four signals" of fossil bone histology as being ontogeny, phylogeny, mechanics, and

environment; the phylogenetic signal is described as being “persistent, but […] never the strongest signal”. Padian *et al.* (2013: 271) consider that “Separating phylogenetic signal of bone microstructure from ontogeny, biomechanics and environment will be extremely difficult, because these other signals are often directly related to phylogeny”.

The reason why qualitative, descriptive histological characters have mostly failed to reflect any significant phylogenetic signal and always been identified as being mostly influenced by autapomorphic, functional constraints, is that these characters are the result of the categorization of continuous features into discrete characters relative to bone matrix and bone tissue types, following a reference nomenclature established by Francillon-Vieillot *et al.* (1990) and de Ricqlès *et al.* (1991). These seminal works allowed a generation of palaeohistologists to provide accurate descriptions of the bone histology in major vertebrate taxa and to identify numerous characteristics of bone growth mecanisms, and brought evidence of extremely high levels of homoplasy ocurring at the histological level for discrete features. The discretisation of the variation present in vertebrate bone histology at all organization levels into unequivocal characters has been used to describe patterns of variation in entire bone sections. This may have resulted in ambiguous interpretations of some of these characters, especially because some of them have recently been considered dubious due to methodological biases for identifying some bone tissue types (Bromage *et al.*, 2003; Lee, 2013; Stein & Prondvai, 2014). For this reason, the ‘traditional’, descriptive histological nomenclature can still be regarded as a very powerful tool to describe the comparative anatomy of bone, but it is unsuitable for a precise account of the variation of bone microstructure in a phylogenetic context, and its use may have prevented previous workers from identifying all signals accounting for this variation, including the phylogenetic one. It is worth noting that the bone histological features showing a high phylogenetic signal (and

hence a potential interest in systematics) at the phylogenetic level considered in this study (palaeognaths) can show a homoplastic pattern of variation at more inclusive levels (birds, dinosaurs, archosaurs, diapsids, etc).

Phylogenetic comparative methods (PCMs, *sensu* Harvey & Pagel, 1991) include a very wide variety of techniques to incorporate the phylogenetic information in the analysis of quantitative features. The measure of phylogenetic signal itself (*sensu* Blomberg & Garland, 2002 – see also Münkemüller *et al.*, 2012) has been considerably developed since the first attempt by Felsenstein (1985) to take it into account using phylogenetically independent contrasts; the four indexes used in this paper are only a few examples inside an array of methods that are now available to describe and quantify the influence of phylogenetic constraints. In this study, the use of PCMs allowed us to find significant and congruent measures of the phylogenetic signal in osteohistological features, not only at the macrostructural level, but also at the microstructural one. This shows that the use of an exhaustive sample inside a given clade and a strict frame of homology for the measure of quantitative characters is essential to find phylogenetic information, which can be described independently from the three other signals present in bone histology and is otherwise inaccessible in this type of features. We believe that this methodology provides a new way to study bone histology in a phylogenetic context. PCMs should be consistently used in palaeohistological studies to ensure a better understanding of the often neglected, but now easily measurable, phylogenetic signal.

Acknowledgements

We thank Aurore Canoville and Andrew Lee for providing helpful comments on the manuscript, the MNHN, NHMW, LACM, and NMNH for kindly providing material for this histological study, and the Société Française de Biologie des Tissus Minéralisés (SFBTM) for allowing us to present an early version of this study at the JFBTM congress in 2011. This work was supported by the Spanish Government (CGL2011-23919 to JC), the Centre National de la Recherche Scientifique and the Université Pierre et Marie Curie (operating grant of UMR 7193 to LJL, HL, AdR and JC).

Conclusions de la première partie

- **Un signal phylogénétique significatif peut être observé pour un grand nombre de caractères ostéohistologiques, à différents niveaux de l'arbre phylogénétique des vertébrés, et pour différentes méthodes de mesure de ce signal.**

- **L'utilisation d'un échantillonnage exhaustif et d'un cadre d'homologie strict permet d'affiner ces résultats et d'identifier un signal significatif pour des caractères ostéocytaires, traditionnellement considérés comme peu informatifs.**

- **Les méthodes phylogénétiques comparatives sont un outil essentiel en histologie osseuse quantitative, et devraient être appliquées à l'ensemble des analyses comparatives au sein de cette discipline.**

PARTIE II

L’évolution de la croissance osseuse et du thermométabolisme chez les archosauromorphes

II – 1. Evidence for high bone growth rate in *Euparkeria* obtained using a new paleohistological inference model for the humerus

Lucas J. Legendre, Loïc Segalen et Jorge Cubo

Publication originale *in*: *Journal of Vertebrate Paleontology*, **33**: 1343–1350 (Novembre 2013).

Résumé

L'étude de l'évolution du taux de croissance osseuse et du taux métabolique chez les archosaures (crocodiliens, dinosaures – oiseaux compris – et ptérosaures) et leurs proches groupes-frères est devenu une préoccupation majeure au sein de la communauté des paléontologues au cours des dernières années. Dans cette étude, nous estimons le taux de croissance osseuse d'*Euparkeria* en utilisant un nouveau modèle d'inférence statistique pour l'humérus. Nous avons modifié l'échantillonnage taxonomique d'espèces existantes utilisées dans des études antérieures, sur lequel nous avons effectué des mesures quantitatives de caractères histologiques et du taux de croissance osseuse. Les valeurs du taux de croissance osseuse estimées chez *Euparkeria* sont cruciales pour comprendre la condition ancestrale chez les archosaures, car ce taxon est considéré comme l'un des plus proches parents du crown group des archosaures. Nous avons obtenu un taux de croissance osseuse instantané de 6,12 µm/jour, ce qui suggère qu'*Euparkeria* partageait avec d'autres archosauromorphes non-archosaures (*Prolacerta*, *Proterosuchus* et *Erythrosuchus*) un taux de croissance élevé compatible avec un métabolisme endotherme. Cet état dérivé pourrait avoir été hérité par certains pseudosuchiens du Trias, comme le suggère le taux de croissance osseuse instantané élevé (14,52 µm/jour) estimé dans cette étude chez *Postosuchus*. Les pseudosuchiens du Jurassique pourraient avoir perdu l'endothermie lors de la transition d'habitats terrestres et d'une prédation active vers des habitats aquatiques et des comportements de prédation de type embuscade, de telle sorte que les crocodiliens du Crétacé seraient des ectothermes secondaires, ce qui est suggéré par les valeurs de $\delta^{18}O$. En conclusion, nous apportons de nouveaux résultats en faveur de l'hypothèse d'un état ancestral endotherme chez le dernier ancêtre commun des archosaures, et considérons que les archosauromorphes non-archosaures et les pseudosuchiens du Trias pourraient avoir présenté un thermométabolisme plus proche de celui des dinosaures que de celui des lépidosauriens ou des tortues.

Abstract
The study of bone growth rate and metabolic rate evolution in archosaurs (crocodiles, dinosaurs including birds, and pterosaurs) and close outgroups has become a subject of major interest among paleontologists in recent years. In this paper, we estimate the bone growth rate of *Euparkeria* using a new statistical inference model for the humerus. We modified the taxonomic range of extant species used in previous studies, on which we performed quantitative measurements of histological features and bone growth rates. Bone growth rate values estimated for *Euparkeria* are crucial in understanding the ancestral condition for archosaurs because this taxon is considered one of the closest relatives to the archosaur crown-group. We obtained an instantaneous growth rate of 6.12 μm/day, suggesting that *Euparkeria* shared with other non-archosaurian archosauromorphs (*Prolacerta*, *Proterosuchus* and *Erythrosuchus*) a condition of high growth rate compatible with endothermy. This derived state may have been inherited by some Triassic pseudosuchians, as suggested by the high instantaneous bone growth rate (14.52 μm/day) estimated in this study for *Postosuchus*. Jurassic pseudosuchians may have lost endothermy during the transition from terrestrial habitats and active predation to aquatic habitats and sit-and-wait predation behaviors, so that Cretaceous crocodiles may be secondarily ectotherms, as suggested by $\delta^{18}O$ values. In conclusion, we provide new evidence for the hypothesis of an ancestral endothermic state for the last common ancestor of archosaurs, and predict that non-archosaurian archosauromorphs and Triassic pseudosuchians may have been characterized by a thermometabolism more similar to that of dinosaurs than to that of lepidosaurs and turtles.

Introduction

The evolution of thermometabolism in archosaurs has been a matter of debate among paleontologists and evolutionary biologists for decades. Since Ostrom (1969, 1974) described the osteology of *Deinonychus* and *Archaeopteryx* and discovered evidence for a dinosaurian origin of birds, considerations on bone histological features have proved to be crucial in determining whether fossil archosaurs, and dinosaurs in particular, had an ectothermic or an endothermic thermometabolic condition. Numerous studies on thermoregulatory physiology of dinosaurs found evidence for endothermy in the 1970s, most notably those of Bakker (1972, 1974), but these results were highly criticized because they were based only on

qualitative observations of global similarities between birds and dinosaurs, or on unreliable features such as brain size or erect stance (see Benton, 1979, for a full review of arguments pro/against endothermy in dinosaurs). Moreover, these studies lack analyses of evolutionary patterns, because they were published before the rise of cladistics in paleontology (Cracraft, 1981).

Recent investigations on physiological (Farmer & Sanders, 2010), anatomical (Summers, 2005), bone histological (Tumarkin-Deratzian, 2007), and developmental (Seymour *et al.*, 2004) features support the evolutionary hypothesis according to which the last common ancestor of archosaurs was endothermic and living crocodiles have reverted to an ectothermic state. Paleontological studies are needed to constrain the temporal and phylogenetic frameworks of the origin of endothermy in archosauromorphs, and its loss in pseudosuchians (*i.e*. taxa more closely related to crocodiles than to birds inside archosauria). It has experimentally been shown that bone tissue contains a metabolic signal: resting metabolic rate is related to bone growth rate, which, in turn, is related to bone histology (Montes *et al.*, 2007, 2010). Thus, the analysis of bone histology of extinct archosaurs and closely related taxa may prove useful in understanding the origin and evolution of endothermy in archosauromorphs. A series of recent paleohistological studies has allowed the reconstruction of evolutionary patterns of bone growth rates and metabolic rates in non-archosaurian archosauromorphs (comprehensive review in Botha-Brink & Smith, 2011). Among these taxa, *Euparkeria* is generally considered as the closest known relative to the archosaur crown-group (Nesbitt *et al.*, 2009; Nesbitt, 2011; *contra* Dilkes & Sues, 2009). Thus, estimating the bone growth rate of this taxon is crucial for the estimation of the ancestral state of archosaurs. An objective of the present paper is to estimate the bone growth rate of *Euparkeria* using the approach developed by Cubo *et al.* (2012), who performed

quantitative measurements of histological features and experimental quantifications of bone growth rates on a sample of extant species of amniotes and compiled a predictive equation that enabled them to estimate the instantaneous bone growth rates for extinct species. Cubo *et al.* (2012) computed predictive models on the basis of three long bones: the femur, humerus, and tibia. Cross-validation tests revealed that although the femoral equation performed well, the two other models were not statistically significant and therefore growth rates of the humeri and tibiae could not be estimated based on their fossil sample. Modification of the original sample of extant taxa with the addition of new species is likely to improve the significance and predictive power of these models. Thus, we attempt to build new predictive equations for the humerus and tibia by modifying the taxonomic sample of extant amniote species used by Cubo *et al.* (2012). Finally, we discuss the congruence between our results and published data obtained using the oxygen isotope proxy to infer the thermometabolic status of extinct vertebrates (e.g. Barrick, Showers & Fischer, 1996; Fricke & Rogers, 2000; Amiot *et al.*, 2006).

Material and methods

Material

We used the 52 specimens belonging to 16 species of extant amniotes already sampled in Cubo *et al.* (2012), with the addition of eight new specimens belonging to two species of extant birds: the chicken *Gallus gallus* and the king penguin *Aptenodytes patagonicus*. The penguin specimens were previously used by de Margerie *et al.* (2004) and the chicken specimens by Montes *et al.* (2007) to estimate the relationship between bone microstructure and bone growth rate, and between bone growth rate, body mass and metabolic rate,

respectively. These species were added to improve the significance of our predictive models for the two bones included in this study, *i.e.* the humerus and tibia.

Our predictive models were used to estimate bone growth rates in the following extinct diapsids: *Euparkeria capensis* SAM-PK-7868 (stylopod, *i.e.* either humerus or femur; originally indexed in de Ricqlès *et al.* (2008) as SAM 7868) among non-archosaurian archosauromorphs; *Postosuchus kirkpatricki* UCMP 28353 (humerus) within pseudosuchians; and *Lesothosaurus diagnosticus* MNHN IG27 (tibia), *Maiasaura peeblesorum* MOR 005 (tibia), *Coelophysis bauri* AMNH 27435 (tibia), *Allosaurus fragilis* UUVP 154 (tibia), *Thecodontosaurus antiquus* YPM 2192 (tibia) and *Lourinhanosaurus antunesi* (tibia) among ornithodirans. *Postosuchus*, *Maiasaura*, *Coelophysis* and *Allosaurus* were sampled, and their histological features measured, in Cubo *et al.* (2012). *Euparkeria* and *Lesothosaurus* specimens were previously described by de Ricqlès *et al.* (2008), *Thecodontosaurus* by Benton *et al.* (2000), and *Lourinhanosaurus* by de Ricqlès *et al.* (2001) and were analyzed quantitatively in this study. High-resolution histological images (M153039 and M153041) of the *Euparkeria* specimen are archived as Project 880 in Morphobank (http://www.morphobank.org/index.php).

Phylogenetic information was taken from Cubo *et al.* (2012) for all taxa with the following exceptions. The *Coelophysis* stratigraphic range spreads from the early Norian to the late Rhaetian (Spielmann *et al.*, 2007). *Euparkeria* is considered the closest relative to crown group Archosauria (Gower & Weber, 1998; Nesbitt, 2011) and dates from the Anisian onward (Rubidge, 2005). As a basal sauropodomorph dinosaur, *Thecodontosaurus* is sister group to all theropod dinosaurs (including birds) in our tree; specimens were found in the fissure deposits of Durdham Down in Bristol, UK, dated from the Rhaetian (Whiteside &

Marshall, 2008). *Lourinhanosaurus* is an allosauroid theropod (Mateus, 1998) from the Lourinhã Formation (Kimmeridgian–Tithonian) in Portugal (Antunes & Mateus, 2003; Mateus *et al.*, 2006). Divergence times for *Gallus* and *Aptenodytes*, as for extant bird species already used by Cubo *et al.* (2012), were taken from Pyron (2010).

Both bone growth rates and bone tissue types undergo ontogenetic variation, which is why we incorporated ontogenetic control into our comparative analyses. We always measured bone growth rate in regions formed during the phase of sustained high growth rate (*i.e.* after the end of the acceleration phase, and before the beginning of the deceleration phase, both phases being easily identifiable on the bone sections we used). We selected these regions by assuming that bone tissues formed before and after the selected region are histologically similar and were formed at the same rate as bone tissue of the selected region.

Variables

Periosteal bone growth rate. This is the dependent variable that is to be estimated in extinct species. Bone growth rate was quantified in extant species using in vivo fluorescent labeling (Montes *et al.*, 2007). The histological thin sections were observed under ultraviolet light (Zeiss Axiovert 35; Jena, Germany) and digitally imaged (Olympus, Japan). The highest density across the fluorescent label was used as the endpoint of the fluorescent mark. We measured bone growth rates in μm/day using the image analysis software ImageJ (Schneider, Rasband & Eliceiri, 2012) as the distance (in μm) between two consecutive fluorescent labels, or between the last label and the bone periphery, divided by the elapsed time (days). This distance was measured as the difference between the radius of the external circle (delimited

by either the external label or the bone periphery) and the radius of the internal one (delimited by the internal label) for each bone section.

Vascular orientation. Blood vessels in the bones were lost during sample preparation in extant taxa, and during the fossilization process in extinct taxa. Thus, this variable measures the orientation of the vascular canals, *i.e.* the cavities that had contained the blood vessels and associated connective tissues during life. We determined the orientation of vascular canals by inserting the largest ellipse into each vascular cavity using Image J. When a conspicuous anastomosis was observed between two cavities, each cavity was measured independently. To improve repeatability, the orientation of each vascular cavity was measured using the radial index (*sensu* de Boef & Larsson, 2007). The orientation of these cavities was computed as the angle between the major axis of each ellipse and a vector tangent to bone periphery; thus, vascular canals extending parallel to the bone periphery have angles approaching 0° and those extending parallel to the radius of the bone cross-section have angles approaching 90° (de Boef & Larsson, 2007). Vascular canal orientation is a continuously varying trait; to incorporate this trait in our character matrix, we categorized this continuous variation into three orientation classes (see Table 1). These types of standard vascular canal orientation were defined in our transverse sections as follows: circular canals (C), which run roughly parallel to the bone periphery (0° + 22.5°; 180° – 22.5°); radial canals (R), which run roughly orthogonal to the bone periphery (90° ± 22.5°); and oblique canals (O), *i.e.* those canals excluded from the intervals corresponding to radial canals and to circular ones (see de Margerie, Cubo & Castanet, 2002; de Margerie *et al.*, 2004; de Boef & Larsson, 2007). Thus, we used three variables to describe the major vascular orientations found on each bone section: proportion of circular canals (C/[C+R+O]), proportion of radial canals (R/[C+R+O]), and proportion of oblique canals (O/[C+R+O]). In avascular bones, the proportions of circular, radial and oblique canals were considered as zero.

Table 1. Measured values for all seven osteohistological features, on humeri obtained from new specimens sampled for this study. For other specimens in the humeri sample, see supplementary material of Cubo *et al.* (2012) deposited at Dryad: doi:10.5061/dryad.j2m25n82/

Histological features	Species	Mean values for each specie	n
Cell density (osteocyte/μm^2)	*Gallus gallus*	0.002	3
	Aptenodytes patagonicus	0.002	4
	Euparkeria capensis	0.002	1
	Postosuchus kirkpatricki	0.001	1
Cell size (μm^2)	*Gallus gallus*	31.21	3
	Aptenodytes patagonicus	43.35	4
	Euparkeria capensis	54.9	1
	Postosuchus kirkpatricki	20.71	1
Cell shape	*Gallus gallus*	0.469	3
	Aptenodytes patagonicus	0.547	4
	Euparkeria capensis	0.46	1
	Postosuchus kirkpatricki	0.519	1
Radial index	*Gallus gallus*	0.106	3
	Aptenodytes patagonicus	0.294	4
	Euparkeria capensis	0.158	1
	Postosuchus kirkpatricki	0.067	1
Oblique index	*Gallus gallus*	0.386	3
	Aptenodytes patagonicus	0.427	4
	Euparkeria capensis	0.292	1
	Postosuchus kirkpatricki	0.3	1
Circular index	*Gallus gallus*	0.508	3
	Aptenodytes patagonicus	0.28	4
	Euparkeria capensis	0.55	1
	Postosuchus kirkpatricki	0.633	1
Vascular density (canals/mm^2)	*Gallus gallus*	143.4	3
	Aptenodytes patagonicus	49.3	4
	Euparkeria capensis	43.94	1
	Postosuchus kirkpatricki	0.0001	1

Vascular density. Vascular density was measured by Cubo *et al.* (2005) as the ratio of total vascular canal area to primary bone area; here we measured the number of canals divided by mm^2 because the osteons are not yet entirelly filled in our sample of extant species. As for vascular orientation, branching cavities were considered as two different entities rather than as a single vascular canal. Sections showing a single vascular canal were considered to be avascular, because this single vascular canal most probably corresponds to a Volkmann canal (*i.e.* a blood vessel running from the periosteum to the endosteum).

Cellular variables. Cellular shape, size and density were carefully measured both in extant and extinct taxa. As for vascular canals, we measured the shape, size, and density of cavities (osteocyte lacunae) that contained bone cells (the osteocytes). Where possible in extant species (*i.e.* where the bone section contained enough osteocyte lacunae), we measured 30 osteocyte lacunae for each of the four main transects we defined on our sections (rostral, lateral, medial and caudal), *i.e.* 120 osteocyte lacunae per bone section.

Cellular shape was quantified as the ratio between the minor and the major axes of these cavities ($0 < \text{cellular shape} \leq 1$). A value of 1 means that the lacuna is perfectly circular.

Cellular size was computed using the major (M) and minor (m) axes of the osteocyte lacuna and assuming its geometry as that of an ellipse ($\pi \times M/2 \times m/2$).

Cellular density was quantified as the number of lacunae divided by the surface in μm^2.

We performed all measurements using a microscope focused on a single layer of osteocyte lacunae. Thus, the measurements refer to this single layer of osteocyte lacunae whatever the thickness of the ground section. Cellular density was computed including all osteocyte lacunae of the quoted single layer. To ensure that cell lacunae were measured near their mid axis, only the largest osteocyte lacunae included in this layer were measured to compute cell size and shape (Organ *et al.*, 2011).

Phylogenetic Comparative Methods

Constructing paleobiological models of bone growth rate estimation. The paleobiological growth rate inference models were constructed using multiple linear regression tested for significance using permutations (Legendre *et al.*, 1994) using the

computer program Permute! version 3.4 alpha 9 (Casgrain, 2009). We obtained a standardized coefficient for each variable (a'), which was unstandardized into a raw coefficient (a) by using the expression:

$$a_1 = a'_1 * (s_Y / s_{X1})$$

where s_Y is the standard deviation of the dependent variable and s_{X1} is the standard deviation of the independent variable under analysis. The intercept was computed using the following equation:

$$b = Y_{mean} - a_1 * X_{1\,mean} - a_2 * X_{2\,mean} - \ldots a_n * X_{n\,mean}$$

The dependent variable (to be estimated in extinct taxa) was bone growth rate. As independent variables, we used all histological features. The multiple regression method takes into account the redundancy of information, called colinearity, among independent variables. Using redundant variables may inflate the coefficient of determination (R^2). However, contrary to studies of variation partitioning (Cubo *et al.*, 2008), here we are not concerned with R^2, the only statistical parameter of interest for our study being the P-value of the cross-validation test (see below).

Computing confidence intervals for bone growth rate estimations in fossils. Each extinct taxon of our sample was transformed into a node by splitting it into two sister taxa of standardized branch lengths of 2 Ma. Values of the two newly created terminal taxa were empirically modified in order to obtain, at the newly created node occupying the phylogenetic position of our extinct taxon, the bone growth rate estimated for this extinct taxon. A 95% confidence interval was then computed for each extinct taxon following the method of Laurin

(2004) for nodes other than the root node, using the PDAP module in Mesquite (Midford, Garland Jr. & Maddison, 2003).

Cross-validation tests. In regression analysis, any equation will fit better on the data set used to create it than on a new data set. This effect is known as shrinkage. In our study, predictive equations were optimized for the samples used to create them, which prevented them from performing as well in other samples (e.g. for estimating bone growth rate in our sample of extinct taxa). Thus cross-validation tests were necessary to determine whether we can be confident in the reliability of our models or not. We compiled 16 subsamples for each bone, each of them including every species in the sample but one. For each subsample, a predictive regression (of bone growth rate) was computed and used to estimate predicted scores for the species not included in the subsample. Then, the predicted bone growth rates (obtained using the 16 predictive equations) were correlated with observed scores (experimentally measured growth rates). This method (leave-one-out cross validation) provides a significant improvement compared with that used by Cubo *et al.* (2012), who performed cross-validation tests by splitting the sample of each bone into two arbitrary subsamples, the first one to compute an inference model, the other one to perform bone growth rate estimations, to be correlated with bone growth rate empirical measurements (2-fold cross-validation). Leave-one-out cross-validation performs better because it avoids this arbitrary split of the sample and, on the other hand, allows us to work with larger sample sizes.

Results

Humerus and tibia predictive equations obtained with all species of the sample were significant (humerus: $R^2 = 0.814$, $p = 0.013$; tibia: $R^2 = 0.755$, $p = 0.022$; tested computing 9999 permutations), when tested with all the data.

Cross-validation tests showed that the correlation between predicted growth rates and observed scores were not significant. For the humerus, however, we observed that both subsamples obtained from removing respectively one or the other ratite species (*i.e. Struthio camelus* and *Dromaius novaehollandiae*) showed much more significant predictive equations ($p < 0.01$) than other subsamples. In fact, the transverse diameters of the humeri of *Struthio camelus* and *Dromaius novaehollandiae* are placed below the regression line in a sample of flightless birds (Cubo & Casinos, 1997). This means that the humeri of these birds have smaller diameters than expected for their body masses (compared with other flightless birds also characterized by having smaller wing bones than flying birds). This is probably the outcome of a heterochronic mechanism of either earlier cessation or slower growth rate, which, by modifying bone histology, would disrupt the relationship between bone growth rate and histological features. The inclusion of “outliers” in the sample (species with a very derived morphology, e.g. ratites characterized by paedomorphic forelimbs and peramorphic hindlimbs in which the functional relationship between bone growth rate and bone histology has been disrupted by heterochronic mechanisms) decreases the coefficient of determination (describing how well the predictive equation fits the set of data from which it was derived) as well as the explanatory and predictive power of the equation. Thus we removed both ratite species from our sample and compiled a new equation for the humerus. The king penguin also has a very derived condition, but in this case the functional relationship between bone growth rate and bone histology (on which the predictive model is based) was not disrupted.

Summarizing, the significance of the model does not exclusively rely on the sample size but also on the choice of relevant species characterized by a strong functional relationship between their bone growth rate and bone histology.

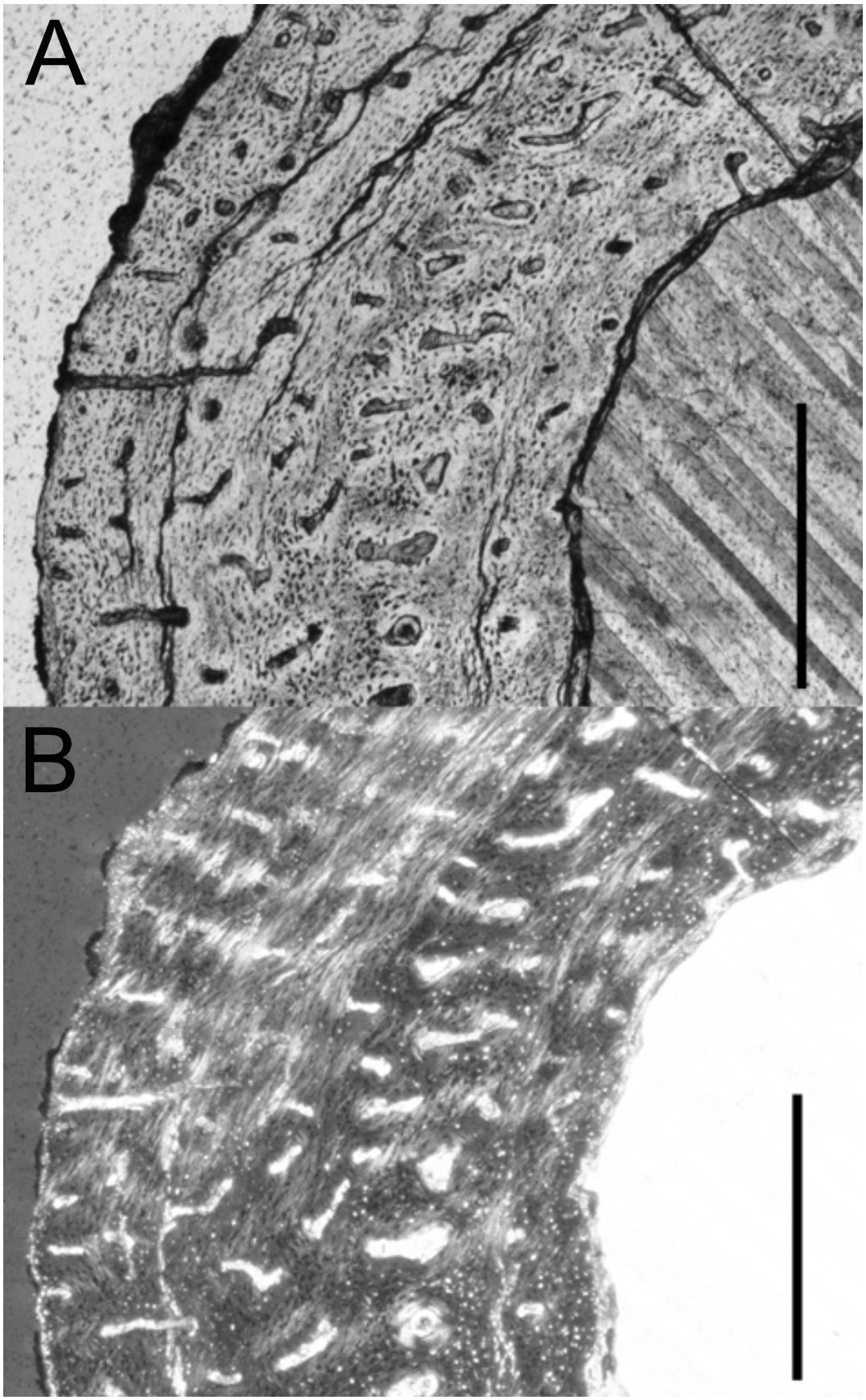

Figure 1. Humeral cross-section of *Euparkeria* (SAM-PK-7868) in ordinary (**A**) and polarized (**B**) lights. Both scale bars equal 0.5 mm.

New predictive equations were computed for the humerus and tibia using the quoted subsample (excluding ratites). The corresponding cross-validation tests show that although the humeus model was significant (p = 0.032; tested computing 9999 permutations), the tibia model was still non-significant. Hence this last model will be excluded from the following analyses and discussion. For the humerus, we obtained the following predictive model (R^2 = 0.896, p = 0.003) tested computing 9999 permutations (the b coefficients and the intercepts are not standardized):

Humeral growth rate = -97.9159 + 0.8420 x Vascular density + 15252.3752 x Cellular density + 109.3471 x Cellular shape + 1.3826 x Cellular size – 167.3197 x Proportion of circular canals + 0.6198 x Proportion of oblique canals – 34.1275 x Proportion of radial canals

We quantified all the histological variables in our fossil samples (Figs. 1, 2), applied the humeral predictive equation to them, and obtained the following bone growth rate estimations and 95% confidence intervals: *Euparkeria* SAM-PK-7868: 6.12 µm / day (0 – 15.68 µm / day); *Postosuchus* UCMP 28353: 14.52 µm / day (4.93 – 24.11 µm / day).

According to de Ricqlès *et al.* (2008), *Euparkeria* SAM-PK-7868 is an undertermined stylopod, and potentially either a femur or a humerus. Without a proper identification for this sample, the bone growth rate estimation performed above may be irrelevant. Some evidence suggesting that the stylopod SAM-PK-7868 is a humerus was obtained from analysis of the k index variation: SAM-PK-7868 has a k index (k = 0.435) closer to that of the humerus SAM-PK-13666 (k = 0.44) than to the mean k indices of femora SAM-PK-K10010 (k = 0.73) and SAM-PK-K10548 (k = 0.53) published by Botha-Brink & Smith (2011). Definitive evidence

in favor of stylopd SAM-PK-7868 being a humerus was obtained from bone size and ontogenetic stage. J. Botha-Brink (pers. comm.) provided digital images of complete sections of *Euparkeria* samples, so that we were able to compare the size of these sections with that of our stylopod. The cross-sectional area of our presumed humerus SAM-PK-7868 (14.15 mm^2) is similar to that of the confirmed humerus SAM-PK-13666 (12.20 mm^2), and less than half of the cross-sectional area of the femora SAM-PK-K10010 (30.26 mm^2) and SAM-PK-K10548 (33.74 mm^2). Two hypotheses have to be analyzed: the stylopod SAM-PK-7868 is either a < 50% adult-sized femur or an adult-sized humerus. Considering that Ewer (1965) suggested that all *Euparkeria* specimens were approximately of the same ontogenetic stage (subadults or adults), and that the outer layer of SAM-PK-7868 cortex has lower vascular density than deeper layers (Fig. 3), we conclude that this specimen undoubtedly corresponds to an adult-sized humerus. The presence of the deltopectoral crest on the plane of section may indicate that this section is not entirely diaphyseal but rather metaphyseal (two complete cross-sections were uploaded into Morphobank: one from which the histological measuments were performed [M153043] and other that was used to compute bone size [M153044]; http://www.morphobank.org/index.php/Projects/ProjectOverview/project_id/880).

Discussion

Evolution of Growth Patterns and Metabolic Rates in Archosauromorpha

The evolution of bone growth rates and metabolic rates in Archosauromorpha is a subject of major interest among paleontologists. Gross (1934) discovered fibrolamellar bone tissue (*i.e.* formed at high growth rate and compatible with a high metabolic rate) in *Erythrosuchus* – one of the most basal archosauriformes. This result, confirmed by de Ricqlès

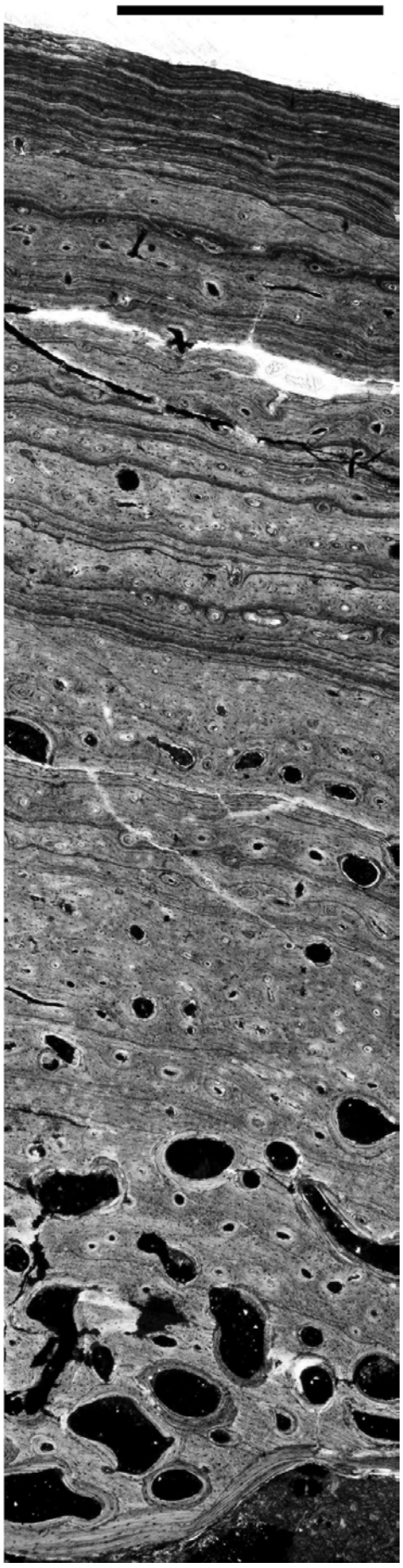

(1976), attracted the attention of many paleontologists towards non-archosaurian archosauromorphs as key taxa to understand the thermometabolism of the last common ancestor of archosaurs (e.g. de Ricqlès *et al.*, 2008; Nesbitt *et al.*, 2009; Botha-Brink & Smith, 2011; Werning *et al.*, 2011). Among these contributions, that by Botha-Brink and Smith (2011) is particularly relevant because these authors performed for the first time bone growth rate estimations in non-archosaurian archosauromorphs. Their estimates are the most conservative possible values because they were computed by measuring the amount of cortex deposited between two successive growth rings (assuming that a growth ring is deposited annually), divided by 380 days of a Triassic year (Botha-Brink and Smith, 2011). Considering that these taxa may have grown for only 6 months (*i.e.* spring and summer), the growth rate estimates would in fact double (J. Botha-Brink, pers. comm.). Moreover,

Figure 3. Humeral cross-section of *Postosuchus* (UCMP 28353) in ordinary light. Scale bar equals 0.5 mm.

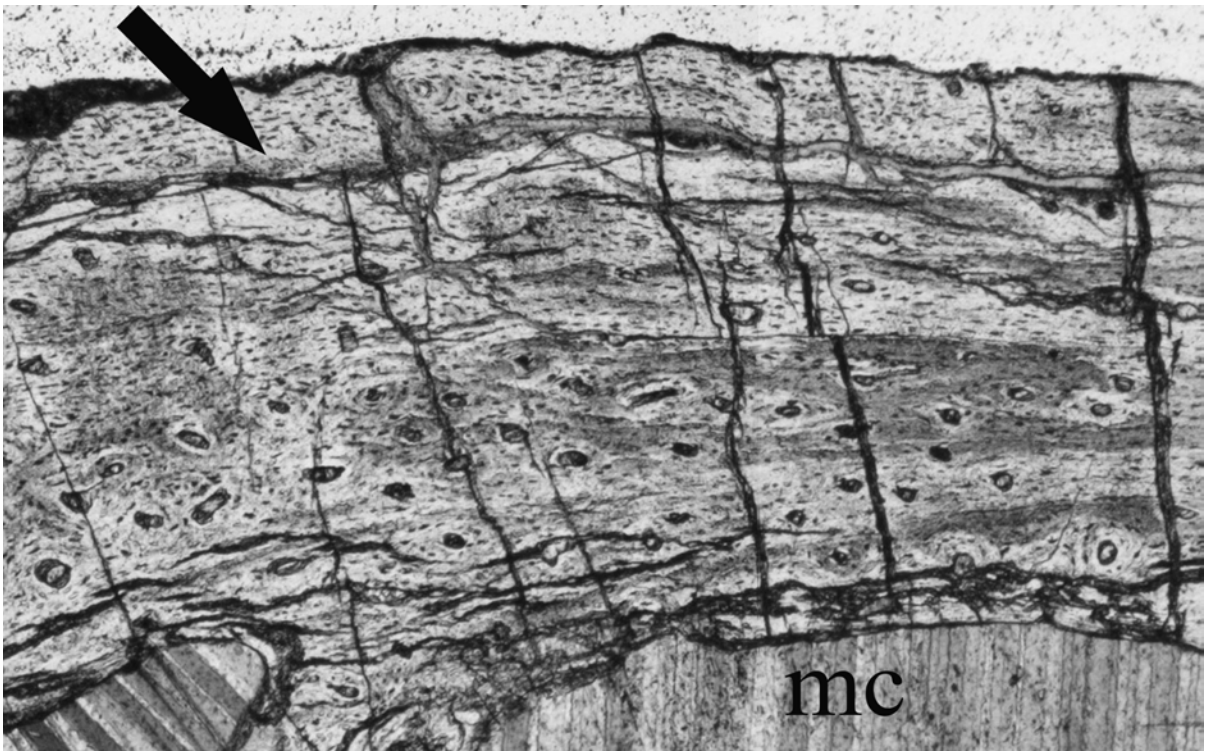

Figure 4. Humeral cross-section of *Euparkeria* (SAM-PK-7868) in ordinary light. Black arrow: peripheral parallel-fibered bone tissue. **Abbreviations**: **mc**, medullary cavity.

these values are also averaged using all analyzed skeletal elements, *i.e.* certain elements may have grown more quickly than others. As an outcome of this interest on non-archosaurian archosauromorphs, we now have a larger picture of evolutionary patterns of bone tissue and associated growth rates in these taxa. These are (from taxa more distantly related to to taxa more closely related to Archosauria) as follows (Fig. 4):

Trilophosaurus (Werning & Irmis, 2011; observations performed on femora, humeri, tibiae and ulnae) and Rhynchosauria (de Ricqlès *et al.,* 2008; observations made on ribs) may have retained the primitive condition that characterizes lepidosaurs, with lamellar-zonal bone tissue formed at very slow growth rates.

Prolacerta, Proterosuchus and *Erythrosuchus* grew at rates of, respectively, 2.1 – 4.2 µm/day, 11.3 – 22.6 µm/day, and 21 - 42 µm/day and shared the derived capacity of forming fibrolamellar bone tissue (Botha-Brink & Smith, 2011). These estimations were performed on

tibiae, femora, and fibulae in *Prolacerta* and *Proterosuchus,* and on ribs, a tibia, and a radius in *Erythrosuchus,* assuming either a growth period of 380 days by Triassic year or a growth period restricted to the spring and summer (Botha-Brink & Smith, 2011). The juvenile *Proterosuchus* femur and tibia show a radial bone tissue pattern, with vascular canals arranged perpendicular to the periosteum and no growth rings or annuli (Botha-Brink & Smith, 2011). Extant bone tissue patterns of this type have been found in the chicken by Montes *et al.* (2007), with an associated instantaneous bone growth rate of 47.01 μm/day for the tibiotarsus, and in the king penguin by de Margerie *et al.* (2004), with an instantaneous bone growth rate interval of roughly 50 – 165 μm/day in the humerus. *Erythrosuchus* possesses a dense reticular pattern in the tibia, which has also been found in the tibiotarsi of emus and ostriches by Castanet *et al.* (2000), with associated instantaneous bone growth rates of 30.1 and 35.8 – 42 μm/day, respectively. Although it is highly unlikely that *Proterosuchus* and *Erythrosuchus* grew at rates as high as those characterizing the quoted bird species, the presence of radial and reticular bone tissue suggest that they showed higher bone growth rates than those estimated for more basal archosauromorphs.

Vancleavea shows a reversion to the primitive condition, and is characterized by lamellar-zonal bone tissue formed at very slow growth rates (Nesbitt *et al.*, 2009; observations performed on a femur).

Chanaresuchus is characterized by early rapid growth, as suggested by the inner region of the bone cortex formed by fibrolamellar bone tissue (de Ricqlès *et al.*, 2008; observations made on an undetermined long bone).

Euparkeria, the closest sister group to archosaurs (Nesbitt *et al.*, 2009; Nesbitt, 2011), is characterized by the presence in femur, humerus, tibia, and fibula of parallel-fibered bone tissue formed at bone growth rates of 1.4 - 2.8 μm/day assuming either a growth period of 380

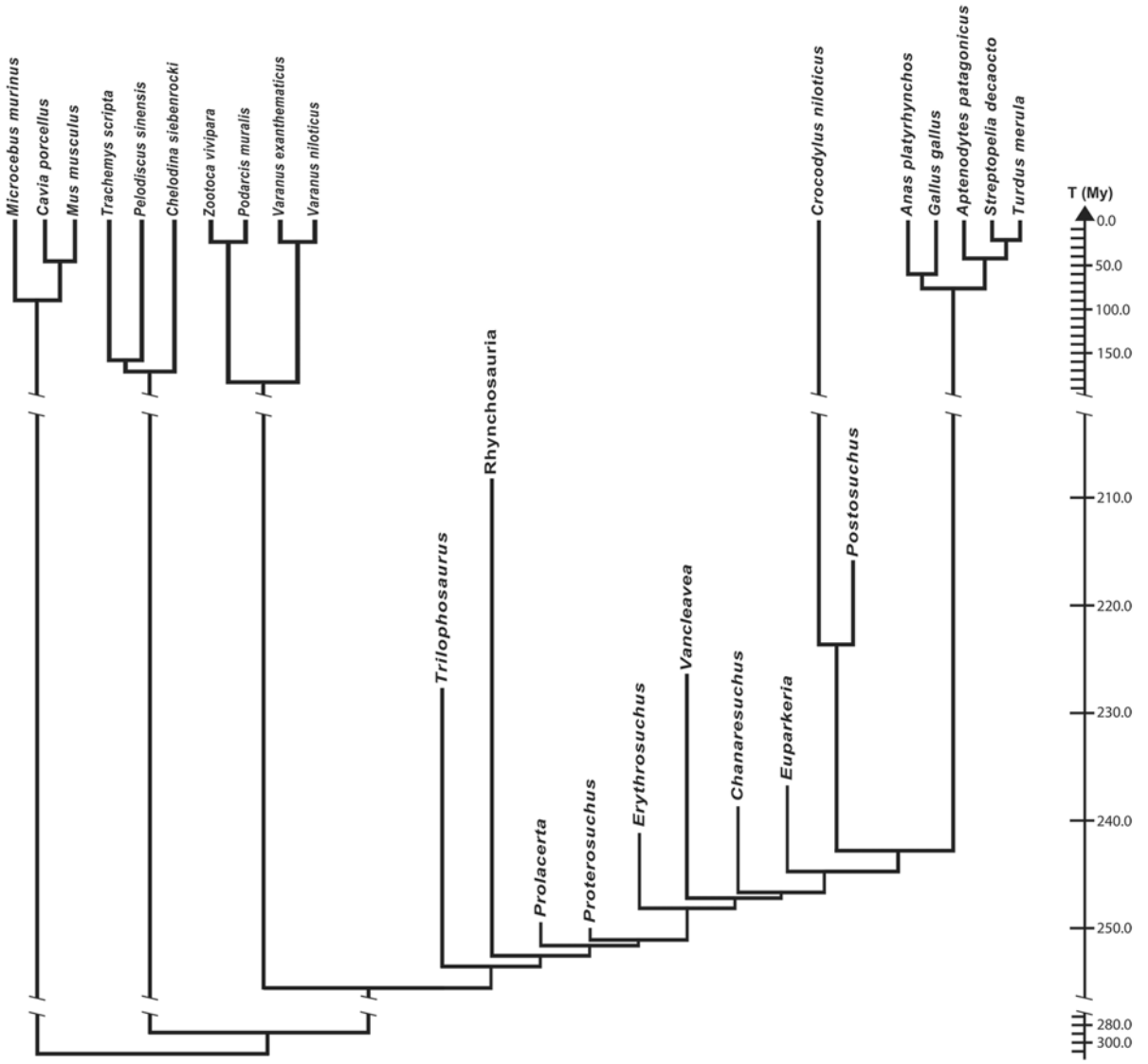

Figure 1. Phylogenetic relationships of taxa analysed or discussed in the text, taken from Botha-Brink & Smith (2011) and Cubo *et al.* (2012). Timescale in million years.

days by Triassic year or a growth period restricted to the spring and summer (Botha-Brink & Smith, 2011).

Summarizing, *Trilophosaurus* and Rhynchosauria may have retained the primitive condition (lamellar-zonal bone tissue formed at very slow growth rates) and the last common ancestor of *Prolacerta* and birds may have acquired the derived condition (fibrolamellar bone tissue formed at high to very high growth rates). Within this last clade, *Vancleavea* may have undergone a reversion to the primitive condition (lamellar bone tissue; Nesbitt et al., 2009).

We constructed a new paleohistological model of bone growth rate inference for the humerus using an improved procedure (compared to that used by Cubo *et al.*, 2012 – see above) and used it notably to estimate the bone growth rate of the *Euparkeria* humerus based on SAM-PK-7868 (see above). We obtained an estimated growth rate value of 6.12 μm/day, the 95% confidence interval of which (0 – 15.68 μm / day) includes the prediction made by J. Botha-Brink (pers. comm.) for humerus SAM-PK-13666 of 1.98 – 3.97 μm/day (lower value obtained assuming a growth period of 380 days by Triassic year, higher value obtained assuming a growth period restricted to a 6-months period). Our bone growth rate estimate is congruent with the presence of an extensive fibrolamellar complex in humerus SAM-PK-7868 (Fig. 1; see also the histological description of this specimen by de Ricqlès *et al.*, 2008). The formation of fibrolamellar bone during the phase of sustained high growth rate may be an apomorphic feature shared by *Prolacerta, Proterosuchus, Erythrosuchus, Chanaresuchus, Euparkeria*, and the last common ancestor of archosaurs. In this phylogenetic context, the last common ancestor of archosaurs may have been characterized by high growth rates and high metabolic rates compatible with endothermy. This derived state may have been inherited by ornithodirans (pterosaurs and dinosaurs including birds) and by Triassic pseudosuchians (taxa more closely related to crocodiles than to birds), as previously suggested by de Ricqlès *et al.* (2008), Botha-Brink & Smith (2011), and Werning *et al.* (2011). Within this last group, we inferred an instantaneous bone growth rate of 14.52 μm/day for the humerus of *Postosuchus* (Fig. 2), a taxon that was able to form densely vascularized fibrolamellar bone tissue (de Ricqlès, Padian & Horner, 2003). Pseudosuchians may have lost endothermy during the transition in the Jurassic from a terrestrial habitat and active predation to an aquatic habitat and a sit-and-wait predation behavior, resulting in extant crocodiles becoming secondarily ectothermic (Seymour *et al.*, 2004).

Do Isotopic Analyses suggest that Crocodiles are Secondarily Ectothermic?

The analysis of the oxygen isotopic composition of phosphate in biogenic apatite (bone, teeth) has been used to estimate the ectothermic or endothermic status of extinct vertebrates (e.g. Barrick *et al.*, 1996; Fricke & Rogers, 2000; Amiot *et al.*, 2006). Considering that oxygen isotope fractionation between PO_4 and body water is thermally dependant (Longinelli & Nuti, 1973), several studies have shown that for animals living in the same biota and having the same water strategies (obligate or non-obligate drinkers), the $\delta^{18}O_{PO4}$ values are expected to be different between endotherms and ectotherms (Amiot *et al.*, 2004, 2006). In terrestrial ecosystems, the water source depends on the isotopic composition of meteoric water, which is in turn controlled by latitude and air temperature (Dansgaard, 1964; Fricke & O'Neil, 1999). Model curves of present-day $\delta^{18}O$ values of endothermic and ectothermic vertebrates have been established as a function of the latitude. According to these models, endothermic vertebrates are expected to have higher $\delta^{18}O$ values than ectothermic ones above 50° latitude, but ectothermic vertebrates should be similar to endotherms, or display higher $\delta^{18}O$ values at low latitudes (Amiot *et al.*, 2004, 2006).

While results obtained in dinosaurs are compatible with endothermy (thus supporting the hypothesis of a widespread high metabolic rate in Cretaceous dinosaurs), the isotopic values obtained for Cretaceous crocodiles and turtles suggest that these animals were ectothermic (Amiot *et al.*, 2006). This last result is compatible with our hypothesis of an ancestral endothermic state for the last common ancestor or archosaurs because, as quoted above, crocodylomorphs may have lost their endothermic condition when they became aquatic in the Jurassic. The other prediction derived from our hypothesis suggests that Triassic pseudosuchians and non-archosaurian archosauromorphs may have been

characterized by $\delta^{18}O$ values more similar to those of endothermic Triassic dinosaurs than to those of ectothermic Triassic lepidosaurs and turtles.

Acknowledgements

We thank very much J. Botha-Brink (Karoo Paleontology, National Museum, Bloemfontein, South Africa) and H. Woodward (Museum of the Rockies, Bozeman, Montana, U.S.A.) for helpful comments on an earlier version of the manuscript, and M. Laurin (Museum National d'Histoire Naturelle, Paris, France) for comments and linguistic revision. This study was funded by the grants CLG2012-34459, CGL2011-23919, and CGL2010-15243 of the Spanish Government (to JC), and by the CNRS and the UPMC (operating grants of UMR 7193 to all authors).

II – 2. Paleohistological evidence for ancestral endothermy in archosaurs

Lucas J. Legendre, Guillaume Guénard, Jennifer Botha-Brink et Jorge Cubo

Résumé
L'évolution de la production métabolique de chaleur chez les archosaures fait depuis longtemps l'objet d'un débat en paléontologie. L'étude de l'histologie osseuse chez les organismes fossiles fournit des informations cruciales sur leur taux de croissance osseuse, et indirectement sur leur taux métabolique, qui ont été utilisées pour étudier l'évolution du thermométabolisme chez les archosaures. Des caractères compatibles avec un taux de croissance osseuse élevé et un métabolisme endotherme ont été identifiés chez plusieurs espèces fossiles d'archosaures, dont des dinosaures non-aviens. Néanmoins, aucune estimation quantitative du taux métabolique n'a jamais été effectuée sur des fossiles en utilisant des caractères ostéohistologiques. Ici, nous avons construit un modèle statistique prédictif dans un cadre phylogénétique en utilisant un échantillonnage de vertébrés actuels et fossiles et un ensemble de caractères ostéohistologiques dans le but d'estimer les taux métaboliques d'archosauromorphes fossiles. Nos résultats montrent que les dinosaures théropodes du Mésozoïque présentent des taux métaboliques comparables à ceux des oiseaux actuels, que les archosaures partagent un taux métabolique primitivement plus élevé que celui des ectothermes actuels, et que l'acquisition de cet état de caractère dérivé a eu lieu à un niveau bien plus inclusif de la phylogénie, au sein des archosauromorphes non-archosaures.

Abstract
The evolution of metabolic heat production in archosaurs has long been a matter of debate in palaeontology. The study of fossil bone histology provides crucial information on bone growth rate (and indirectly metabolic rate), which has been used to investigate the evolution of thermometabolism in archosaurs. Several species of fossil archosaurs, including non-avian dinosaurs, have been shown to exhibit features compatible with a high metabolic rate and endothermy. However, no quantitative estimation of metabolic rate has ever been performed on fossils using bone histological features. Here we performed statistical predictive modeling in a phylogenetic context using a sample of extant and extinct vertebrates and a set of bone histological features in order to estimate metabolic rates of fossil archosauromorphs. Our results show that Mesozoic theropod dinosaurs exhibit metabolic rates very close to those found in modern birds, that archosaurs share an ancestral metabolic rate significantly higher than extant ectotherms, and that this derived high metabolic rate was acquired at a much more inclusive level of the phylogenetic tree, among non-archosaurian archosauromorphs.

The Archosauria clade includes extant crocodiles and birds, as well as numerous extinct groups such as pterosaurs and non-avian dinosaurs. The latter group has always been a matter of controversy regarding their capacity for metabolic heat production (Ostrom, 1969; Bakker, 1971). The hypothesis of endothermy being a synapomorphy of modern birds among sauropsids has been challenged countless times during the 1970s, after the discovery of the dinosaurian origin of birds (Bakker, 1974), but these studies were all based on observations of global similarities between birds and dinosaurs, and only qualitative features were used without performing any quantitative estimation of thermometabolism. For this reason, evidence of endothermy in dinosaurs was considered inconclusive by most palaeontologists; dinosaurs were labelled ectothermic with probable homeothermy given their large size (Benton, 1979), and non-avian archosaurs considered as ectothermic by most palaeontologists.

However, over the past decade, investigations on thermometabolism in fossil vertebrates have increased dramatically (Nespolo *et al.*, 2011). Evidence for an endothermic ancestral condition of heat production at the archosaur node, and a reversal in modern-day crocodiles to an ectothermic state, has been raised in different fields of biology including development (Seymour *et al.*, 2004), physiology (Farmer & Sanders, 2010), anatomy (Summers, 2005), and palaeohistology (de Ricqlès *et al.*, 2008).

It has been shown experimentally that bone tissue contains a metabolic signal: resting metabolic rate is related to bone growth rate, which, in turn, is related to bone histology (Montes *et al.*, 2007). Thus, the analysis of bone histology of extinct archosauromorphs proves useful in understanding the origin and evolution of endothermy. A series of palaeohistological studies has allowed the reconstruction of evolutionary patterns of bone

growth rates in non-archosaurian archosauromorphs using qualitative assessments of bone histological features (de Ricqlès *et al.*, 2008; Botha-Brink & Smith, 2011). More recently, two studies used quantitative histological characters to build statistical predictive models and estimate bone growth rates of fossil archosauromorphs (Cubo *et al.*, 2012; Legendre, Segalen & Cubo, 2013). All these predictions provided indirect information on the evolution of metabolic rate in archosaurs, but they were not estimations of thermometabolism itself.

To date, no study has provided quantitative estimations of metabolic rate in extinct diapsids using bone histological features. Although the relationship between bone growth rate and metabolic rate is statistically significant, no definitive answer to the origin of endothermy in archosaurs can be found without a precise estimation of metabolic rate. Furthermore, even if phylogenetic signal is known to be a major influence on the variation of osteohistological variables (Cubo et al. 2012; Legendre *et al.*, 2013; Legendre *et al.*, in press), to date no inference model has included phylogenetic information in the form of predictive variables. Thus this study involves two further steps in investigating the evolution of thermometabolism in diapsids: the direct estimation of quantitative values of mass-specific metabolic rate in extinct diapsids, and the use of phylogenetic variables as predictive ones.

Guénard *et al.* (2013) recently published a powerful new approach to deal with phylogenetic information in predictive modeling: the structure of a phylogenetic tree is expressed as a set of eigenfunctions, termed phylogenetic eigenvector maps (PEM), which depict a set of patterns of phenotypic variation among species from the structure of the phylogenetic tree. Thus, a subset of eigenfunctions from a PEM can be selected to predict phenotypic values of traits for species that are represented in a tree, but for which trait data are otherwise lacking – which is the case in fossil species for traits that can only be measured

in vivo, such as metabolic rate. For this reason, we selected this approach to estimate mass-specific resting metabolic rate (mass-specific RMR, in mL O_2 h^{-1} $g^{-0.67}$) in this study, using histological parameters (Supplementary Tables 1–3) and phylogenetic information. The value 0.67 is the allometric exponent of the ratio surface to volume versus body mass for geometrically similar organisms. It has been used to correct the effect of body mass on mass-specific RMR, assuming that the effect of body mass on metabolic rate is mediated by the fact that both the surface to volume ratio and the caloric loss per mass unit decrease as body mass increases (Withers, 1992; White & Seymour, 2005; Montes *et al.*, 2007).

We built three inference models (humerus, femur and tibia) that showed high statistical significance ($R^2 > 0.99$; $p < 10^{-6}$). We thus obtained three mass-specific RMR estimations for specimens with all three long bones included in the sample. However, mass-specific RMR is an organism-level parameter. We used the higher estimation for each specimen in further analyses because an organism with a mass-specific RMR typical of endotherms can grow slowly (e.g. *Microcebus murinus*; Castanet *et al.*, 2004), but the converse does not hold (a specimen with low mass-specific RMR does not have a high bone growth rate because this process involves a high protein turnover that is very energy consuming; Montes *et al.*, 2007). Moreover, osteohistological features included in the model were measured in regions formed during the phase of sustained high bone growth rate (Cubo *et al.*, 2012). For a given body mass, the resting metabolic rate of endotherms are more than one order of magnitude higher than those of turtles, lepidosaurs and crocodiles (Clarke & Pörtner, 2010). These differences are the outcome of metabolic heat production through the mitochondrial uncoupling activity in endotherms (Walter & Seebacher, 2009). The RMR (mLO_2 h^{-1}) of mammals is 12 times higher, and those of birds 15 times higher, than those of ectotherms of similar body masses (Clarke & Pörtner, 2010). We can observe this large gap

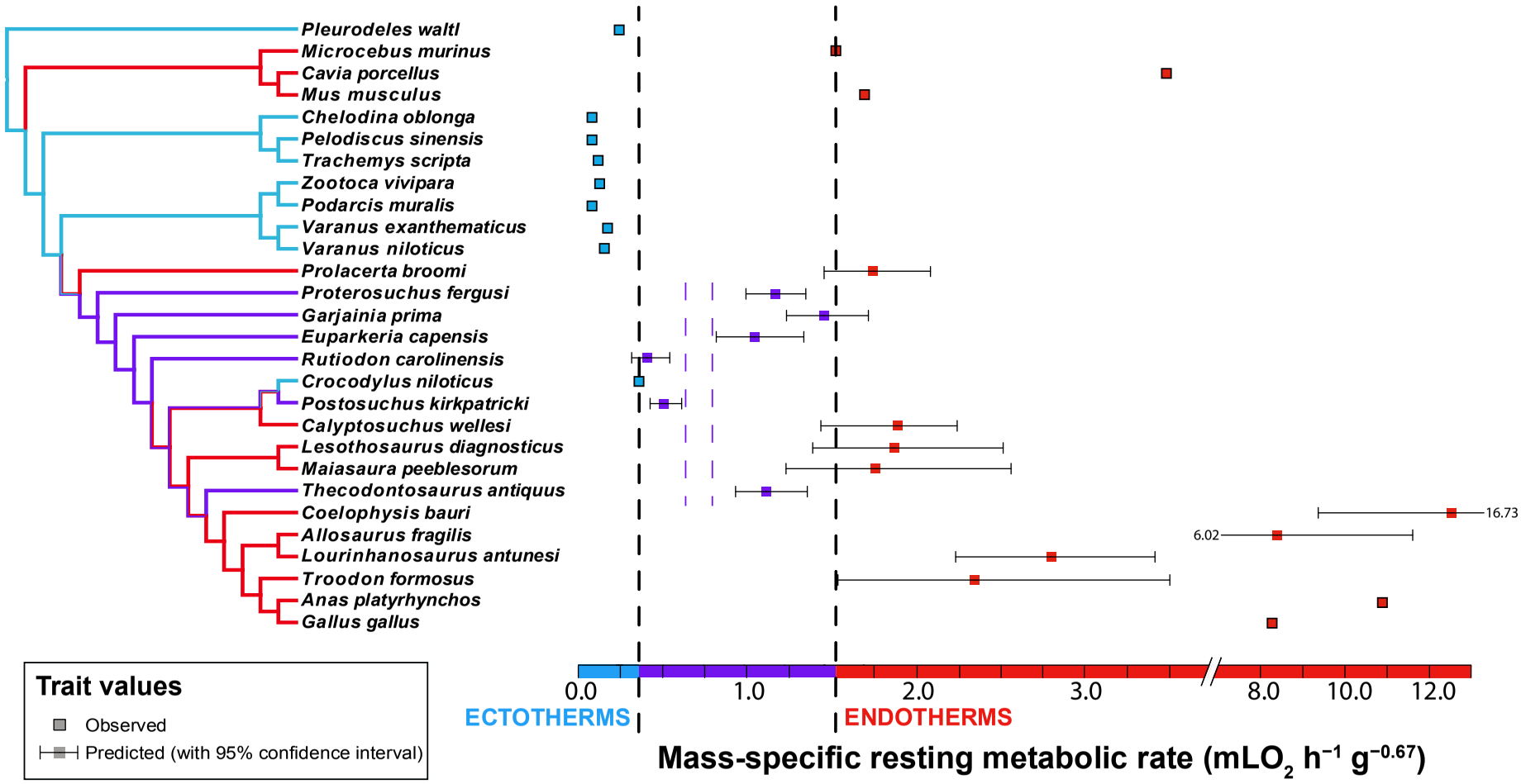
Pleurodeles waltl
Microcebus murinus
Cavia porcellus
Mus musculus
Chelodina oblonga
Pelodiscus sinensis
Trachemys scripta
Zootoca vivipara
Podarcis muralis
Varanus exanthematicus
Varanus niloticus
Prolacerta broomi
Proterosuchus fergusi
Garjainia prima
Euparkeria capensis
Rutiodon carolinensis
Crocodylus niloticus
Postosuchus kirkpatricki
Calyptosuchus wellesi
Lesothosaurus diagnosticus
Maiasaura peeblesorum
Thecodontosaurus antiquus
Coelophysis bauri
Allosaurus fragilis
Lourinhanosaurus antunesi
Troodon formosus
Anas platyrhynchos
Gallus gallus
16.73
6.02
Trait values
Observed
Predicted (with 95% confidence interval)
0.0
1.0
2.0
3.0
8.0
10.0
12.0
ECTOTHERMS
ENDOTHERMS
Mass-specific resting metabolic rate (mLO2 h−1 g−0.67)

Figure 1. Mass-specific resting metabolic rate for all species included in our sample**.** The black dotted lines delimit the values attributed respectively to truly ectothermic (blue), truly endothermic (red), and intermediate (purple) metabolic rates for all species. The purple dotted lines delimit a small gap between values of metabolic rates for fossil species, inside the large gap of intermediate mass-specific RMR values. The resulting optimization of the character is plotted on the associated phylogeny (blue: true ectothermy, red: true endothermy, purple: intermediate metabolic rate).

---

among values in our sample: *Crocodylus* shows the highest mass-specific RMR observed in our sample of ectotherms (0.34 $mLO_2\ h^{-1}\ g^{-0.67}$) and *Microcebus* the lowest mass-specific RMR observed in the sample of endotherms (1.53 $mLO_2\ h^{-1}\ g^{-0.67}$; Figure 1). Thus we conclude that mass-specific RMR inferences equal to, or lower than, 0.34 $mLO_2\ h^{-1}\ g^{-0.67}$ correspond to ectothermic animals, whereas inferences equal to, or higher than, 1.53 $mLO_2\ h^{-1}\ g^{-0.67}$ correspond to endotherms.

The analysis of evolutionary patterns (Figure 1) shows that, among non-archosaur archosauromorphs, *Prolacerta* shows a high value of mass-specific RMR (1.73 $mLO_2\ h^{-1}\ g^{-0.67}$) compatible with the hypothesis of a ancestral high metabolism at the archosauromorph node, whereas *Proterosuchus*, *Garjainia*, and *Euparkeria* show values intermediate between extant ectotherms and endotherms (from 1.04 $mLO_2\ h^{-1}\ g^{-0.67}$ for *Euparkeria* to 1.45 $mLO_2\ h^{-1}\ g^{-0.67}$ for *Garjainia*). The phytosaur *Rutiodon* shows a much lower value (0.41 $mLO_2\ h^{-1}\ g^{-0.67}$) very close to that of *Crocodylus*, which is congruent with the strong similarities in morphology and lifestyle between phytosaurs and crocodilians. This finding supports a previous study by Cubo *et al.* (2012) who, using a different approach, inferred a bone growth rate for *Rutiodon* lower than those measured in extant ectotherms. Among pseudosuchians, *Calyptosuchus* has a very high mass-specific RMR (1.88 $mLO_2\ h^{-1}\ g^{-0.67}$), typical of extant endotherms, whereas *Postosuchus* presents a lower value (0.51 $mLO_2\ h^{-1}\ g^{-0.67}$), which may indicate a reversion to a low heat production state shared with extant crocodilians.

Most seven non-avian dinosaur species share high metabolic rate values. Both ornithopod dinosaurs *Lesothosaurus* and *Maiasaura* present a mass-specific RMR typical of extant endotherms, but the sauropodomorph dinosaur *Thecodontosaurus* exhibits an intermediate value (1.12 $mLO_2\ h^{-1}\ g^{-0.67}$, the lowest value among dinosaurs). Highest values in the whole sample are found in theropod dinosaurs, all higher than 2 $mLO_2\ h^{-1}\ g^{-0.67}$. *Allosaurus* and *Coelophysis*, with respective values of 8.36 and 12.5 $mLO_2\ h^{-1}\ g^{-0.67}$, have mass-specific RMR similar to those of modern birds.

A recent comprehensive study (Grady *et al.*, 2014) estimated the resting metabolic rate of fossil dinosaurs using body mass growth rate as independent variable, and found them to be 'mesotherms' (*i.e.* with a metabolic rate intermediate to those of ectotherms and endotherms). Our results do not agree with those obtained by this study: we have found a conspicuous gap between mass-specific RMR of endotherms and ectotherms, and all non-avian dinosaur species but one clearly placed in the cluster of endotherms. Though the intermediate values of mass-specific RMR estimated for most non-archosaurian archosauromorphs in the present study can neither be associated to endothermy nor ectothermy, the ancestral condition at the archosaur node is significantly above a typical ectothermic metabolism as measured in our sample of extant species. Among archosauromorphs with values of mass-specific RMR intermediate between those of ectotherms and endotherms, we can observe that *Rutiodon* and *Postosuchus* share very low values (0.41 and 0.51 $mLO_2\ h^{-1}\ g^{-0.67}$, respectively), whereas all other archosauromorphs present values higher than 1 $mLO_2\ h^{-1}\ g^{-0.67}$. This might reflect the existence of a smaller gap of values inside the larger gap observed in extant species, which implies that *Rutiodon* and *Postosuchus* shared a metabolism more similar to that of extant ectotherms, and that all fossil archosauromorphs with values of mass-specific RMR higher than 1 $mLO_2\ h^{-1}\ g^{-0.67}$ presented a metabolism more similar to that of extant endotherms.

Hence, what has been described as ‘mesothermy’ probably consists in a whole array of physiological responses to different environmental constraints (Supplementary Information). These various metabolic strategies appeared independently during the evolution of archosauromorphs, and cannot be interpreted as a homologous character state in a phylogenetic context.

Results of the optimization onto the phylogenetic tree of archosauromorphs are congruent with the hypothesis of an ancestral high metabolic rate shared by all species in the archosaur crown group, and suggest that this derived state may have been acquired by the last common ancestor of *Prolacerta* and *Gallus*. Archosauromorphs like *Prolacerta* must have shared a series of physiological adaptations linked to true endothermy, including a four-chambered heart similar to that of mammals, crocodiles, and birds. The separation of a high systemic blood pressure from a low pulmonary blood pressure may have allowed a high hematocrit (linked to high oxygen consumption), high viscosity blood to flow through the body, as well as sufficient blood pressure to enable efficient ultrafiltration in the kidneys (Seymour *et al.*, 2004). The endothermic state may also explain the histological profile compatible with high bone growth rate observed in a large archosauromorph like *Erythrosuchus* (Gross, 1934; de Ricqlès *et al.*, 2008; Botha-Brink & Smith, 2011).

Our sample of fossil pseudosuchians does not allow us to identify the ancestral condition for this node. Though the rauisuchian *Postosuchus* presents a low mass-specific RMR value, some crocodylomorphs (*i.e.* pseudosuchians closer to extant crocodiles than they are from rauisuchians) like *Hesperosuchus* or *Terrestrisuchus* (de Ricqlès *et al.*, 2003, 2008) display morphological characteristics very similar to those of endotherms, like parasagittal stance, and, in the case of *Terrestrisuchus*, a histological profile compatible with high bone

growth rate. A larger sample of pseudosuchians is likely to solve this problem and to improve our understanding of the evolution of metabolic rate in this clade.

It has been argued that endothermy in dinosaurs was restricted to the smaller species, since very large dinosaurs like sauropods or hadrosaurs would have required an impossibly large heart and too high lung ventilation rates to sustain mammalian- or avian-like metabolic rates, and because the internal temperature linked to body size may have been too elevated (McNab, 1978; Benton, 1979; Seebacher, 2003; Seymour *et al.*, 2004). In this context, the lower mass-specific RMR values found for sauropodomorph *Thecodontosaurus* and hadrosaurid *Maiasaura* compared to that of other dinosaurs in our sample is congruent with these observations. Conversely, theropod dinosaurs exhibit very high mass-specific RMR values, similar to those of modern birds, which is congruent with the high systemic blood pressure inferred for such bipedal, active predators (Seymour, 1976).

Methods summary

The models were built using 57 specimens belonging to 14 extant species, and 14 extinct species, of tetrapods. Histological bone sections have been sampled and described in previous studies (Montes *et al.*, 2007; Cubo *et al.*, 2012). They were observed using a Zeiss Axiovert microscope and digitally imaged. We measured eight histological quantitative characters – vascular density; relative proportions of circular, longitudinal, oblique, and radial vascular canals; osteocyte shape, size and density – on each bone section following a standardized procedure for each of them (Cubo *et al.*, 2012). The dependent variable in our models – resting metabolic rate – was taken from published literature, as well as phylogenetic relationships between all species (Cubo *et al.*, 2012; Legendre *et al.*, 2013; see Figure 2). We

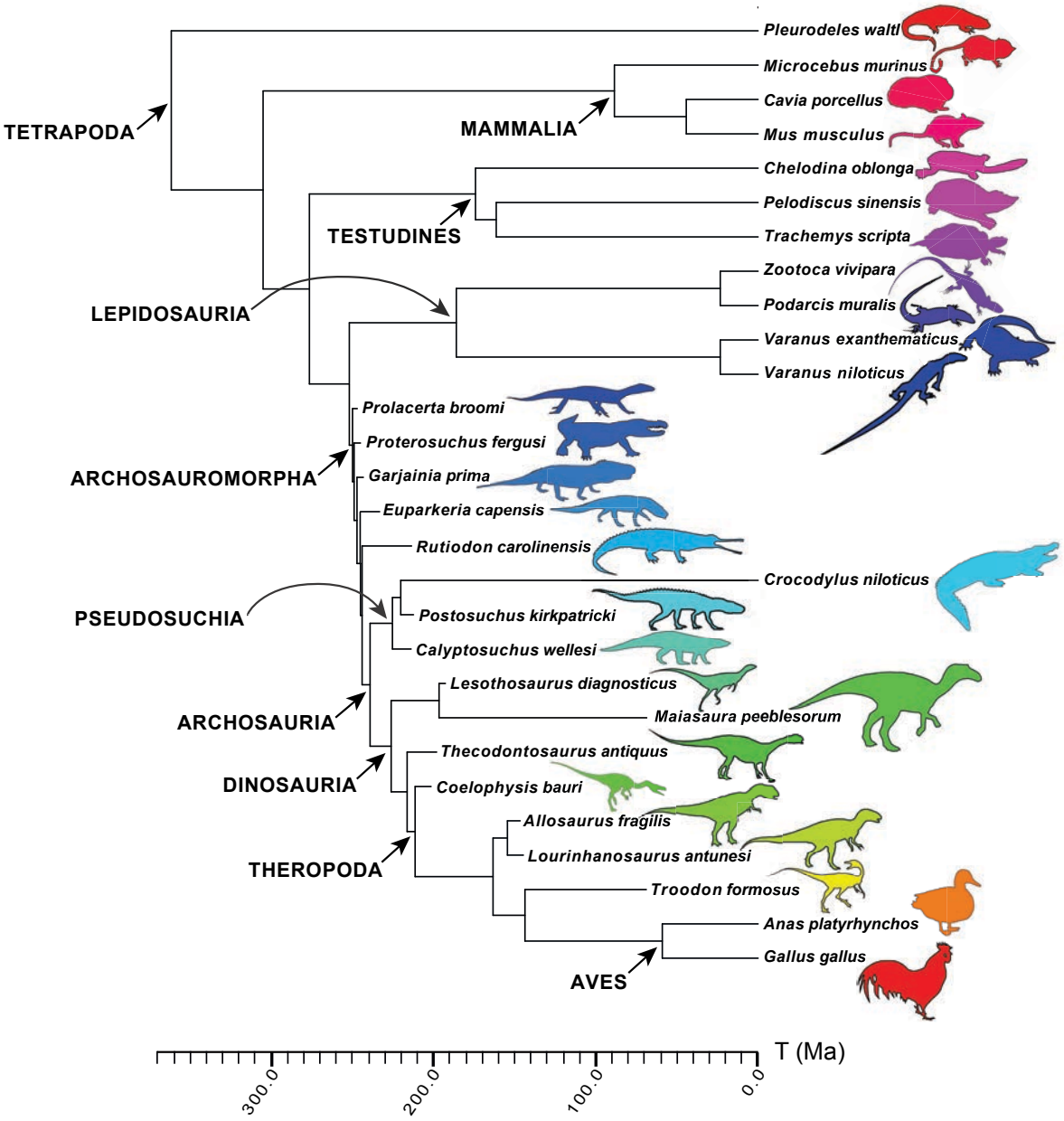

Figure 2. Phylogenetic relationships between species included in our sample, with branch lengths. Clades discussed in the text are labelled. Timescale in million years (Ma).

used the R package MPSEM (Guénard *et al.*, 2013) to convert the phylogeny into PEM and predict values of the dependent variable for fossil species; a predictive model was compiled for each of the three bones (femur, humerus and tibia). Independent variables for each model consisted of these PEM, with the addition of one of the eight histological characters per model, both selected using their AICc values. All models were cross-validated using leave-one-out cross-validation. Values of resting metabolic rate with 95% confidence intervals were

then estimated for each fossil species in our sample.

Supplementary information

Supplementary discussion

Mesothermy and the scaling of metabolic rates

In their recent study on the thermometabolism of dinosaurs, Grady *et al.* (2014) built a predictive model for resting metabolic rate (RMR) based on ontogenetic growth using a sample of 381 species of vertebrates. All 21 non-avian dinosaurs in their sample were unambiguously found to be what they labelled 'mesothermic', *i.e.* with RMR values intermediate between those of extant ectotherms and endotherms. Though numerous examples of extant vertebrate species with intermediate metabolic rates are quoted as being present-day mesotherms (e.g. tunas, lamnid sharks, leatherback sea turtles), some of them are acknowledged as presenting significantly different metabolic heat productions from each other. For example, echidnas are described as able to maintain a thermal set point, but their body temperature (T_b) range is subject to an important variation due to a very low metabolic rate and a limited capacity to thermoregulate. For this reason, they are classified as being 'near the intersection of mesothermy and endothermy', but are identified as mesotherms on the basis of their high thermal lability (Grady *et al.*, 2014).

However, thermal lability is also important in a number of small poikilothermic mammals; mouse lemurs (*Microcebus*), for example, alternate between an active phase with a preferred range of body temperature around 37°C and a torpor phase with lower temperatures (Schmid, Ruf & Heldmaier, 2000). This torpor is conditioned by environmental constraints

such as low ambient temperatures (T_a); for this reason, mouse lemurs display very low RMR values and large temperature ranges compared to those of other placental mammals, but they do not fit into the definition of mesothermy because of their inability to maintain a high T_b when T_a is below their preferred range (Grady *et al.*, 2014). Conversely, lamnid sharks and tunas display high RMR values compared to those of ectotherms because they present many convergent physiological adaptations to fast swimming, like the ability to retain metabolic heat produced by continuous activity of red muscles during swimming to elevate their global body heat (Bernal *et al.*, 2001), but resting metabolic heat production in these taxa is not significantly different from that of ectotherms. Thus, the existence of a difference between mesothermy and ectothermy / endothermy is still controversial (Ruben, 1995).

The interval of RMR values between 'true' endotherms and ectotherms comprises mostly large ectotherms that have acquired the autapomorphic ability to maintain a high metabolic rate in an aquatic environment where true endothermy would be impossible, or small endotherms that have acquired the autapomorphic ability to modify their preferred range of T_b in a dry environment with large variations of T_a. These autapomorphies probably correspond to various metabolic adaptations associated with very specific physiological constraints, and the use of the term 'mesothermy' to describe a mosaic of different heat production strategies may thus be misleading. Grady *et al.* (2014, p. 1268) are right when they state that « the modern dichotomy of endothermic versus ectothermic is overly simplistic », but creating a trichotomy with the addition of a single mesothermic state is likely another simplification; a comprehensive review of all metabolic strategies in vertebrates without using discrete categories is yet to come.

Comparison between methods used in this study and in Grady *et al.* (2014)

In the present study, we used osteohistological features and phylogenetic eigenvector maps (PEM) as independent variables in our predictive modeling of mass-specific RMR ; these variables were all measured for this study. *A contrario*, Grady *et al.* (2014) built their predictive model using growth rate as an independent variable; growth rate was compiled from measurements from previous studies, and expressed as maximum growth rate (G_{max}), in g day^{-1}. However, not all growth rates taken from literature were originally measured in g day^{-1}, which might generate some uncertainty and conversion errors. For example, *Psittacosaurus mongoliensis* is identified has having a G_{max} of 5.82 kg $year^{-1}$ (Erickson, Curry-Rogers & Yerby, 2001). In Grady *et al.* (2014) this number becomes 13.8 g day^{-1}, which would imply a number of 422 days in an Early Cretaceous year, from which *Psittacosaurus* is dated; even when considering the variation of length of a day over time (Myhrvold, 2013), this estimation is incorrect. Similarly, *Tenontosaurus tilletti* has a G_{max} of 27 kg $year^{-1}$ (Lee & Werning, 2008), which would require an impossibly small number of days (139) in a Middle Cretaceous year to match the value of 194.5 g day^{-1} used by Grady *et al.* (2014). Some estimations of growth rates for extinct dinosaur species may thus be biased by these conversion rates.

The other major difference between this study and that of Grady *et al.* (2014) is the type of phylogenetic regression used for building predictive models. The construction of PEM for a given trait involve weighting the edges (*i.e.* branches) of the phylogenetic tree on the basis of the among-species phylogenetic covariance matrix of this trait, using a steepness parameter *a* – related to Pagel's κ (Pagel, 1999) and to the Ornstein-Uhlenbeck selection strength parameter α (Butler & King, 2004) – to describe the relationship between changes in traits values and branch lengths in the tree (*a* = 0 under purely neutral evolution). This

procedure is a significant improvement on the arbitrary assumption of purely neutral evolution (*i.e.* following a Brownian motion model) assumed by phylogenetic independent contrasts (PICs; Felsenstein, 1985) used by Grady *et al.* (2014), which imply a strict relationship between the variation of a given trait and branch length information for the corresponding phylogeny. Furthermore, although most of the species in their sample of non-avian dinosaurs have been the matter of precise dating studies in the literature (Cubo *et al.*, 2012; Legendre *et al.*, 2013), no branch length information was included by Grady *et al.* (2014) in their trees for both non-avian dinosaurs and crocodilians, which adds an important bias to the way their model takes into account phylogenetic information.

In conclusion, a better characterization of both datasets and modeling procedures are required for further modeling of archosauromorph metabolic rate. Grady *et al.*'s study is the most comprehensive work ever performed on dinosaurs in a phylogenetic perspective, and is a strong attempt to solve one of the oldest mysteries in palaeontology; the present study is a further description of the thermometabolism evolutionary pattern in archosauromorphs, using a new and powerful predictive method and the largest osteohistological dataset ever assembled for this clade. However, some riddles on metabolic heat production of archosaurs still remain unanswered. Future works on this matter will have to rely on larger datasets, better knowledge of the phylogeny, and more accurate characterization of heat production in extant vertebrates, in order to improve our understanding of the metabolism of dinosaurs and other archosauromorphs.

Table S1. Resting metabolic rate measured for extant species and osteohistological characters measured for all species in the sample, with the number of specimens for each of them, for femora of all specimens.

Species	**Number of specimens**	**Resting metabolic rate ($mLO_2\ h^{-1}\ g^{-0.67}$)**	**Relative proportion of circular vascular canals**	**Relative proportion of longitudinal vascular canals**	**Relative proportion of oblique vascular canals**
Anas platyrhynchos	4	10.865	0.367	0.356	0.185
Cavia porcellus	3	3.477	0.369	0.359	0.236
Chelodina oblonga	2	0.085	0.085	0.000	0.000
Crocodylus niloticus	3	0.336	0.207	0.449	0.267
Mus musculus	5	1.696	0.346	0.394	0.241
Pelodiscus sinensis	4	0.083	0.000	0.000	0.000
Zootoca vivipara	4	0.124	0.000	0.000	0.000
Podarcis muralis	3	0.084	0.000	0.000	0.000
Trachemys scripta	4	0.117	0.000	0.000	0.000
Varanus exanthematicus	2	0.173	0.000	0.313	0.063
Varanus niloticus	1	0.157	0.000	0.000	0.000
Microcebus murinus	3	1.526	0.213	0.470	0.239
Gallus gallus	3	8.289	0.359	0.262	0.265
Pleurodeles waltl	5	0.084	0.000	0.000	0.000
Calyptosuchus wellesi	1	-	0.367	0.367	0.200
Lesothosaurus diagnosticus	1	-	0.267	0.467	0.233
Troodon formosus	1	-	0.933	0.033	0.033
Allosaurus fragilis	1	-	0.767	0.133	0.100
Rutiodon carolinensis	1	-	0.500	0.333	0.133
Maiasaura peeblesorum	1	-	0.600	0.133	0.233
Proterosuchus fergusi	1	-	0.058	0.400	0.217

Table S1. Continued.

Species	Relative proportion of radial vascular canals	Vascular density (vascular canals / mm^2)	Osteocyte density (osteocyte / μm^2)	Osteocyte size (μm^2)	Osteocyte shape
Anas platyrhynchos	0.092	128.695	0.0025	20.644	0.496
Cavia porcellus	0.036	106.281	0.0019	34.155	0.497
Chelodina oblonga	0.000	0.000	0.0009	28.125	0.615
Crocodylus niloticus	0.078	33.077	0.0007	29.694	0.475
Mus musculus	0.020	183.789	0.0012	29.485	0.480
Pelodiscus sinensis	0.000	0.000	0.0009	24.486	0.522
Zootoca vivipara	0.000	0.000	0.0021	13.677	0.427
Podarcis muralis	0.000	0.000	0.0011	11.992	0.438
Trachemys scripta	0.000	0.000	0.0014	28.963	0.495
Varanus exanthematicus	0.125	14.286	0.0011	33.362	0.463
Varanus niloticus	0.000	0.000	0.0010	39.700	0.479
Microcebus murinus	0.078	46.912	0.0039	30.008	0.587
Gallus gallus	0.113	90.861	0.0025	27.733	0.524
Pleurodeles waltl	0.000	0.000	0.0006	134.939	0.595
Calyptosuchus wellesi	0.067	282.651	0.0041	33.151	0.500
Lesothosaurus diagnosticus	0.033	218.121	0.0027	103.046	0.370
Troodon formosus	0.000	90.065	0.0015	69.503	0.447
Allosaurus fragilis	0.000	227.895	0.0055	31.252	0.470
Rutiodon carolinensis	0.033	153.226	0.0011	37.294	0.411
Maiasaura peeblesorum	0.033	38.354	0.0011	44.413	0.551
Proterosuchus fergusi	0.325	24.002	0.0010	27.931	0.558

Table S2. Resting metabolic rate measured for extant species and osteohistological characters measured for all species in the sample, with the number of specimens for each of them, for humeri of all specimens.

Species	**Number of specimens**	**Resting metabolic rate ($mLO_2\ h^{-1}\ g^{-0.67}$)**	**Relative proportion of circular vascular canals**	**Relative proportion of longitudinal vascular canals**	**Relative proportion of oblique vascular canals**
Anas platyrhynchos	4	10.865	0.527	0.272	0.172
Cavia porcellus	3	3.477	0.314	0.286	0.317
Chelodina oblonga	3	0.085	0.000	0.000	0.000
Crocodylus niloticus	1	0.336	0.234	0.489	0.234
Mus musculus	5	1.696	0.312	0.312	0.302
Pelodiscus sinensis	5	0.083	0.000	0.000	0.000
Zootoca vivipara	4	0.124	0.000	0.000	0.000
Podarcis muralis	2	0.084	0.000	0.000	0.000
Trachemys scripta	4	0.117	0.000	0.000	0.000
Varanus exanthematicus	3	0.173	0.000	0.179	0.154
Varanus niloticus	1	0.157	0.000	0.000	0.000
Microcebus murinus	3	1.526	0.227	0.490	0.223
Gallus gallus	3	8.289	0.545	0.285	0.153
Pleurodeles waltl	5	0.298	0.000	0.000	0.000
Euparkeria capensis	1	-	0.000	0.900	0.067
Postosuchus kirkpatricki	1	-	0.433	0.500	0.067
Garjainia prima	1	-	0.133	0.125	0.342
Prolacerta broomi	1	-	0.092	0.417	0.208

Table S2. Continued.

Species	Relative proportion of radial vascular canals	Vascular density (vascular canals / mm^2)	Osteocyte density (osteocyte / μm^2)	Osteocyte size (μm^2)	Osteocyte shape
Anas platyrhynchos	0.028	172.948	0.0023	24.291	0.509
Cavia porcellus	0.082	112.748	0.0020	34.986	0.485
Chelodina oblonga	0.000	0.000	0.0012	24.278	0.563
Crocodylus niloticus	0.043	48.957	0.0007	34.602	0.485
Mus musculus	0.074	98.517	0.0012	22.624	0.526
Pelodiscus sinensis	0.000	0.000	0.0012	20.926	0.497
Zootoca vivipara	0.000	0.000	0.0033	10.454	0.442
Podarcis muralis	0.000	0.000	0.0009	11.953	0.404
Trachemys scripta	0.000	0.000	0.0012	27.135	0.516
Varanus exanthematicus	0.000	5.542	0.0012	36.293	0.435
Varanus niloticus	0.000	0.000	0.0014	38.164	0.471
Microcebus murinus	0.060	71.309	0.0038	28.516	0.527
Gallus gallus	0.017	114.114	0.0024	31.206	0.469
Pleurodeles waltl	0.000	0.000	0.0008	107.919	0.553
Euparkeria capensis	0.033	48.157	0.0025	54.896	0.460
Postosuchus kirkpatricki	0.000	189.542	0.0013	20.712	0.519
Garjainia prima	0.400	50.771	0.0024	38.865	0.597
Prolacerta broomi	0.283	73.892	0.0014	32.306	0.619

Table S3. Resting metabolic rate measured for extant species and osteohistological characters measured for all species in the sample, with the number of specimens for each of them, for tibiae of all specimens.

Species	**Number of specimens**	**Resting metabolic rate ($mLO_2\ h^{-1}\ g^{-0.67}$)**	**Relative proportion of circular vascular canals**	**Relative proportion of longitudinal vascular canals**	**Relative proportion of oblique vascular canals**
Anas platyrhynchos	4	10.865	0.394	0.423	0.175
Cavia porcellus	3	3.477	0.328	0.484	0.141
Chelodina oblonga	1	0.085	0.000	0.000	0.000
Crocodylus niloticus	3	0.336	0.318	0.383	0.271
Mus musculus	3	1.696	0.440	0.274	0.214
Pelodiscus sinensis	3	0.083	0.000	0.000	0.000
Zootoca vivipara	1	0.124	0.000	0.000	0.000
Podarcis muralis	3	0.084	0.000	0.000	0.000
Trachemys scripta	5	0.117	0.000	0.000	0.000
Varanus exanthematicus	2	0.173	0.000	0.000	0.000
Varanus niloticus	1	0.157	0.000	0.000	0.000
Microcebus murinus	3	1.526	0.108	0.542	0.251
Gallus gallus	4	8.289	0.294	0.537	0.136
Pleurodeles waltl	5	0.298	0.000	0.000	0.000
Allosaurus fragilis	1	-	0.900	0.100	0.000
Coelophysis bauri	1	-	0.500	0.367	0.133
Lesothosaurus diagnosticus	1	-	0.733	0.200	0.067
Lourinhanosaurus antunesi	1	-	0.800	0.033	0.133
Maiasaura peeblesorum	1	-	0.533	0.308	0.142
Thecodontosaurus antiquus	1	-	0.100	0.533	0.300
Garjainia prima	1	-	0.125	0.225	0.275
Prolacerta broomi	1	-	0.108	0.600	0.192
Proterosuchus fergusi	1	-	0.075	0.175	0.475

Table S3. Continued.

Species	Relative proportion of radial vascular canals	Vascular density (vascular canals / mm^2)	Osteocyte density (osteocyte / μm^2)	Osteocyte size (μm^2)	Osteocyte shape
Anas platyrhynchos	0.008	149.983	0.0022	19.064	0.516
Cavia porcellus	0.047	107.370	0.0017	31.000	0.462
Chelodina oblonga	0.000	0.000	0.0015	19.956	0.589
Crocodylus niloticus	0.027	37.287	0.0010	31.432	0.480
Mus musculus	0.071	96.908	0.0023	35.120	0.529
Pelodiscus sinensis	0.000	0.000	0.0098	24.919	0.471
Zootoca vivipara	0.000	0.000	0.0032	9.388	0.483
Podarcis muralis	0.000	0.000	0.0013	11.401	0.402
Trachemys scripta	0.000	0.000	0.0014	23.302	0.486
Varanus exanthematicus	0.000	0.000	0.0008	41.051	0.536
Varanus niloticus	0.000	0.000	0.0012	19.448	0.485
Microcebus murinus	0.099	41.074	0.0038	28.430	0.618
Gallus gallus	0.033	91.200	0.0034	31.148	0.507
Pleurodeles waltl	0.000	0.000	0.0006	134.939	0.595
Allosaurus fragilis	0.000	210.890	0.0003	23.326	0.407
Coelophysis bauri	0.000	734.742	0.0113	3.477	0.476
Lesothosaurus diagnosticus	0.000	31.565	0.0017	33.361	0.590
Lourinhanosaurus antunesi	0.033	39.097	0.0017	38.053	0.502
Maiasaura peeblesorum	0.017	37.976	0.0020	52.750	0.577
Thecodontosaurus antiquus	0.067	14.899	0.0017	64.729	0.502
Garjainia prima	0.375	45.408	0.0007	66.621	0.732
Prolacerta broomi	0.100	60.714	0.0013	19.089	0.637
Proterosuchus fergusi	0.275	31.102	0.0016	26.047	0.626

Acknowledgements

This work was supported by the Université Pierre et Marie Curie and the Centre National de la Recherche Scientifique (operating grant of UMR 7193 to LJL and JC), and by the Spanish Government (CGL2011-23919 to JC).

Author Contribution

LJL and JC designed the study and wrote the paper. LJL performed measurements on bone histological sections. LJL and GG performed analytical work and figures. JBB contributed histological data and assisted in data interpretation and writing the paper. All authors discussed the results and commented on the manuscript.

Conclusions de la seconde partie

◆ **Les caractères ostéohistologiques quantitatifs sont de bons prédicteurs du taux de croissance osseuse et du taux métabolique des vertébrés fossiles.**

◆ **Les archosauromorphes fossiles présentent tous des taux métaboliques au repos supérieurs à ceux des ectothermes typiques ; certains d'entre eux, notamment la majorité des dinosaures de notre échantillonnage, sont clairement identifiés comme endothermes par notre modèle, avec des taux métaboliques comparables à ceux des mammifères ou des oiseaux.**

◆ **Si plusieurs incertitudes demeurent quant à l'apparition de ce caractère au sein des archosauromorphes et à son évolution au sein de la lignée des pseudosuchiens, ces résultats démontrent clairement l'apparition d'un métabolisme élevé au sein des archosauromorphes non-archosaures, et d'une perte de ce métabolisme chez les crocodiliens actuels, probablement en réponse aux contraintes de leur environnement aquatique.**

◆ **Un échantillonnage plus conséquent dans les registres actuel et fossile permettra certainement de visualiser plus précisément l'évolution du thermométabolisme au sein du clade des archosauromorphes.**

Conclusion générale et perspectives

Le signal phylogénétique en histologie osseuse

Les principaux résultats de ce travail sont à la fois d'ordre biologique et méthodologique. En effet, si nous nous sommes focalisés sur l'évolution du thermométabolisme et des caractères ostéohistologiques qui lui sont liés au sein des archosaures, cette étude a également fourni plusieurs pistes de réflexion relatives à l'utilisation de données ostéohistologiques dans un cadre phylogénétique.

Nous avons pu confirmer les résultats préliminaires obtenus par Cubo *et al.* (2005) sur les sauropsidés, aussi bien pour un clade plus inclusif – les amniotes – que pour un clade moins inclusif – les paléognathes – en utilisant pour ce dernier un échantillonnage exhaustif et un large jeu de données. Les caractères quantitatifs ostéohistologiques sont donc bien porteurs d'une information phylogénétique facilement identifiable et mesurable par de multiples méthodes, et cette information peut être utilisée lors de la construction de modèles statistiques prédictifs.

Dans une revue des méthodes quantitatives utilisées pour inférer les taux de croissance globaux des dinosaures non-aviens, Myhrvold (2013) a montré que bon nombre des études sur le sujet, dont des analyses de coupes histologiques, présentent des résultats difficilement reproductibles et des échantillonnages soumis à d'importants biais. Dans cette perspective, le cadre strict d'homologie, utilisé dans notre étude sur les paléognathes aussi bien pour les spécimens que pour les caractères, a permis d'identifier un fort signal phylogénétique pour des caractères jusque là considérés comme peu informatifs. Il apparaît donc absolument indispensable d'appliquer ce type de méthodologie et ce cadre systématique à toute étude

paléohistologique souhaitant incorporer des méthodes phylogénétiques comparatives, ce qui est le cas d'un nombre croissant d'entre elles (Stein & Werner, 2014; Huttenlocker, 2014).

L'endothermie des archosaures

Le principal résultat de la thèse est l'apport du modèle prédictif statistique qui identifie formellement les archosaures comme présentant primitivement un taux métabolique élevé, supérieur à celui des ectothermes actuels, également partagé par les archosauromorphes non-archosaures inclus dans notre échantillonnage. Cela confirme donc l'hypothèse, formulée pour la première fois par de Ricqlès (1978), selon laquelle les crocodiles ont acquis secondairement une ectothermie qui leur a conféré un avantage énergétique certain au cours de leur retour au milieu aquatique.

Toutefois, ce résultat préliminaire ne résout pas entièrement la condition primitive présente au nœud archosaures. En effet, si le modèle construit à l'aide des Phylogenetic Eigenvector Maps (PEM) permet de prédire efficacement les taux métaboliques de nos spécimens fossiles, notre échantillonnage assez restreint d'archosauromorphes non-archosaures et de pseudosuchiens fossiles laisse une incertitude quant à l'endothermie primitive éventuelle de ces groupes. Il est intéressant de noter que *Euparkeria*, une espèce identifiée comme présentant un faible taux de croissance osseuse par Botha-Brink & Smith (2011) et un taux de croissance bien plus élevé par notre modèle prédictif du taux de croissance osseuse (voir Partie II. – 1), s'est vu attribué un taux métabolique intermédiaire entre ceux des endothermes et des ectothermes, ce qui est cohérent avec une certaine variabilité intraspécifique du taux de croissance osseuse, probablement influencé par les importants bouleversements climatiques au Trias moyen (Botha-Brink & Smith, 2011). Ces

conditions climatiques ont certainement joué un rôle essentiel dans l'apparition de métabolismes plus élevés que ceux des autres diapsides chez les premiers archosauromorphes.

L'article de Grady *et al.* (2014), qui identifie les dinosaures comme mésothermes (*i.e.* présentant un métabolisme « intermédiaire » entre celui des ectothermes et des endothermes), n'est pas exempt de biais ni d'imprécisions méthodologiques. Il insiste pourtant sur une information essentielle, souvent passée sous silence dans les multiples articles sur le thermométabolisme des dinosaures : la capacité de produire sa propre chaleur corporelle n'est pas un caractère discret, et le débat sur le métabolisme des archosaures ne se résume pas à une simple dichotomie endothermie / ectothermie. De multiples conditions métaboliques, souvent liées à des contraintes d'ordre environnemental, peuvent être observées au sein des vertébrés, selon que l'on s'intéresse à la capacité à maintenir sa température corporelle à un niveau constant (Seymour, 2013), à l'intervalle préférentiel de température corporelle, à l'activité enzymatique ou à la consommation d'oxygène au repos (Ruben, 2005), à l'alternance entre endothermie et ectothermie observée chez certains vertébrés (e.g. Schmid, Ruf & Heldmaier, 2000 ; Bernal *et al.*, 2001) identifiés comme « mésothermes » par Grady *et al.* (2014)… Il existe donc une multitude d'adaptations physiologiques liées à la production de chaleur, conditionnées par le milieu de vie dans lequel elles apparaissent, qui ne saurait être correctement prise en compte par un caractère binaire tel qu'utilisé couramment dans la littérature.

Dans cette optique, il apparaît donc comme indispensable de définir plus clairement les multiples stratégies évolutives au sein des vertébrés et de se baser sur un échantillonnage intégrant le plus possible de ces stratégies pour mieux retracer l'évolution du thermométabolisme au sein de clades aussi diversifiés que celui des archosauromorphes. De

nombreux groupes d'archosauromorphes (les dinosaures, bien sûr, mais également les erythrosuchidés, sauropodomorphes, pseudosuchiens, crocodylomorphes…), dont la condition primitive n'est pas formellement identifiée par notre modèle, et pour lesquels peu d'études quantitatives ont été menées dans ce sens, pourraient être intégrés à une telle approche, et leur métabolisme pourrait ainsi être plus clairement défini. Sur le long terme, cela permettrait d'inférer le thermométabolisme de ces groupes à un niveau très inclusif de l'arbre, et de comparer ces résultats à la succession des différentes conditions climatiques au cours des temps géologiques (Haywood, Valdes & Markwick, 2004 ; Selwood & Valdes, 2006 ; Belcher & McElwain, 2008) afin de mieux comprendre les processus à l'œuvre derrière l'acquisition de ces modifications du thermométabolisme au cours de l'évolution. Il serait également intéressant de modéliser d'autres caractères liés au thermométabolisme, d'appliquer d'autres méthodes phylogénétiques comparatives telles que les PGLS (Phylogenetic Generalized Least Squares ; Grafen, 1989), ou encore de prendre en considération le métabolisme spécifique de certains organes plutôt que la production de chaleur à l'échelle de l'organisme, afin d'estimer les bilans énergétiques des différents groupes d'archosauromorphes.

Bibliographie

Abouheif E. **1999**. A method for testing the assumption of phylogenetic independence in comparative data. *Evolutionary Ecology Research* **1**: 895–909.

Adams DC, Church JO. **2011**. The evolution of large-scale body size clines in *Plethodon* salamanders: evidence of heat-balance or species-specific artifact? *Ecography* **34**: 1067–1075.

Agassiz, JLR. 1833–1844. Recherches sur les Poissons Fossiles. Neuchâtel: Imprimerie Petitpierre.

Alvarenga HMF. **1983.** Uma ave ratitae do Paleoceno Brasileiro: Bacia Calcaŕia de Itaboraí, Estado do Rio de Janeiro, Brasil. *Geologia: Boletim do Museu Nacional do Rio de Janeiro* **41**: 1–7.

Amiot R, Lécuyer C, Buffetaut E, Fluteau F, Legendre S, Martineau F. 2004. Latitudinal temperature gradient during the Cretaceous Upper Campanian–Middle Maastrichtian: $\delta^{18}O$ record of continental vertebrates. *Earth and Planetary Science Letters* **226**: 255–272.

Amiot R, Lécuyer C, Buffetaut E, Escarguel G, Fluteau F, Martineau F. 2006. Oxygen isotopes from biogenic apatites suggest widespread endothermy in Cretaceous dinosaurs. *Earth and Planetary Science Letters* **246**: 41–54.

Amprino R. 1947. La structure du tissu osseux envisagée comme l'expression de différences dans la vitesse de l'accroissement. *Archives de Biologie* **58**: 315–330.

Antunes MT, Mateus O. 2003. Dinosaurs of Portugal. *Comptes rendus Palevol* **2**: 77–95.

Baker AJ, Daugherty CH, Colbourne R, McLennan JL. **1995**. Flightless brown kiwis of New Zealand possess extremely subdivided population structure and cryptic species like small mammals. *Proceedings of the National Academy of Sciences* **92**: 8254–8258.

Bakker RT. 1971. Dinosaur physiology and the origin of mammals. *Evolution* **25**: 636–658.

Bakker RT. 1972. Anatomical and ecological evidence of endothermy in dinosaurs. *Nature* **238**: 81–85.

Bakker RT. 1974. Dinosaur Bioenergetics – A Reply to Bennett and Dalzell, and Feduccia. *Evolution* **28**: 497–503.

Barrick RE, Showers WJ, Fischer AG. 1996. Comparison of thermoregulation of four ornithischian dinosaurs and a varanid lizard from the Cretaceous Two Medicine Formation; evidence from oxygen isotopes. *Palaios* **11**: 295–305.

Belcher CM, McElwain JC. **2008**. Limits for combustion in low O_2 redefine paleoatmospheric predictions for the Mesozoic. *Science* **321**: 1197–1200.

Benjamini Y, Hochberg Y. 1995. Controlling the false discovery rate: a practical and powerful approach to multiple testing. *Journal of the Royal Statistical Society: Series B (Statistical Methodology)* **57**: 289–300.

Benton MJ. 1979. Ectothermy and the Success of Dinosaurs. *Evolution* **33**: 983–997.

Benton MJ. 2004. Origin and relationships of Dinosauria. In: Weishampel DB, Dodson PR, Osmólka H, eds. *The Dinosauria (2nd edition)*. Berkeley, CA: University of California Press, 7–19.

Benton MJ, Juul L, Storrs GW, Galton PM. 2000. Anatomy and systematics of the prosauropod dinosaur *Thecodontosaurus antiquus* from the Upper Triassic of Southwest England. *Journal of Vertebrate Paleontology* **20**: 77–108.

Bernal D, Dickson KA, Shadwick RE, Graham JB. **2001**. Review: Analysis of the evolutionary convergence for high performance swimming in lamnid sharks and tunas. *Comparative Biochemistry and Physiology Part A: Molecular & Integrative Physiology* **129**: 695–726.

Bertelli S, Chiappe LM. **2005**. Earliest Tinamous (Aves: Palaeognathae) from the Miocene of Argentina and Their Phylogenetic Position. *Contributions in Science* **502**: 1–20.

Bertelli S, Giannini NP, Goloboff PA. **2002**. A phylogeny of the tinamous (Aves: Palaeognathiformes) based on integumentary characters. *Systematic Biology* **51**: 959–979.

Blomberg SP, Garland, T. **2002**. Tempo and mode in evolution: phylogenetic inertia, adaptation and comparative methods. *Journal of Evolutionary Biology* **15**: 899–910.

Blomberg SP, Garland T, Ives AR. **2003**. Testing for phylogenetic signal in comparative data: behavioral traits are more labile. *Evolution* **57**: 717–745.

de Boef M, Larsson HCE. 2007. Bone microstructure: quantifying bone vascular orientation. *Canadian Journal of Zoology* **85**: 63–70.

Boles WE. **2001**. A new emu (Dromaiinae) from the Late Oligocene Etadunna Formation. *Emu* **101**: 317–321.

Botha-Brink J, Smith RMH. 2011. Osteohistology of the Triassic Archosauromorphs *Prolacerta*, *Proterosuchus*, *Euparkeria*, and *Erythrosuchus* from the Karoo Basin of South Africa. *Journal of Vertebrate Paleontology* **31**: 1238–1254.

Bourdon E, Castanet J, de Ricqlès A, Scofield P, Tennyson A, Lamrous H, Cubo J. 2009a. Bone growth marks reveal protracted growth in New Zealand kiwi (Aves, Apterygidae). *Biology Letters* **5**: 639–642.

Bourdon E, de Ricqlès A, Cubo J. 2009b. A new Transantarctic relationship: morphological evidence for a Rheidae–Dromaiidae–Casuariidae clade (Aves, Palaeognathae, Ratitae). *Zoological Journal of the Linnean Society* **156**: 641–663.

Bromage TG, Goldman HM, McFarlin SC, Warshaw J, Boyde A, Riggs CM. **2003**. Circularly polarized light standards for investigations of collagen fiber orientation in bone. *The Anatomical Record* **274B**: 157–168.

de Buffrénil V, Houssaye A, Böhme W. 2008. Bone vascular supply in monitor lizards (Squamata: Varanidae): influence of size, growth, and phylogeny. *Journal of Morphology* **269**: 533–543.

Butler MA, King AA. **2004**. Phylogenetic comparative analysis: a modeling approach for adaptive evolution. *The American Naturalist* **164**: 683–695.

Caldwell MW. 1999. Squamate phylogeny and the relationships of snakes and mosasauroids. *Zoological Journal of the Linnean Society* **125**: 115–147.

Casgrain P. 2009. *Permute! version 3.4 alpha 9.* Available via http://adn.biol.umontreal.ca/~numericalecology/old/permute-index.html

Castanet J, Curry Rogers K, Cubo J, Boissard JJ. 2000. Periosteal bone growth rates in extant ratites (ostriche and emu). Implications for assessing growth in dinosaurs. *Comptes Rendus de l'Académie des Sciences de Paris, Sciences de la Vie / Life Sciences* **323**: 543–550.

Castanet J, Croci S, Aujard F, Perret M, Cubo J, de Margerie E. **2004**. Lines of arrested growth in bone and age estimation in a small primate: *Microcebus murinus*. *Journal of Zoology* **263**: 31–39.

Clarke A, Pörtner HO. **2010**. Temperature, metabolic power and the evolution of endothermy. *Biological Reviews* **85**: 703–727.

Cope ED. 1869. Synopsis of the extinct Batrachia, Reptilia and Aves of North America. *Transactions of the America Philosophical Society* **14**: 1–252.

Cracraft J. 1981. Pattern and Process in Paleobiology: The Role of Cladistic Analysis in Systematic Paleontology. *Paleobiology* **7**: 456–468.

Cracraft J. 2001. Avian evolution, Gondwana biogeography and the Cretaceous-Tertiary mass extinction event. *Proceedings of the Royal Society B: Biological Sciences* **268**: 459–469.

Cubo J, Casinos A. 1997. Flightlessness and long bone allometry in Palaeognathiformes and Sphenisciformes. *Netherlands Journal of Zoology* **47**: 209–226.

Cubo J, Laurin M. 2011. Perspectives on vertebrate evolution: topics and problems.

Comptes rendus Palevol **10**: 285–292.

Cubo J, Le Roy N, Martinez-Maza C, Montes L. 2012. Paleohistological estimation of bone growth rate in extinct archosaurs. *Paleobiology* **38**: 335–349.

Cubo J, Ponton F, Laurin M, de Margerie E, Castanet J. 2005. Phylogenetic signal in bone microstructure of sauropsids. *Systematic Biology* **54**: 562–574.

Cubo J, Legendre P, de Ricqlès A, Montes L, de Margerie E, Castanet J, Desdevises Y. 2008. Phylogenetic, functional, and structural components of variation in bone growth rate of amniotes. *Evolution & Development* **10**: 217–227.

Curran-Everett D. 2000. Multiple comparisons: philosophies and illustrations. *American Journal of Physiology – Regulatory, Integrative and Comparative Physiology* **279**: 1–8.

Dansgaard W. 1964. Stable isotopes in precipitation. *Tellus* **16**: 436–468.

Desdevises Y, Legendre P, Azouzi L, Morand S. 2003. Quantifying phylogenetically structured environmental variation. *Evolution* **57**: 2467–2652.

Dilkes D, Sues HD. 2009. Redescription and Phylogenetic Relationships of *Doswellia kaltenbachi* (Diapsida: Archosauriformes) from the Upper Triassic of Virginia. *Journal of Vertebrate Paleontology* **29**: 58–79.

Diniz-Filho JAF, de Sant'Ana CER, Bini LM. 1998. An eigenvector method for estimating phylogenetic inertia. *Evolution* **52**: 1247–1262.

Diniz-Filho JAF, Bini LM, Rangel TF, Morales-Castilla I, Olalla-Tárraga MÁ, Rodríguez MÁ, Hawkins BA. **2012**. On the selection of phylogenetic eigenvectors for ecological analyses. *Ecography* **35**: 239–249.

Dumont M, Laurin M, Jacques F, Pellé E, Dabin W, de Buffrénil V. 2013. Inner architecture of vertebral centra in terrestrial and aquatic mammals: a two-dimensional comparative study. *Journal of Morphology* **274**: 570–584.

Enlow DH, Brown SO. 1956. A comparative histological study of fossil and recent bone tissues. Part I. *Texas Journal of Science* **8**: 405–443.

Enlow DH, Brown SO. 1957. A comparative histological study of fossil and recent bone tissues. Part II. *Texas Journal of Science* **9**: 186–214.

Enlow DH, Brown SO. 1958. A comparative histological study of fossil and recent bone tissues. Part III. *Texas Journal of Science* **10**: 187–230.

Erickson GM, Rogers KC, Yerby SA. **2001**. Dinosaurian growth patterns and rapid avian growth rates. *Nature* **412**: 429–433.

Estes R. 1982. The Fossil Record and Early Distribution of Lizards. In: Rhodin AGJ, Miyata K, eds. *Advances in Herpetology and Evolutionary Biology: Essays in honor of E. E.*

Williams. Cambridge, MA: Harvard University Press, 365–398.

Estes R, de Queiroz K, Gauthier J. 1988. Phylogenetic Relationships within Squamata. In: Estes R, Pregill G, eds. *Phylogenetic Relationships of the Lizard Families*. Stanford, CA: Stanford University Press, 119–281.

Evans, SE. 2003. At the feet of the dinosaurs: the early history and radiation of lizards. *Biological Reviews* **78**: 513–551.

Ewer RF. 1965. The Anatomy of the Thecodont Reptile *Euparkeria capensis* Broom. *Philosophical Transactions of the Royal Society of London B* **248**: 379–435.

Farmer CG, Sanders K. 2010. Unidirectional airflow in the lungs of alligators. *Science* **327**: 338–340.

Feduccia A. 1973. Dinosaurs as reptiles. *Evolution* **27**: 166–169.

Feduccia A. **1974**. Endothermy, Dinosaurs, and Archaeopteryx. *Evolution* **28**: 503–504.

Felsenstein J. **1985**. Phylogenies and the Comparative Method. *The American Naturalist* **125**: 1–15.

Francillon-Vieillot, H, de Buffrénil V, Castanet J, Géraudie J, Meunier FJ, Sire JY, Zylberberg L, de Ricqlès A. **1990**. Microstructure and Mineralization of Vertebrate Skeletal Tissues. In: Carter JG, ed. *Skeletal Biomineralization: Patterns, Processes and Evolutionary Trends. Volume I.* New York, NY: Van Nostrand Reinhold, 471–530.

Freckleton RP, Cooper N, Jetz W. **2011**. Comparative Methods as a Statistical Fix: The Dangers of Ignoring an Evolutionary Model. *The American Naturalist* **178**: E10–E17.

Fricke HC, O'Neil JR. 1999. The correlation between $^{18}O/^{16}O$ ratios of meteoric water and surface temperature: its use in investigating terrestrial climate change over geologic time. *Earth and Planetary Science Letters* **170**: 181–196.

Fricke HC, Rogers RR. 2000. A multiple taxon / multiple locality approach to providing oxygen isotope evidence for warm-blooded theropod dinosaurs. *Geology* **28**: 799–802.

Gaffney ES, Meylan PA. 1988. A phylogeny of turtles. In: Benton MJ, ed. *The Phylogeny and Classification of the Tetrapods*. Oxford, UK: Clarendon Press, 157–219.

Gould SJ. 2002. The Structure of Evolutionary Theory. Cambridge, MA: Belknap Press.

Gower DJ, Weber E. 1998. The braincase of *Euparkeria*, and the evolutionary relationships of birds and crocodilians. *Biological Reviews* **73**: 367–411.

Grafen A. **1989**. The Phylogenetic Regression. *Philosophical Transactions of the Royal Society B: Biological Sciences* **326**: 119–157.

Grady JM, Enquist BJ, Dettweiler-Robinson E, Wright NA, Smith FA. 2014. Evidence for mesothermy in dinosaurs. *Science* **344**: 1268–1272.

Gross W. 1934. Die Typen des mikroskopischen Knochenbaues bei foslen Stegocephalen und Reptilien. *Zeitschrift für Anatomie und Entwicklungsgeschichte* **103**: 731–764.

Guénard G, Legendre P, Peres-Neto P. 2013. Phylogenetic eigenvector maps: a framework to model and predict species traits. *Methods in Ecology and Evolution* **4**: 1120–1131.

Hackett SJ, Kimball RT, Reddy S, Bowie RCK, Braun EL, Braun MJ, Chojnowski JL, Cox A, Han K-L, Harshman J, Huddleston CJ, Marks BD, Miglia KJ, Moore WS, Sheldon FH, Steadman DW, Witt CC, Yuri T. 2008. A phylogenomic study of birds reveals their evolutionary history. *Science* **320**: 1763–1768.

Haddrath O, Baker AJ. **2012**. Multiple nuclear genes and retroposons support vicariance and dispersal of the palaeognaths, and an Early Cretaceous origin of modern birds. *Proceedings of the Royal Society B: Biological Sciences* **279**: 4617–4625.

Harrison GL, McLenachan PA, Phillips MJ, Slack KE, Cooper A, Penny D. 2004. Four new avian mitochondrial genomes help get to basic evolutionary questions in the late Cretaceous. *Molecular Biology and Evolution* **21**: 974–983.

Harshman J, Braun EL, Braun MJ, Huddleston CJ, Bowie RCK, Chojnowski JL, Hackett SJ, Han KL, Kimball RT, Marks BD, Miglia KJ, Moore WS, Reddy S, Sheldon FH, Steadman DW, Steppan SJ, Witt CC, Yuri T. **2008**. Phylogenomic evidence for multiple losses of flight in ratite birds. *Proceedings of the National Academy of Sciences* **105**: 13462–13467.

Harvey PH, Pagel MD. 1991. The Comparative Method in Evolutionary Biology. Oxford: Oxford University Press.

Havers C. 1691. Osteologia nova, or some new Observations of the Bones, and the Parts belonging to them, with the manner of their Accretion and Nutrition. Leyde: G Wishoff.

Haywood AM, Valdes PJ, Markwick PJ. **2004**. Cretaceous (Wealden) climates: a modelling perspective. *Cretaceous Research* **25**: 303–311.

Hennig W. **1975**. 'Cladistic Analysis or Cladistic Classification?': A Reply to Ernst Mayr. *Systematic Zoology* **24**: 244–256.

Houde PW. 1988. Paleognathous birds from the early Tertiary of the Northern Hemisphere. *Publications of the Nuttall Ornithological Club* **22**: 1–148.

Houde PW, Haubold H. **1987**. *Palaeotis weigelti* restudied: a small Middle Eocene ostrich (Aves: Struthioniformes). *Palaeovertebrata* **17**: 27–42.

Houssaye A, Tafforeau P, Herrel A. Amniote vertebral microanatomy – what are the major trends? *Biological Journal of the Linnean Society*. In press.

Houssaye A, Boistel R, Böhme W, Herrel A. 2013. Jack of all trades master of all? Snake vertebrae have a generalist inner organization. *Naturwissenschaften* **100**: 997–1006.

Horner JR, Padian K, de Ricqlès A. 2001. Comparative osteohistology of some embryonic and perinatal archosaurs: developmental and behavioral implications for dinosaurs. *Paleobiology* **27**: 39–58.

Hulbert AJ, Else PL. **2000**. Mechanisms Underlying the Cost of Living in Animals. *Annual Review of Physiology* **62**: 207–235.

Huttenlocker AK. **2014**. Body size reductions in nonmammalian eutheriodont therapsids (Synapsida) during the End-Permian mass extinction. *PLOS ONE* **9**: e87553.

Huttenlocker AK, Woodward H, Hall BK. 2013. The Biology of Bone. In: Padian K, Lamm ET, eds. *Bone Histology of Fossil Tetrapods: Advancing Methods, Analysis and Interpretation.* Berkeley, CA: University of California Press, 13-34.

Ives AR, Midford PE, Garland T. **2007**. Within-species variation and measurement error in phylogenetic comparative methods. *Systematic Biology* **56**: 252–270.

Janvier P. 1996. Early vertebrates. Oxford: Oxford University Press.

Johnston P. **2011**. New morphological evidence supports congruent phylogenies and Gondwana vicariance for palaeognathous birds. *Zoological Journal of the Linnean Society* **163**: 959–982.

Jombart T, Balloux F, Dray S. 2010. adephylo: new tools for investigating the phylogenetic signal in biological traits. *Bioinformatics* **26**: 1907–1909.

Kembel SW, Cowan PD, Helmus MR, Cornwell WK, Morlon H, Ackerly DD, Blomberg SP, Webb CO. 2010. Picante: R tools for integrating phylogenies and ecology. *Bioinformatics* **26**: 1463–1464.

Langer MC, Ezcurra, MD, Bittencourt JS, Novas FE. 2010. The origin and early evolution of dinosaurs. *Biological Reviews* **85**: 55–110.

Laurin M. 2004. The evolution of body size, Cope's rule and the origin of amniotes. *Systematic Biology* **53**: 594–622.

Laurin M, Reisz RR. 1995. A reevaluation of early amniote phylogeny. *Zoological Journal of the Linnean Society* **113**: 165–223.

Laurin M, Canoville A, Quilhac A. 2009. Use of paleontological and molecular data in supertrees for comparative studies: the example of lissamphibian femoral microanatomy. *Journal of Anatomy* **215**: 110–123.

Laurin M, Girondot M, Loth MM. **2004**. The evolution of long bone microstructure and lifestyle in lissamphibians. *Paleobiology* **30**: 589–613.

Laurin M, Gussekloo SWS, Marjanović D, Legendre L, Cubo J. 2012. Testing gradual and speciational models of evolution in extant taxa: the example of ratites. *Journal of Evolutionary Biology* **25**: 293–303.

Lee AH. 2013. Woven bone is not optically extinct under polarized light. *International Symposium on Paleohistology 2013*: abstract III.9.

Lee AH, Werning S. **2008**. Sexual maturity in growing dinosaurs does not fit reptilian growth models. *Proceedings of the National Academy of Sciences* **105**: 582–587.

Lee MSY. 2001. Molecules, morphology, and the monophyly of diapsid reptiles. *Contributions to Zoology* **70**: 1–18.

Legendre LJ, Segalen L, Cubo J. **2013**. Evidence for high bone growth rate in *Euparkeria* obtained using a new paleohistological inference model for the humerus. *Journal of Vertebrate Paleontology* **33**: 1343–1350.

Legendre L, Le Roy N, Martinez-Maza C, Montes L, Laurin M, Cubo J. **2013**. Phylogenetic signal in bone histology of amniotes revisited. *Zoologica Scripta* **42**: 44–53.

Legendre LJ, Bourdon E, Scofield RP, Tennyson AJD, Lamrous H, de Ricqlès A, Cubo J. Bone histology, phylogeny, and palaeognathous birds (*Aves*, Palaeognathae). *Biological Journal of the Linnean Society*. In press.

Legendre P, Lapointe FJ, Casgrain P. 1994. Modeling brain evolution from behavior: a permutational regression approach. *Evolution* **48**: 1487–1499.

Legendre P. 2000. Comparison of permutation methods for the partial correlation and partial Mantel tests. *Journal of Statistical Computation and Simulation* **67**: 37–73.

Leonard L, Dyke GJ, Van Tuinen M. 2005. A new specimen of the fossil palaeognath *Lithornis* from the Lower Eocene of Denmark. *American Museum Novitates* **3491**: 1–11.

Livezey BC, Zusi RL. **2007**. Higher-order phylogeny of modern birds (Theropoda, Aves: Neornithes) based on comparative anatomy. II. Analysis and discussion. *Zoological Journal of the Linnean Society* **149**: 1–95.

Longinelli A, Nuti S. 1973. Revised phosphate–water isotopic temperature scale. *Earth and Planetary Science Letters* **19**: 373–376.

Lyson TR, Bever GS, Bhullar BAS, Joyce WG, Gauthier JA. 2010. Transitional fossils and the origin of turtles. *Biology Letters* **6**: 830–833.

Maddison WP. 1991. Squared-change parsimony reconstructions of ancestral states for continuous-valued characters on a phylogenetic tree. *Systematic Zoology* **40**: 304–314.

Maddison WP, Maddison DR. 2011. *Mesquite: a modular system for evolutionary analysis. Version 2.75.* Available via http://mesquiteproject.org.

Maddison WP, Maddison DR, Midford PE. 2011. *TreeFarm package of modules for Mesquite. Version 2.75.* Available via http://mesquiteproject.org.

Mantel N. 1967. The detection of disease clustering and a generalized regression approach. *Cancer Research* **27**: 209–220.

de Margerie E. 2002. Laminar bone as an adaptation to torsional loads in flapping flight. *Journal of Anatomy* **201**: 521–526.

de Margerie E, Cubo J, Castanet J. **2002**. Bone typology and growth rate: testing and quantifying 'Amprino's rule' in the mallard *Anas platyrhynchos*. *Comptes rendus biologies* **325**: 221–230.

de Margerie E, Robin JP, Verrier D, Cubo J, Groscolas R, Castanet J. 2004. Assessing a relationship between bone microstructure and growth rate: a fluorescent labeling study in the king penguin chick (*Aptenodytes patagonicus*). *The Journal of Experimental Biology*, **207**: 869–879.

Marín-Moratalla N, Cubo J, Jordana X, Monconill-Sole B, Kohler M. Correlation of quantitative bone histology data with life history and climate: a phylogenetic approach. *Biological Journal of the Linnean Society*. In press.

Marjanović D, Laurin M. 2007. Fossils, molecules, divergence times, and the origin of lissamphibians. *Systematic Biology* **56**: 369–388.

Mateus O. 1998. *Lourinhanosaurus antunesi*, A New Upper Jurassic Allosauroid (Dinosauria: Theropoda) from Lourinhã, Portugal. *Memórias da Academia de Ciências de Lisboa* **37**: 111–124.

Mateus O, Wallen A, Antunes MT. 2006. The large theropod fauna of the Lourinhã Formation (Portugal) and its similarity to the Morrison Formation, with a description of a new species of *Allosaurus*. *New Mexico Museum of Natural History and Science Bulletin* **36**: 1–7.

Mayr E. 1961. Cause and effect in biology. *Science* **10**: 1501–1506.

Mayr G. 2009. Paleogene Fossil Birds. Berlin: Springer.

McNab BK. 1978. The evolution of endothermy in the phylogeny of mammals. *The American Naturalist* **112**: 1–21.

Meunier FJ. 2011. The Osteichthyes, from the Paleozoic to the extant time, through histology and palaeohistology of bony tissues. *Comptes Rendus Palevol* **10**: 347–355.

Midford PE, Garland Jr. T, Maddison WP. 2011. *PDAP package for Mesquite (Version 1.16).* Available via mesquiteproject.org/pdap_mesquite/index.Html

Montes L, Castanet J, Cubo J. **2010**. Relationship between bone growth rate and bone tissue organization in amniotes: first test of Amprino's rule in a phylogenetic context. *Animal Biology* **60**: 25–41.

Montes L, Le Roy N, Perret M, de Buffrénil V, Castanet J, Cubo J. **2007**. Relationships between bone growth rate, body mass and resting metabolic rate in growing amniotes: a phylogenetic approach. *Biological Journal of the Linnean Society* **92**: 63–76.

Mourer-Chauviré C, Senut B, Pickford M, Mein P. 1996. The oldest representative of the genus *Struthio* (Aves: Struthionidae), *Struthio coppensi* n. sp., from the Lower Miocene of Namibia. *Comptes-Rendus de l'Académie des Sciences* **322**: 325–332.

Müller J, Reisz RR. 2005. Four well-constrained calibration points from the vertebrate fossil record for molecular clock estimates. *BioEssays* **27**: 1069–1075.

Münkemüller T, Lavergne S, Bzeznik B, Dray S, Jombart T, Schiffers K, Thuiller W. **2012**. How to measure and test phylogenetic signal. *Methods in Ecology and Evolution* **3**: 743–756.

Myhrvold NP. **2013**. Revisiting the estimation of dinosaur growth rates. *PLOS ONE* **8**: e81917.

Nesbitt SJ. 2011. The early evolution of archosaurs: relationships and the origin of major clades. *Bulletin of the American Museum of Natural History* **352**: 1–292.

Nesbitt SJ, Stocker MR, Small BJ, Downs A. 2009. The osteology and relationships of *Vancleavea campi* (Reptilia: Archosauriformes). *Zoological Journal of the Linnean Society* **157**: 814–864.

Nespolo RF, Bacigalupe LD, Figueroa CC, Koteja P, Opazo JC. **2011**. Using new tools to solve an old problem: the evolution of endothermy in vertebrates. *Trends in Ecology & Evolution* **26**: 414–423.

Organ CL, Canoville A, Reisz RR, Laurin M. **2011**. Paleogenomic data suggest mammal-like genome size in the ancestral amniote and derived large genome size in amphibians. *Journal of Evolutionary Biology* **24**: 372–380.

Organ CL, Shedlock AM, Meade A, Pagel M, Edwards SV. 2007. Origin of avian genome size and structure in non-avian dinosaurs. *Nature* **446**: 180–184.

Ostrom JH. 1969. A new theropod dinosaur from the Lower Cretaceous of Montana. *Postilla* **128**: 1–17.

Ostrom JH. 1974. *Archaeopteryx* and the Origin of Flight. *The Quarterly Review of Biology* **49**: 27–47.

Padian K. 2013. Why Study the Bone Microstructure of Fossil Tetrapods? In: Padian K, Lamm ET, eds. *Bone Histology of Fossil Tetrapods: Advancing Methods, Analysis and Interpretation.* Berkeley, CA: University of California Press, 1–12.

Padian K, Horner JR, de Ricqlès A. **2004**. Growth in small dinosaurs and pterosaurs: the evolution of archosaurian growth strategies. *Journal of Vertebrate Paleontology* **24**: 555–571.

Padian, K, de Ricqlès A, Horner JR. 2001. Dinosaurian growth rates and bird origins. *Nature* **412**: 405–408.

Padian K, de Boef Miara M, Larsson HCE, Wilson L, Bromage T. 2013. Research Applications and Integration. In: Padian K, Lamm ET, eds. *Bone Histology of Fossil Tetrapods: Advancing Methods, Analysis and Interpretation.* Berkeley, CA: University of California Press, 265–285.

Pagel M. **1999**. Inferring the historical patterns of biological evolution. *Nature* **401**: 877–884.

Paradis E. **2012**. Analysis of Phylogenetics and Evolution with R (2nd edition). Berlin: Springer.

Paton T, Haddrath O, Baker AJ. 2002. Complete mitochondrial DNA genome sequences show that modern birds are not descended from transitional shorebirds. *Proceedings of the Royal Society B: Biological Sciences* **269**: 839–846.

Phillips MJ, Gibb GC, Crimp EA, Penny D. **2010**. Tinamous and Moa Flock Together: Mitochondrial Genome Sequence Analysis Reveals Independent Losses of Flight among Ratites. *Systematic Biology* **59**: 90–107.

de Pinna MCC. **1991**. Concepts and tests of homology in the cladistic paradigm. *Cladistics* **7**: 367–394.

Piras P, Teresi L, Buscalioni AD, Cubo J. 2009. The shadow of forgotten ancestors differently constrains the fate of Alligatoroidea and Crocodyloidea. *Global Ecology and Biogeography* **18**: 30–40.

Pyron RA. 2010. A likelihood method for assessing molecular divergence time estimates and the placement of fossil calibrations. *Systematic Biology* **59**: 185–194.

Queckett JT. 1849a. On the Intimate Structure of Bone as composing the Skeleton in the four great Classes of Animals, viz., Mammals, Birds, Reptiles and Fishes, with some Remarks on the great Value of the Knowledge of such Structure in determining the Affinities of Minute Fragments of Organic Remains. *Transactions of the Microscopical Society of London* **2**: 46–58.

Queckett JT. 1849b. Additional Observations on the Intimate Structure of Bone.

Transactions of the Microscopical Society of London **2**: 59–64.

Queckett JT. 1855. Descriptive and illustrated catalogue of the histological series contained in the Museum of the Royal College of Surgeons of England, vol. 2. Structure of the Skeleton of Vertebrate Animals. London, UK: R. and J.E. Taylor.

Reisz RR, Müller J. 2004. Molecular timescales and the fossil record: a paleontological perspective. *Trends in Genetics* **20**: 237–241.

Rensberger JM, Watabe M. 2000. Fine structure of bone dinosaurs, birds and mammals. *Nature* **406**: 619–623.

Revell LJ. 2010. Phylogenetic signal and linear regression on species data. *Methods in Ecology & Evolution* **1**: 319–329.

Revell LJ. 2012. phytools: an R package for phylogenetic comparative biology (and other things). *Methods in Ecology & Evolution* **3**: 217–223.

de Ricqlès A. 1975. Recherches paléohistologiques sur les os longs des tétrapodes VII. — Sur la classification, la signification fonctionnelle et l'histoire des tissus osseux des tétrapodes. Première partie. *Annales de Paléontologie* **61**: 51–129.

de Ricqlès A. 1976. Recherches paléohistologiques sur les os longs des tétrapodes VII. — Sur la classification, la signification fonctionnelle et l'histoire des tissus osseux des tétrapodes. Deuxième partie. *Annales de Paléontologie* **62**: 71–126.

de Ricqlès A. 1977a. Recherches paléohistologiques sur les os longs des tétrapodes VII. — Sur la classification, la signification fonctionnelle et l'histoire des tissus osseux des tétrapodes. Deuxième partie, suite. *Annales de Paléontologie* **63**: 33–56.

de Ricqlès A. 1977b. Recherches paléohistologiques sur les os longs des tétrapodes VII. — Sur la classification, la signification fonctionnelle et l'histoire des tissus osseux des tétrapodes. Deuxième partie, fin. *Annales de Paléontologie* **63**: 133–160.

de Ricqlès A. **1978**. Recherches paléohistologiques sur les os longs des Tétrapodes. VII. — Sur la classification, la signification fonctionnelle et l'histoire des tissus osseux des Tétrapodes. Troisième partie. *Annales de Paléontologie* **64**: 85–111.

de Ricqlès AJ. **2011**. Vertebrate palaeohistology: Past and future. *Comptes Rendus Palevol* **10**: 509–515.

de Ricqlès A, Castanet J, Francillon-Vieillot H. 2004. The "message" of bone tissue in paleoherpetology. *Italian Journal of Zoology, Supplement* **1**: 3–12.

de Ricqlès AJ, Padian K, Horner JR. 2003. On the bone histology of some Triassic pseudosuchian archosaurs and related taxa. *Annales de Paléontologie* **89**: 67–101.

de Ricqlès A, Mateus O, Antunes MT, Taquet P. 2001. Histomorphogenesis of embryos of

Upper Jurassic Theropods from Lourinhã (Portugal). *Comptes-Rendus de l'Académie des Sciences de Paris, Sciences de la Terre et des Planètes / Earth and Planetary Sciences* **332**: 647–656.

de Ricqlès A, Meunier FJ, Castanet J, Francillon-Vieillot H. **1991**. Comparative microstructure of bone. In: Hall BK, ed. *Bone, Volume 3: Bone matrix and bone specific products.* Boca Raton, FL: CRC Press, 1–78.

de Ricqlès A, Padian K, Knoll F, Horner JR. 2008. On the origin of high growth rates in archosaurs and their ancient relatives: complementary histological studies on Triassic archosauriforms and the problem of a "phylogenetic signal" in bone histology. *Annales de Paléontologie* **94**: 57–76.

Rieppel O. 1988. The classification of the Squamata. In: Benton MJ, ed. *The Phylogeny and Classification of the Tetrapods*. Oxford, UK: Clarendon Press, 261–293.

Rieppel O, Reisz RR. 1999. The origin and early evolution of turtles. *Annual Review of Ecology and Systematics* **30**: 1–22.

Ruben J. **1995**. The evolution of endothermy in mammals and birds: from physiology to fossils. *Annual Review of Physiology* **57**: 69–95.

Rubidge BS. 2005. Re-uniting lost continents – fossil reptiles from the ancient Karoo and their wanderlust. *South African Journal of Geology* **108**: 135–172.

Sander PM. 2000. Longbone histology of the Tendaguru sauropods: implications for growth and biology. *Paleobiology* **26**: 466–488.

Santos T, Diniz-Filho JAF, Rangel T, Bini LM. 2012. *PVR: computes phylogenetic eigenvectors regression (PVR) and phylogenetic signal-representation curve (PSR) (with null and Brownian expectations), Version 0.2.1*. Available via: http://cran.r-project.org/web/packages/PVR/index.html

Schmid J, Ruf T, Heldmaier G. **2000**. Metabolism and temperature regulation during daily torpor in the smallest primate, the pygmy mouse lemur (*Microcebus myoxinus*) in Madagascar. *Journal of Comparative Physiology B* **170**: 59–68.

Schneider CA, Rasband WS, Eliceiri KW. 2012. NIH Image to ImageJ: 25 years of image analysis. *Nature Methods* **9**: 671–675.

Seebacher F. **2003**. Dinosaur body temperatures: the occurrence of endothermy and ectothermy. *Paleobiology* **29**: 105–122.

Seilacher A. 1970. Arbeitskonzept zur Konstruktions-Morphologie. *Lethaia* **3**:393–396.

Sellwood BW, Valdes PJ. **2006**. Mesozoic climates: General circulation models and the rock record. *Sedimentary Geology* **190**: 269–287.

Seymour RS. 1976. Dinosaurs, endothermy, and blood pressure. *Nature* **262**: 207–208.

Seymour RS. **2013**. Maximal aerobic and anaerobic power generation in large crocodiles versus mammals: implications for dinosaur gigantothermy. *PLOS ONE* **8**: e69361.

Seymour RS, Bennett-Stamper CL, Johnston SD, Carrier DR, Grigg GC. 2004. Evidence for Endothermic Ancestors of Crocodiles at the Stem of Archosaur Evolution. *Physiological and Biochemical Zoology* **77**: 1051–1067.

Sibley CG, Ahlquist JE. 1990. Phylogeny and Classification of Birds: A Study in Molecular Evolution. New Haven, CT: Yale University Press.

Slack KE, Delsuc F, McLenachan PA, Arnason U, Penny D. 2006. Resolving the root of avian mitogenomic tree by breaking up long branches. *Molecular Phylogenetics and Evolution* **42**: 1–13.

Smith JV, Braun EL, Kimball RT. **2013**. Ratite Nonmonophyly: Independent Evidence from 40 Novel Loci. *Systematic Biology* **62**: 35–49.

Spielmann JA, Lucas SG, Rinehart LF, Hunt AP, Heckert AB, Sullivan RM. 2007. Oldest records of the Late Triassic theropod dinosaur *Coelophysis bauri*. *New Mexico Museum of Natural History and Science Bulletin* **41**: 384–401.

Stein K, Prondvai E. **2014**. Rethinking the nature of fibrolamellar bone: an integrative biological revision of sauropod plexiform bone formation. *Biological Reviews* **89**: 24–47.

Stein KWH, Werner J. **2013**. Preliminary analysis of asteocyte lacunar density in long bones of tetrapods: All measures are bigger in sauropod dinosaurs. *PLOS ONE* **8**: e77109.

Summers AP. 2005. Warm-hearted crocs. *Nature* **434**: 833–834.

Tennyson AJD, Worthy TH, Jones CM, Scofield RP, Hand SJ. 2010. Moa's Ark: Miocene fossils reveal the great antiquity of moa (Aves: Dinornithiformes) in Zealandia. *Records of the Australian Museum* **62**: 105–114.

Tumarkin-Deratzian AR. 2007. Fibrolamellar Bone in Wild Adult *Alligator mississipiensis*. *Journal of Herpetology* **41**: 341–345.

Van Tuinen M, Sibley CG, Hedges SB. 2000. The early history of modern birds inferred from DNA sequences of nuclear and mitochondrial ribosomal genes. *Molecular Biology Evolution* **17**: 451–457.

Walter I, Seebacher F. **2009**. Endothermy in birds: underlying molecular mechanisms. *The Journal of Experimental Biology* **212**: 2328–2336.

Werning S, Irmis RB. 2011. Reconstructing growth of the basal archosauromorph *Trilophosaurus*. *Society for Integrative and Comparative Biology 2010 Annual Meeting*: abstract 39.2.

Werning S, Irmis R, Smith N, Turner A, Padian K. 2011. Archosauromorph bone histology reveals early evolution of elevated growth and metabolic rates. *Programs and Abstracts, 71st Annual Meeting, Society of Vertebrate Paleontology* p. 213.

White CR, Seymour RS. 2005. Sample size and mass range effects on the allometric exponent of basal metabolic rate. *Comparative Biochemistry and Physiology – Part A: Molecular & Integrative Physiology* **142**: 74–78.

Whiteside DI, Marshall JEA. 2008. The age, fauna and palaeoenvironment of the Late Triassic fissure deposits of Tytherington, South Gloucestershire, UK. *Geological Magazine* **145**: 105–147.

Withers PC. 1992. Comparative Animal Physiology. Boston, MA: Brooks/Cole.

Worthy TH, Holdaway RN. 2002. The Lost World of the Moa: Prehistoric Life of New Zealand. Bloomington: Indiana University Press.

Worthy TH, Scofield RP. **2012**. Twenty-first century advances in knowledge of the biology of moa (Aves: Dinornithiformes): a new morphological analysis and moa diagnoses revised. *New Zealand Journal of Zoology* **39**: 87–153.

Worthy TH, Tennyson AJD, Jones C, McNamara JA, Douglas BJ. **2007**. Miocene waterfowl and other birds from central Otago, New Zealand. *Journal of Systematic Palaeontology* **5**: 1–39.

Worthy TH, Worthy JP, Tennyson AJD, Salisbury SW, Hand SJ, Scofield RP. 2013. Miocene fossils show that kiwi (*Apteryx*, Apterygidae) are probably not phyletic dwarves. In: Göhlich UB, Kroh A, eds. *Proceedings of the 8th International Meeting of the Society of Avian Paleontology and Evolution*. Vienna, Austria: Verlag Naturhistorisches Museum Wien, 63–80.

Zardoya R, Meyer A. 2001. The evolutionary position of turtles revised. *Naturwissenschaften* **88**: 193–200.

ANNEXES

Publications collatérales à la thèse

Annexe I – Testing gradual and speciational models of evolution in extant taxa: the example of ratites

Michel Laurin, Sander W. S. Gussekloo, David Marjanović,

Lucas Legendre et Jorge Cubo

Publication originale *in*: *Journal of Evolutionary Biology* **25**: 293–303 (Février 2012)

Abstract

Ever since Eldredge and Gould proposed their model of punctuated equilibria, evolutionary biologists have debated how often this model is the best description of nature and how important it is compared to the more gradual models of evolution expected from natural selection and the neo-Darwinian paradigm. Recently, Cubo proposed a method to test whether morphological data in extant ratites are more compatible with a gradual or with a speciational model (close to the punctuated equilibrium model). As shown by our simulations, a new method to test the mode of evolution of characters (involving regression of standardized contrasts on their expected standard deviation) is easier to implement and more powerful than the previously proposed method, but the Mesquite module CoMET (aimed at investigating evolutionary models using comparative data) performs better still. Uncertainties in branch length estimates are probably the largest source of potential error. Cubo hypothesized that heterochronic mechanisms may underlie morphological changes in bone shape during the evolution of ratites. He predicted that the outcome of these changes may be consistent with a speciational model of character evolution because heterochronic changes can be instantaneous in terms of geological time. Analysis of a more extensive data set confirms his prediction despite branch length uncertainties: evolution in ratites has been mostly speciational for shape-related characters. However, it has been mostly gradual for size-related ones.

Keywords: birds – comparative studies – morphometrics – phylogenetics – simulations

Introduction

The proposal of the model of punctuated equilibria by Gould & Eldredge (1977) triggered a debate about the tempo and mode of evolution. Several palaeontological studies attempted to determine which of the two main models (natural selection with variable rates of evolution, or punctuated equilibria characterized by long periods of stasis interrupted by brief periods of change that coincide with cladogenetic events) was most compatible with data from several successive populations representing a few evolving lineages sampled over relatively long periods of time (several tens of thousands of years to a few million years). Based on a review of the literature (including previous reviews), Benton & Pearson (2001) argued that both patterns occur in the fossil record of eukaryotes, but that in unicellular eukaryotes of the marine plankton, gradual evolution prevails, whereas in metazoans, a punctuated equilibrium pattern may be more common. However, this latter conclusion remains tentative because the fossil record of metazoans is much less complete than that of many unicellular organisms with mineralized skeletons.

Evolutionary models of characters are interesting because they can produce evidence for the presence of selection and trends, limits on character value, and patterns of change and thus contribute to refining evolutionary theory. Determining the correct evolutionary model is also important because modern comparative methods used to test character correlation and infer ancestral values assume a Brownian motion model, whereas strong departures from this model can lead to inaccurate results (Díaz-Uriarte & Garland, 1996; Martins, Diniz-Filho & Housworth, 2002). Punctuated equilibrium is such a departure. Comparative data that result from such an evolutionary model can be analysed by most comparative tests, but instead of using branch lengths proportional to evolutionary time or to the variance observed in other

characters (which may have evolved according to other models), branches of equal lengths on a tree including a representative sample of all known (extant and extinct) lineages of a clade should be used. Using appropriate branch lengths should lead to more accurate estimates of correlation and ancestral values.

More recently, comparative data from extant taxa have been used to investigate the preponderance of these evolutionary models. Ratites are good candidates to test models of character evolution because this clade contains a low number of species (thus making exhaustive sampling possible). Note that the model of punctuated equilibria has two variants: (i) the punctuational model, in which changes occur at the time of speciation (cladogenesis) only in a single daughter species (clade), and (ii) the speciational model, according to which changes occur at the time of speciation in both daughter species (clades) (Rohlf *et al.*, 1990). Cubo (2003) recently proposed a method to test whether a character evolved according to a gradualist or a speciational model. His test is based on determining which phylogenetic distance matrix best explains the phenotypic distance matrix of the relevant character. One matrix is based on estimated times of divergence between terminal taxa and represents a gradual model of evolution, whereas the other has unitary branch lengths and represents a speciational model of evolution. Thus, Cubo (2003) regressed distance matrices of individual characters against the phylogenetic distance matrices of the taxa assuming gradual evolution (branch lengths reflecting evolutionary time) and a speciational model (branches were of equal lengths). His data set included dimensionless shape variables: the ratio diaphyseal diameter ⁄ total length of stylopodial (humerus and femur) and zeugopodial bones (ulna, radius and tibiotarsus) and the ratio wing length ⁄ leg length. Cubo (2003) tested the significance of these regressions using permutations. This procedure suggested that some phylogenetic distance matrices explained the character data better than others, as shown by

the probability that the regression coefficients reflected random fluctuations. However, in some cases, neither phylogenetic distance matrix seemed to explain the character data, whereas in others, both the gradual and the speciational model of evolution seemed to be compatible with the data. Thus, the resolution of this method may not be optimal. We propose instead to regress standardized contrasts on their expected standard deviation, a test that is implemented in Mesquite, and we use simulations to assess the relative merits of both tests, as well as the performance of a third approach available in the Mesquite module CoMET (Lee *et al.*, 2006).

One of the most sophisticated tools to investigate evolutionary model using comparative data is the Mesquite module CoMET, which uses maximum likelihood and the Akaike Information Criterion (AIC) values to compare the fit of nine evolutionary models to the data (Lee *et al.*, 2006). This implements methods presented in more detail by Oakley *et al.* (2005). The nine models represent all possible combinations of two properties of the model, each of which can follow one of three submodels (Lee *et al.*, 2006: fig. 1). Thus, evolutionary change can be purely phylogenetic (each branch of the reference phylogeny is used), nonphylogenetic (only terminal branches are used, the internal ones are set to 0) or punctuated, in which only one of every pair of sister branches stemming from a node has a positive length (the other is set to 0). The length of the branches can follow the reference phylogeny ('distance' in the terminology of Lee *et al.*, 2006), can be of equal length or can be estimated from the data ('free' in the terminology of Lee *et al.*, 2006). The evolutionary model that Cubo (2003) called gradual is the distance, purely phylogenetic model of Lee *et al.* (2006), whereas Cubo's (2003) speciational model is Lee *et al.*'s (2006) equal, pure phylogenetic model. Note that in this last model, according to Mooers *et al.* (1999), phenotypic change between taxa is proportional to the number of speciation events

(cladogeneses) that have occurred between them.

Later, we use CoMET to reanalyse the data on appendicular bone shape, based on which Cubo (2003) argued for a mostly speciational model of evolutionary change in osteological characters in ‘ratites’. We added 48 characters to this data set. These analyses were performed using a phylogeny based on morphological characters and suggesting that ratites are monophyletic (Bourdon, de Ricqlès & Cubo, 2009), as well as on three molecular phylogenies.

Methods

Analysis of the evolutionary model (gradual/speciational)

We tested the performance of the test developed by Cubo (2003) to determine whether a character evolved according to a gradualist or a speciational model. For this purpose, we simulated the evolution of 100 characters using a Brownian motion model in Mesquite (Maddison & Maddison, 2011) on two phylogenies (Fig. 1a, c) with 36 terminal taxa. These represent the characters that have evolved according to a gradual model. We also simulated the evolution of 100 characters using a Brownian motion model on two phylogenies with unitary branch lengths (Fig. 1b, d); these represent the characters that have evolved according to a speciational model. We then regressed distance matrices obtained from each character against the phylogenetic distance matrices that reflect two phylogenies: (i) the original phylogeny; (ii) a phylogeny with the same topology in which all branches were of equal length. As in Cubo (2003), the test is based on determining which phylogenetic distance matrix (one is based on estimated times of divergence between terminal taxa, whereas the

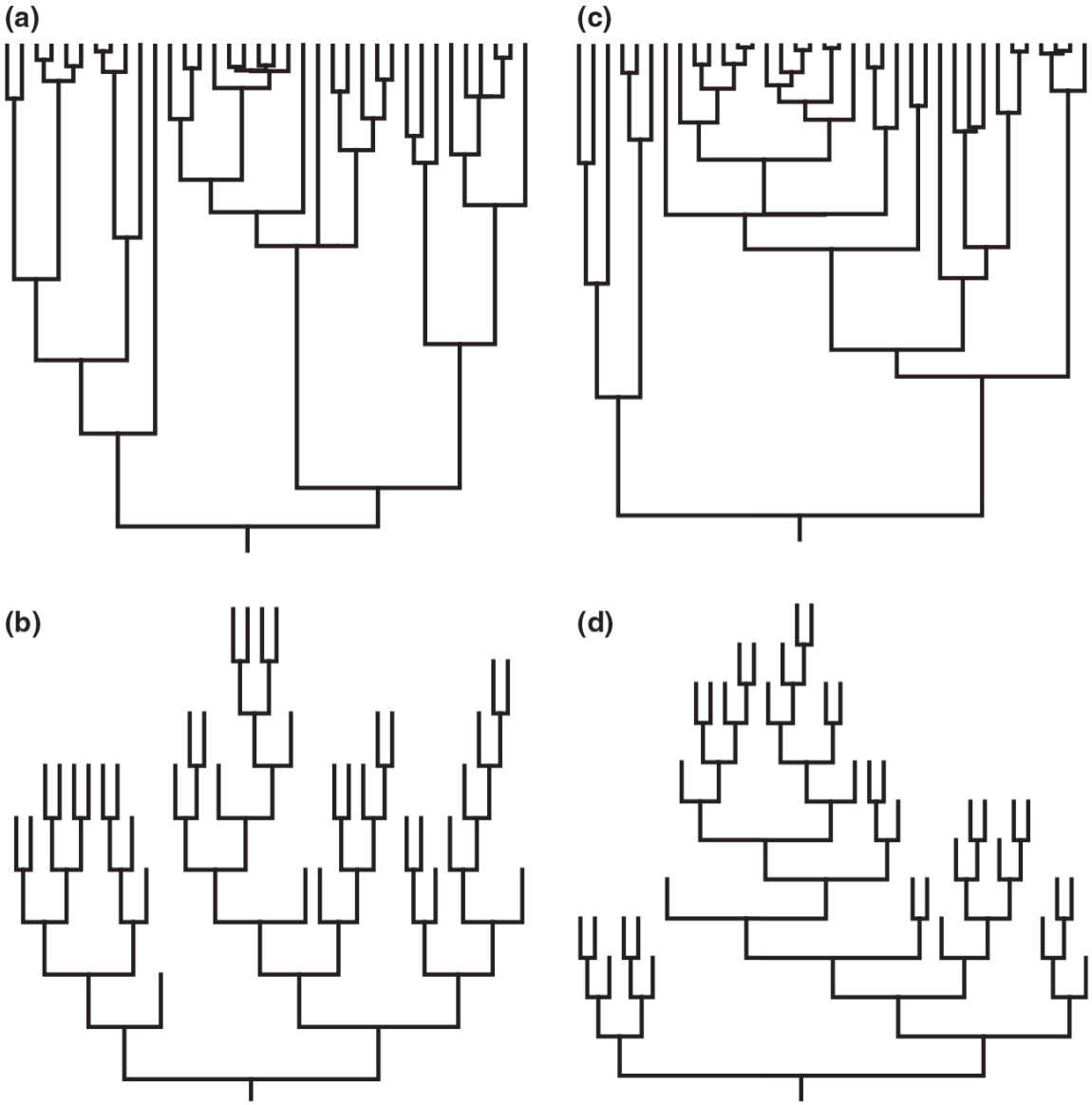

Figure 1. Trees used to establish the validity of two proposed methods to determine whether characters evolved according to a speciational or a gradualistic model of evolution. (a) The first random (Yule) tree produced by Mesquite used to simulate the characters that evolve according to a Brownian motion model. This also represents the true tree (in which branch lengths represent time). (b) Tree of identical topology but in which all branches are of equal length. This tree was used to generate characters that evolve according to a speciational model of evolution. Note that branch lengths do not represent time here; the true tree, in which branch lengths represent time, is still represented by (a). Similar pairs are presented for the second (c, d) random tree, also generated using a Yule process.

other has unitary branch lengths) best explains the distance matrix of the relevant character. For this purpose, we regressed distance matrices of individual characters against the phylogenetic distance matrices using multiple linear regressions. The significance of these regressions was tested using permutations and a forward selection procedure (p-to-enter =

0.05). Cubo (2003) used a similar procedure to discriminate between two main alternative sets of branch lengths: the original branch lengths (implying a gradual model) and equal branch lengths implying a speciational model.

In our tests using Cubo's (2003) original implementation, the procedure using forward selection selects the variable (in this case, a phylogenetic distance matrix representing a tree) with the most significant coefficient of correlation (lowest probability, not necessarily the highest R^2), provided that both the probability of the R^2 and of the b coefficient (slope) are inferior to the p-to-enter (here, 0.05 for the first step of the analysis). Then, the remaining variable(s) are tested to determine whether their addition significantly improves the regression model (using multiple regression); again, if both the probabilities of the R^2 and of the b coefficient are inferior to the p-to-enter value (here 0.025 because at this step, it must be half of the p-to-enter value of the first step), the variable is entered into the model. With two competing trees, this analysis requires up to two steps (a single step is required minimally, in the cases in which none of the trees yields a significant regression). The statistical significance of the R^2 and the b coefficient is tested using 999 permutations in the program Permute! (Casgrain, 2009); the regression on the unpermuted values is added to this sample of randomized data, which makes the test conservative. Thus, up to 3000 individual regressions are used to determine which tree(s) correspond to the model of character evolution. In sum, over 1200000 regressions were performed for this study. Given that the forward selection procedure can select more than one tree, the accuracy score of the test is $1/n$, where n is the number of selected trees, provided that the latter included the correct tree. If none of the trees were selected, the correctness score is 0. The values reported later are the average of the correctness scores for 100 characters.

We also evaluated two other related but somewhat simpler procedures to determine the evolutionary model of a character, which consists of choosing the tree that has the lowest probability (even if it is > 0.05) associated with the explained variance or with the b coefficient in the first step of the forward selection procedure. In case of a tie, the correctness score is $1 / n$, where n is the number of selected trees, provided that the latter includes the correct tree.

We also test the performance of a second method to establish whether a character has evolved according to a gradual or to a speciational model. This method consists in regressing standardized contrasts on their expected standard deviation (based on the branch lengths), a method that is implemented in Mesquite and which is commonly used to determine whether selected branch lengths are adequate to standardize data prior to performing an analysis of phylogenetically independent contrasts (e.g. Laurin, 2004; Cubo *et al.*, 2005). If the character has evolved according to a Brownian motion model and the branch lengths have been estimated correctly, there should be no significant relationship (the slope should be about 0 and its associated probability should be high, typically over 0.05, reflecting adequate contrast standardization), but unitary branch lengths should provide inferior standardization (the probability associated with the slope should be lower). If the character has evolved according to a speciational model, a nonsignificant relationship will usually be found using unitary branch lengths, provided that all cladogeneses are documented (or a representative sample thereof), including those that have given rise to lineages that are now extinct. Conversely, branch lengths reflecting time should yield inferior standardization (with a lower probability associated with the slope). This test thus selects the phylogeny with the highest probability associated with the linear regression slope between standardized contrasts and branch lengths as the best one. Note that the test used by Cubo (2003), as well as any other test that we could

imagine, is also subject to this latter (and most problematic) requirement when a speciational model is among those tested. Clearly, the quality of the fossil record is the most limiting factor in our ability to detect speciational change from comparative data.

Lastly, we tested the performance of CoMET (Lee *et al.*, 2006) by determining which of the two models of interest (pure phylogenetic／distance and pure phylogenetic／equal) best fit the data (lower AIC scores are better). When the best model was neither of these two, we still scored the character on the basis of the fit of both of these models, ignoring the score of the seven other models. We followed the same procedure in our analysis of the empirical ratite data set.

All our tests of the methods relied on two random trees generated by the Yule algorithm of Mesquite, to cover a diversity of tree symmetry and branch length distribution. Testing the impact of tree symmetry, number of taxa, and branch length distribution would of course improve reliability of such tests, but such a procedure would require software development that is beyond the scope of this study.

Description of characters

The skull was described using a total number of 18 continuous characters distributed over the ventral side of the cranium (Table 1). Each character was measured twice using a digital caliper (accuracy 0.01 mm; Sylvac, Crissier, Switzerland). The average of the two values was used for further analysis. To reduce size effects, all character were scaled to the width of the skull measured at the quadrate–jugal articulation (parameter A), which adds 17 continuous characters to the data set. When possible, multiple specimens of a single species

A: Skull width at the quadrate–jugal articulation (standard)
B: Distance between most distal points of *proc. orbitales quadrati*
C: Width at pterygoids at quadrate–pterygoid articulation
D: Width at most rostral part of pterygoids at the pterygoid–palatine connection
E: Maximal width of the right pterygoid in the transversal plane
F: Width of the vomer (caudal)
G: Width of the vomer (rostral)
H: Distance between the *anguli caudolaterales* of the palatal wings (*pars lateralis*)
I: Maximal distance between the lateral margins of the palatal wings at their rostral endings
J: Width between palates at position 'I'
K: Width at most caudal part of the palatines at the pterygoid–palate connection
L: Width between the connection of the *proc. palatinus* and *proc. jugalis* of the maxilla
M: Width of the *rostrum parasphenoidale* incl. *proc. basipterygoidei* if present
N: Distance *foramen magnum* to measurement 'N'
O: Distance *foramen magnum* to most caudal part of an element of the PPC connecting or crossing the *r. parasphenoidale*
P: Maximal length palatine
Q: Width at palatine–maxillae articulation
R: Internal width at palatine–maxillae articulation

Table 1. Description of the continuous morphological characters representing the ventral side of the cranium of ratites and related taxa. These correspond to characters 20–37 (raw measurements) and characters 38–54 (standardized characters) in Data S1–S3. They are denoted by the same letter followed by 'm' (for raw measurement) or 's' (standardized) in Data S1–S3.

were measured to obtain a mean species value for the analysis. When a character was absent, the value for this character was set to be zero. In four cases, the museum specimens were incomplete and some characters could not be measured. Only if less than three characters were impossible to measure was the specimen included in the analysis. In four such cases, missing values were calculated based on the mean relative value of the species in the same genus. These relative values were then used to calculate absolute values for the missing parameter. The characters used in the analyse give a good description of the palatine–pterygoid complex (PPC) (Gussekloo & Zweers, 1999; Gussekloo & Bout, 2002), which plays an important role in the cranial kinesis of birds (Zusi, 1984). The pterygoid, the palatine and in some cases the vomer are bony elements that play an important role in transferring muscle force to either open or close the upper bill (Bock, 1964; Gussekloo, Vosselman & Bout, 2001).

The morphology of appendicular bones was quantified through measurements of total length and diaphyseal diameter of stylopodial bones (humerus and femur) and zeugopodial

bones (ulna, radius and tibiotarsus) to the nearest 0.01 mm using a digital caliper (Roch, Lunéville, France). Dimensionless variables were computed: for each bone, the ratio diaphyseal diameter/total length was calculated (shape characters). In addition, the ratio wing length / leg length was also calculated (limb length was computed as stylopodial length + zeugopodial length). Thirteen appendicular bone characters were added to the data set by Cubo (2003): the 10 size characters used to compute shape characters (*i.e.* total length and diaphyseal diameter of stylopodial and zeugopodial bones) plus tarsometatarsus total length, diaphyseal diameter and shape. Mean values of these ratios for each species were used, assuming no sampling error because of small sample sizes. Data were collected for twelve species, but each character is documented for ten species (not always the same ones). All data can be found in Data S1.

Choice of the reference phylogenies and temporal calibration

Ratite phylogeny is still in a state of flux, with important differences between molecular (Cooper *et al.*, 2001; Haddrath & Baker, 2001; Hackett *et al.*, 2008; Harshman *et al.*, 2008; Phillips *et al.*, 2010; Johnston, 2011; and references therein) and morphological studies (Bourdon *et al.*, 2009, and references therein), and even between studies using the same kind of evidence. Divergence times are even more difficult to estimate within the context of a molecular phylogeny, although Phillips *et al.* (2010) provide a very good starting point. For all these reasons, and because Cubo (2003) had used two phylogenies (Cooper *et al.*, 2001; Haddrath & Baker, 2001), we decided to use four phylogenies to test evolutionary models in ratites. These include those of Cooper *et al.* (2001: fig. 2) and Haddrath & Baker (2001: fig. 2), both as modified by Cubo (2003: fig. 1a), and Phillips *et al.* (2010: fig. 5), which are all molecular phylogenies, as well as a morphological one (Bourdon *et al.*, 2009)

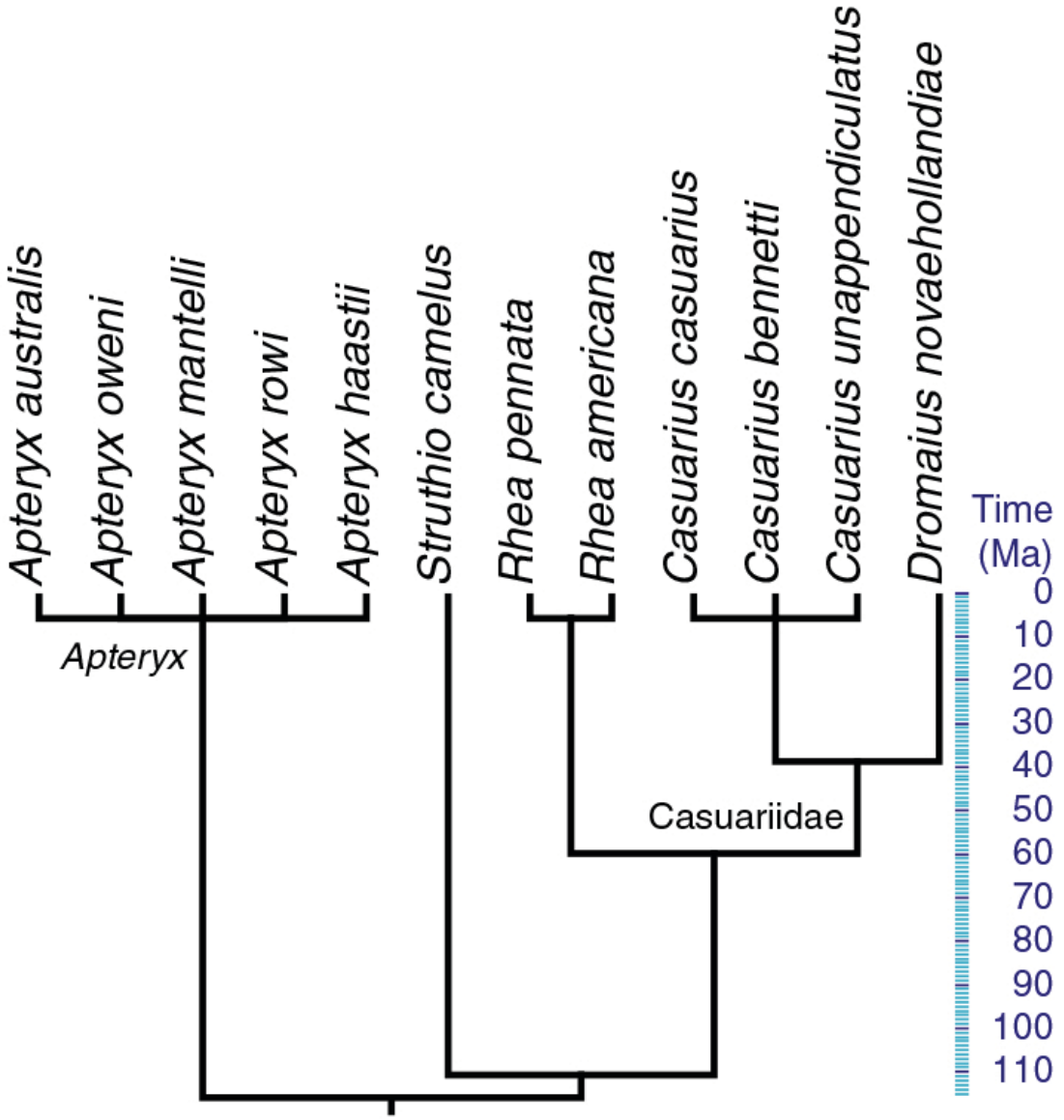

Figure 2. One of the four trees (called 'palaeontological tree' in the text) used for the species-level analysis of the ratite empirical data set. The genus-level analysis was carried out by pruning the tree to retain one terminal taxon per genus and by inserting the generic averages into the remaining taxa.

---

that we dated using a combination of fossil and biogeographical data. These four trees allow us to assess the robustness of our results to phylogenetic uncertainties.

Bourdon *et al.* (2009), using 129 morphological characters, assumed that ratites were monophyletic, but were unable to find evidence for the monophyly of extant Australasian ratites suggested by all molecular studies. Bourdon *et al.* (2009) found the New Zealand

ratites (kiwis plus moas) as the sister group of all other ratites. Within this last clade, the aepyornithids (Madagascar) are the sister group of a clade comprising all other extant ratites. Finally, *Struthio* (Africa) and *Rhea* (South America) are successive sister groups of the Australian *Casuarius-Dromaius* clade (Bourdon *et al.*, 2009).

To date the tree by Bourdon *et al.* (2009), we estimated divergence times using well-known ratite fossils: the minimal age for a node was determined by the age of the oldest fossil included in this node, if there is one. The divergence between *Dromaius* and *Casuarius* was dated to 35–38 Ma, following Boles (2001) and Paton, Haddrath & Baker (2002). The oldest known ratite, *Diogenornis fragilis*, has been identified as a rheid (Alvarenga, 1983; Mayr, 2009), allowing us to estimate an age of 56–59 Ma for the divergence Rheidae/Casuaridae, in the late Palaeocene. Other Tertiary ratite fossils were not relevant in this study, because there were either too recent to estimate the age of other nodes (Mourer-Chauviré *et al.*, 1996; Bertelli & Chiappe, 2005) or not well enough known to unambiguously estimate their position in the phylogeny (Houde, 1986; Houde & Haubold, 1987; Grellet-Tinner & Dyke, 2005; Mayr, 2005; Bibi *et al.*, 2006). A possible exception is the Eocene *Lithornis*, but its affinities may be with tinamous (Grellet-Tinner & Dyke, 2005; Johnston, 2011), which would place it outside ratites and hence outside the sampled taxa on the topology of Bourdon *et al.* (2009).

Vicariance biogeography proved to be congruent with the ages estimated by the use of fossils, and some ornithologists have hypothesized that all ratites are descended from a flightless ancestor that was widespread in Gondwana (see for instance Cracraft, 1973, 1974, 2001; Bourdon *et al.*, 2009). This hypothesis allowed us to use geological events to date parts of the tree. Indeed, South America and Australia remained in contact through Antarctica until the Paleogene (Woodburne & Case, 1996), and sweepstake dispersal was still possible until

the early Eocene (Veevers, Powell & Roots, 1991; Lawver, Gahagan & Coffin, 1992). Thus, we estimated a divergence time between the South American *Rhea* clade and the Australian *Casuarius-Dromaius* clade at 60 Ma, which is consistent with the age of *Diogenornis*, the first South American ratite. The loss of contact between Australia and south-east Papua occurred in the early Eocene (Veevers & McElhinny, 1976), about 25 Ma before the divergence between *Casuarius* and *Dromaius*. Africa drifted away from South America (and thus from Antarctica) in the late Albian (Scotese, 2001), which may fix the divergence between *Struthio* and the clade Rheidae-Casuaridae at 90–110 Ma. However, this is tentative because there is no fossil record of paleognaths in Africa before the Miocene, by which time there are ostriches both there and in Eurasia. Phillips *et al.* (2010: 102) suggest that ostriches invaded Africa from Eurasia in the Miocene, but that is not certain because this is based on claimed close relationships between the mid-Eocene Palaeotis from Messel (Germany) and ostriches, for which Phillips *et al.* (2010: 99) cite Houde (1986), whereas a more recent unpublished analysis cited by Dyke & van Tuinen (2004: 161) has instead found it to be a stem-ratite. We estimated that the divergence between Aepyornithidae and the clade Struthio-Rheidae-Casuaridae occurred between 130 and 110 Ma, as the Madagascar/India block drifted away from Antarctica in the Early Cretaceous (Scotese, 2001).

The palaeogeographic dating roots the clade of paleognathous birds in the Early Cretaceous, a very old estimate compared to the oldest undoubted ratite fossils known from the Paleogene (around half the age of the Early Cretaceous) or indeed the oldest undoubted fossils of crown-group birds (Kurochkin, Dyke & Karhu, 2002; Clarke *et al.*, 2005) and their sister group (Clarke & Chiappe, 2001) from the end of the Cretaceous. The much lower ages implied by the fossil record (Hope, 2002; Clarke, 2004) would require several independent losses of flight among ratites during the Tertiary to explain their distribution and thus much

morphological convergence between the various ratite taxa. This hypothesis is suggested by the most recent molecular phylogenies, which place tinamous within ratites (Hackett *et al.*, 2008; Harshman *et al.*, 2008; Phillips *et al.*, 2010), but this is unproblematic because we have included such phylogenies among those used in our tests; we have not changed the dates of the molecular phylogenies.

A problem in the vicariance model is the case of New Zealand ratites, because New Zealand drifted away from Antarctica after the separation between Madagascar and Antarctica. Assuming ratite monophyly and a single loss of flight, as we have done to date the tree by Bourdon *et al.* (2009), this incongruence can be resolved only by the hypothesis that the initial divergence between the moa-kiwi lineage and all other ratites occurred before the separation of Gondwana and New Zeland, and that differential extinction events led to the extinction of the other ratite lineage in New Zealand, and the extinction of the kiwi-moa lineage on other continents, as suggested by Bourdon *et al.* (2009). The fossil record is so far silent on this question.

We did not find palaeontological or molecular data that could be used to reliably date the divergences between species. Thus, we simply inserted the minimal branch lengths that we enforced throughout all trees (5 Myr) between species, whenever molecular ages were unavailable. This is analogous to the method proposed by Laurin, Canoville & Quilhac (2009) to deal with missing branch length data in comparative analyses. For the two other trees, we used the branch lengths shown in Cubo (2003: fig. 1a). However, to assess whether unreliable branch lengths between closely related species (within genera) favour the speciational model over the gradual one, we performed the analyses using generic averages (first analysis) for all characters and repeated them using species data (second analysis) for the four trees.

Test	True evolutionary model of the characters	Proportion of simulations in which each method yields correct results		
		Tree 1	Tree 2	Average for the two trees
Cubo (2003), matrix selection	Gradual	0.610	0.050	0.330
Cubo (2003), matrix selection, modified	Gradual	0.600	0.170	0.385
Cubo (2003), slope	Gradual	0.605	0.275	0.440
Contrast	Gradual	0.770	0.760	0.765
CoMET	Gradual	0.950	0.970	0.960
Cubo (2003), matrix selection	Speciational	0.610	0.820	0.715
Cubo (2003), matrix selection, modified	Speciational	0.570	0.940	0.755
Cubo (2003), slope	Speciational	0.550	0.935	0.742
Contrast	Speciational	0.970	0.990	0.980
CoMET	Speciational	0.970	0.990	0.980

Table 2. Power of the three tests to determine whether a character evolved according to a gradualistic or a speciational model. These are the test proposed by Cubo (2003), as originally implemented ('matrix selection'), modified to use the smallest probability (even if greater than 0.05) associated with the explained variance, modified to use the probability associated with the slope, the test using phylogenetic independent contrasts and the maximum likelihood test (using AIC scores) implemented in CoMET (Lee *et al.*, 2006). In the tests of Cubo and the new contrast-based test, four trees were used to discriminate between the models: two topologies and two evolutionary models (one in which the branch lengths reflect geological time, and another with unitary branch lengths). The original method by Cubo (2003) is based on linear regressions between phylogenetic distance and phenetic distance matrices. The proportion of the simulations in which the correct tree was selected for all methods is the average for 100 simulations for each of the two trees and for each evolutionary model (speciational and gradual); when Cubo's (2003) original test selected both phylogenetic distance matrices, this simulation was scored as 0.5. The modified version of Cubo's (2003) test is the proportion of times that the correct tree has the lowest probability associated with the explained variance or with the slope, even when these probabilities exceed the 0.05 threshold. When, for a given topology, the probability associated with the slope was the same for both evolutionary models, we scored 0.5. The contrast-based method ('contrasts' in the table) is based on a regression between standardized contrasts and their expected standard deviation (based on branch lengths). The choice of the model is based on the probability associated with the slope (higher is better).

Results

Our simulations indicate that the test proposed by Cubo (2003) to determine whether a character evolved according to a gradualistic or a speciational model has only a moderate success rate (Table 2). When forward selection was used to determine which of the two phylogenetic distance matrices (unitary branch length or branch lengths reflecting evolutionary time) best explained character data, the correct matrix was identified in only 5–82% of the cases (with an average success rate of 52%). This low and very heterogeneous success rate is attributable to the fact that in many cases neither phylogenetic distance matrix

was found to be significantly correlated with the phenotypic data, and when one was, it was often the wrong one; in both cases, this was scored as a failure of the test. Using the probability associated with the explained variance or with the b coefficient to choose between phylogenetic distance matrices gives slightly better, but still very heterogeneous results (17–94% of correct results using the probability associated with the variance; 28–94% of correct results using the b coefficient). This great heterogeneity concerns mostly the Yule two tree, in which a bias in favour of the speciational phylogenetic distance matrix was present, yielding very low success rates (5–27.5%) when the true model of evolution was continuous. Conversely, these three approaches (Cubo's original, or both modifications thereof) on the same tree yielded very high success rates when characters follow speciational evolution (success rate of 82–94%), apparently reflecting the same bias. Note that, of all methods analysed in this study, Cubo's original method is the only one that takes into account exclusively those phylogenetic distance matrices significantly related to the trait under analysis. Variants of this method, although more performant in terms of success rates, select phylogenetic distance matrices on the basis of the lowest probability, even when this probability is higher than 0.05. In other words, even when the analyses conclude that neither of the models significantly explain the variation of the trait under analysis, these methods consider that one of them fit the data better than the other.

Our proposed test, which consists of regressing standardized contrasts against their expected standard deviation, is slightly better, with a global success rate ranging from 76% to 99%, depending on the real evolutionary model of the characters and, to a lower extent, on the tree. The contrast-based method performed overall better with characters evolving according to a speciational model (maximum success rate of 99%) than with characters evolving gradually, according to a Brownian motion model (maximum success rate of 77%). However,

Tree	Data set	Taxonomic level			
		Genus		Species	
		Number of gradual characters	Number of speciational characters	Number of gradual characters	Number of speciational characters
Paleontological and biogeographical	All	39	19	38	16
	Size	26	4	29	1
	Shape	9	15	9	15
Phillips *et al.*, 2010	All	37	17	39	15
	Size	26	4	29	1
	Shape	11	13	10	14
Haddrath & Baker, 2001	All	40	14	38	16
	Size	27	3	29	1
	Shape	13	11	9	15
Cooper *et al.*, 2001	All	35	19	37	17
	Size	25	5	29	1
	Shape	10	14	8	16
Average of four trees	All	36.75	17.25	38	16
	Size	26	4	29	1
	Shape	10.75	13.25	9	15

Table 3. Evolutionary model of ratite osteological characters according to the four tested trees. For the data set, 'all' indicates results for all 54 characters; 'size' indicates results for the 30 unstandardized, size-related characters; 'shape' indicates results for the 24 shape characters.

CoMET outperformed both, with a global success rate around 97%, and not differing significantly between both models. Therefore, only CoMET was used to test the evolutionary model of our ratite data.

The CoMET analyses of the 54 osteological characters of ratites show that about 70% (37) evolved according to a gradual model, and only about 30% (17) according to a speciational model (Table 3). This result represents the grand average over the four trees and using both generic averages and species data; the tree and taxonomic level have little influence on these results. The tree that implies the lowest number of 'gradual' characters (Cooper *et al.*, 2001) still finds 35, whereas the tree that supports the greatest amount of gradual change (Haddrath & Baker, 2001) finds 40, at the genus level (at the species level, the spread is even narrower, from 37 to 39). A paired-sample t test, performed manually (Zar,

1984) and repeated using Statistica, shows that overall more characters evolve according to a gradual than a speciational model (Data S3), both when genera (t^3 = 8.25, P = 0.003726) and species (t^3 = 26.94, P = 0.000112) are used. However, the size characters (measurements) follow predominantly a gradual model (87% to 97%, according to genus- and species-level trees, respectively), whereas the shape characters (ratios of the former) predominantly follow a speciational model (55–63%, according to genus- and species-level trees, respectively). Again, this conclusion does not heavily depend on the selected tree; among the size characters, the trees support from 25 (Cooper *et al.*, 2001) to 27 (Haddrath & Baker, 2001) 'gradual' characters at the genus level (at the species level, all trees find 29). Similarly, among shape characters, these numbers range from 9 (palaeontological tree) to 13 characters (Haddrath & Baker, 2001) at the genus level; these numbers range from 8 in Cooper *et al.* (2001) to 10 in Phillips *et al.* (2010). A paired-sample t test (Zar, 1984) shows that the difference in model between raw and shape measurements is very highly significant (Data S3) for both genera (t^3 = 24.24, P = 0.000154) and species (t^3 = 48.99, P = 0.000019). This suggests a fair amount of independence between raw (size-related) and shape characters. No single tree seems to give outlier values, and each yields one of the highest or lowest values at least once; the two trees that most often yield extreme (but by no means 'outlying') values are those of Haddrath & Baker (2001) and Cooper *et al.* (2001).

Discussion

Speciational vs. gradual models of evolution

A survey of the literature suggests that it will be generally difficult to determine whether characters evolved according to a gradual or a punctuational model, for several

reasons. First, as pointed out previously, the tests that have been proposed so far (including the new test presented earlier) require fairly precise knowledge about the evolutionary time separating the sampled species to assess the fit of a gradual model of evolution to the data. This is currently problematic because neither of the two main sources of timing data currently provides more than a crude estimate of the chronology of taxonomic diversification. Namely, the fossil record is notoriously incomplete, and molecular dating relies on calibration constraints predominantly extracted from the fragmentary fossil record. To illustrate this, of about 320 lissamphibian clades for which Marjanović & Laurin (2007) proposed minimal divergence dates based on the fossil record, only four clades had enough known extinct relatives to estimate their maximum age. Yet, Marjanović & Laurin (2007) demonstrated that these few maximum age constraints were crucial for deriving plausible molecular estimates of the ages of most other clades. Other methodological problems plaguing molecular dating are well known and have been adequately described elsewhere (Rodríguez-Trelles *et al.*, 2002; Shaul & Graur, 2002; Brochu, 2004a, b; Graur & Martin, 2004; Britton, 2005). Maximum ages were used for every calibration constraint by Phillips *et al.* (2010).

Second, assessing the fit of a speciational model to the data requires data about all extant and extinct species of a taxon, or at least a representative sample of the latter (*i.e.* with fairly homogeneous sampling in all groups). This condition is most limiting because < 1% of the species that have ever lived on this planet are known from fossils, according to plausible models and our knowledge of the past biodiversity (Newman, 2001; Laurin, 2005). Mooers *et al.* (1999) argued that a punctuational model can be established using extant species if most of the extant species of a clade are included in the study. However, this method assumes that the proportion of extinct species is homogeneously distributed on the tree or negligible (Mooers *et al.*, 1999), and at least the second is in most cases unrealistic because most species are

already extinct, as mentioned earlier. Thus, in practice, such a test is possible only within a taxon that has a very dense fossil record that allows detection of most cladogenetic events, a very uncommon situation (Prothero, 2004; Laurin, 2010).

Nonetheless, our simulations show that if all the rather restrictive conditions mentioned earlier are met, the correct model of evolution of characters can be inferred by CoMET with great reliability (about 97% global success rate). Thus, the problem does not lie in the statistical analysis of the data, but rather in obtaining a phylogeny with correct topology and branch lengths.

Our results are encouraging because, despite the methodological differences, increased sample of characters and number of phylogenies, they confirm the conclusion by Cubo (2003) that the osteological characters of ratites that reflect shape evolved mostly according to a speciational model. Our results provide additional information by suggesting that this does not apply to size-related characters; thus, over two-thirds of the characters in our sample (which includes 30 size-related and 24 shape-related characters) have evolved according to a gradual model. Size- and shape-related characters appear to follow different models in ratites. These results provide additional support for the hypothesis by Cubo (2003) that heterochronic mechanisms may underlie morphological changes in bone shape during the evolution of ratites because it has been argued that (i) heterochronic changes are instantaneous on a geologic time scale (Gould, 1977), in such a way that the outcome of these changes may be consistent with a speciational model of character evolution, and that (ii) only evolutionary shape changes (and not evolutionary size changes) could be evidence for heterochrony (Gould, 2000).

Our conclusions on these points should be seen as tentative because the uncertainties in branch lengths and topology remain substantial. Nevertheless, the fact that the choice of tree (among the four tested) impacts very little on the results suggests that our results are fairly robust to phylogenetic uncertainties concerning ratites. The palaeontological tree, whose paleobiogeographical dating rests on the highest number of hypotheses, yields results congruent with the other trees, and indeed, it is not one of the two trees (Cooper *et al.*, 2001; Haddrath & Baker, 2001) that most frequently yields extreme (but still not outlying) values. Thus, in this case, there is no sharp difference between morphological and molecular signals.

Acknowledgments

We thank the CNRS and the French Ministry of Research (ML, operating grant to UMR 7207; JC, operating grant to UMR 7193), the Netherlands Organization for Scientific Research (NWO; SG) and the university study subsidy office of Austria (DM) for funding this research.

References

Alvarenga HMF. **1983.** Uma ave ratitae do Paleoceno Brasileiro: Bacia Calcaŕia de Itaboraí, Estado do Rio de Janeiro, Brasil. *Geologia: Boletim do Museu Nacional do Rio de Janeiro* **41**: 1–7.

Benton MJ, Pearson PN. 2001. Speciation in the fossil record. *Trends in Ecology and Evolution* **16**: 405–411.

Bertelli S, Chiappe LM. **2005**. Earliest Tinamous (Aves: Palaeognathae) from the Miocene of Argentina and Their Phylogenetic Position. *Contributions in Science* **502**: 1–20.

Bibi F, Shabel AB, Kraatz BP, Stidham TA. 2006. New fossil ratite (*Aves*: Palaeognathae) eggshell discoveries from the Late Miocene Baynunah Formation of the United Arab

Emirates, Arabian Peninsula. *Palaeontologica Electronica* **9**: 1–13.

Bock WJ. 1964. Kinetics of the avian skull. *Journal of Morphology* **114**: 1–42.

Boles WE. **2001**. A new emu (Dromaiinae) from the Late Oligocene Etadunna Formation. *Emu* **101**: 317–321.

Bourdon E, de Ricqlès A, Cubo J. 2009. A new Transantarctic relationship: morphological evidence for a Rheidae–Dromaiidae–Casuariidae clade (Aves, Palaeognathae, Ratitae). *Zoological Journal of the Linnean Society* **156**: 641–663.

Britton T. 2005. Estimating divergence times in phylogenetic trees without a molecular clock. *Systematic Biology* **54**: 500–507.

Brochu CA. 2004a. Patterns of calibration age sensitivity with quartet dating methods. *Journal of Paleontology* **78**: 7–30.

Brochu CA. 2004b. Calibration age and quartet divergence date estimation. *Evolution* **58**: 1375–1382.

Casgrain P. 2009. *Permute! version 3.4 alpha 9.* Available via http://adn.biol.umontreal.ca/~numericalecology/old/permute-index.html

Clarke JA. 2004. Morphology, phylogenetic taxonomy, and systematics of *Ichthyornis* and *Apatornis* (Avialae: Ornithurae). *Bulletin of the American Museum of Natural History* **286**: 1–179.

Clarke JA, Chiappe LM. 2001. A new carinate bird from the Late Cretaceous of Patagonia (Argentina). *American Museum Novitates* **3323**: 1–23.

Clarke JA, Tambussi CP, Noriega JI, Erickson GM, Ketcham RA. 2005. Definitive fossil evidence for the extant avian radiation in the Cretaceous. *Nature* **433**: 305–308.

Cooper A, Lalueza-Fox C, Anderson S, Rambaut A, Austin J, Ward R. 2001. Complete mitochondrial genome sequences of two extinct moas clarify ratite evolution. *Nature* **409**: 704–707.

Cracraft J. 1973. Continental drift, paleoclimatology, and the evolution and biogeography of birds. *Journal of Zoology* **169**: 455–545.

Cracraft J. 1974. Phylogeny and evolution of the ratite birds. *Ibis* **116**: 494–521.

Cracraft J. 2001. Avian evolution, Gondwana biogeography and the Cretaceous-Tertiary mass extinction event. *Proceedings of the Royal Society B: Biological Sciences* **268**: 459–469.

Cubo J. 2003. Evidence for speciational change in the evolution of ratites (*Aves*: Palaeognathae). *Biological Journal of the Linnean Society* **80**: 99–106.

Cubo J, Ponton F, Laurin M, de Margerie E, Castanet J. 2005. Phylogenetic signal in

bone microstructure of sauropsids. *Systematic Biology* **54**: 562–574.

Díaz-Uriarte R, Garland Jr. T. 1996. Testing hypotheses of correlated evolution using phylogenetically independent contrasts: sensitivity to deviations from Brownian motion. *Systematic Biology* **45**: 27–47.

Dyke GJ, Van Tuinen M. 2004. The evolutionary radiation of modern birds (Neornithes): reconciling molecules, morphology and the fossil record. *Zoological Journal of the Linnean Society* **141**: 153–177.

Gould SJ. 1977. Ontogeny and Phylogeny. Cambridge: Harvard University Press.

Gould SJ. 2000. Of coiled oysters and big brains: how to rescue the terminology of heterochrony, now gone astray. *Evolution and Development* **2**: 241–248.

Gould SJ, Eldredge N. 1977. Punctuated equilibria: the tempo and mode of evolution reconsidered. *Paleobiology* **3**: 115–151.

Graur D, Martin W. 2004. Reading the entrails of chickens: molecular timescales of evolution and the illusion of precision. *Trends in Genetics* **20**: 80–86.

Grellet-Tinner G, Dyke GJ. 2005. The eggshell of the Eocene bird *Lithornis*. *Acta Palaeontologica Polonica* **50**: 831–835.

Gussekloo SWS, Bout RG. 2002. Non-neotenous origin of the palaeognathous (*Aves*) pterygoid-palate complex. *Canadian Journal of Zoology* **80**: 1491–1497.

Gussekloo SWS, Zweers GA. 1999. The paleognathous pterygoid-palatinum complex: a true character? *Netherlands Journal of Zoology* **49**: 29–43.

Gussekloo SWS, Vosselman MG, Bout, RG. 2001. Threedimensional kinematics of skeletal elements in avian prokinetic and rhynchokinetic skulls determined by Roentgen stereophotogrammetry. *Journal of Experimental Biology* **204**: 1735–1744.

Hackett SJ, Kimball RT, Reddy S, Bowie RCK, Braun EL, Braun MJ, Chojnowski JL, Cox A, Han K-L, Harshman J, Huddleston CJ, Marks BD, Miglia KJ, Moore WS, Sheldon FH, Steadman DW, Witt CC, Yuri T. 2008. A phylogenomic study of birds reveals their evolutionary history. *Science* **320**: 1763–1768.

Haddrath O, Baker AJ. 2001. Complete mitochondrial DNA genome sequences of extinct birds: ratite phylogenetics and the vicariance biogeography hypothesis. *Proceedings of the Royal Society B: Biological Sciences* **268**: 939–945.

Harshman J, Braun EL, Braun MJ, Huddleston CJ, Bowie RCK, Chojnowski JL, Hackett SJ, Han KL, Kimball RT, Marks BD, Miglia KJ, Moore WS, Reddy S, Sheldon FH, Steadman DW, Steppan SJ, Witt CC, Yuri T. 2008. Phylogenomic

evidence for multiple losses of flight in ratite birds. *Proceedings of the National Academy of Sciences* **105**: 13462–13467.

Hope S. 2002. The mesozoic radiation of Neornithes. In: Chiappe, LM, Witmer L, eds. *Mesozoic Birds: Above the Heads of Dinosaurs*. Berkeley, CA: University of California Press, 339–388.

Houde P. 1986. Ostrich ancestors found in the northern hemisphere suggest new hypothesis of ratite origins. *Nature* **324**: 563–565.

Houde PW, Haubold H. **1987**. *Palaeotis weigelti* restudied: a small Middle Eocene ostrich (Aves: Struthioniformes). *Palaeovertebrata* **17**: 27–42.

Johnston P. **2011**. New morphological evidence supports congruent phylogenies and Gondwana vicariance for palaeognathous birds. *Zoological Journal of the Linnean Society* **163**: 959–982.

Kurochkin EN, Dyke GJ, Karhu AA. 2002. A new presbyornithid bird (*Aves,* Anseriformes) from the Late Cretaceous of southern Mongolia. *American Museum Novitates* **3386**: 1–11.

Laurin M. 2004. The evolution of body size, Cope's rule and the origin of amniotes. *Systematic Biology* **53**: 594–622.

Laurin M. 2005. The advantages of phylogenetic nomenclature over Linnean nomenclature. In: Minelli A, Ortalli G, Sanga G, eds. *Animal Names, Vol. 1*. Venice, Italy: Instituto Veneto di Scienze, Lettere ed Arti, 67–97.

Laurin M. 2010. How Vertebrates Left the Water. Berkeley, CA: University of California Press.

Laurin M, Canoville A, Quilhac A. 2009. Use of paleontological and molecular data in supertrees for comparative studies: the example of lissamphibian femoral microanatomy. *Journal of Anatomy* **215**: 110–123.

Lawver LA, Gahagan LM, Coffin MF. 1992. The development of paleoseaways around Antarctica. In: Kennett JP, Warnke DA, eds. *The Antarctic Paleoenvironment: A Perspective on Global Change, Part 1*. Washington, DC: American Geophysical Union, 7–30.

Lee C, Blay S, Mooers AØ, Singh A, Oakley TH. 2006. CoMET: a Mesquite package for comparing models of continuous character evolution on phylogenies. *Evolutionary Bioinformatics Online* **2**: 193–196.

Maddison WP, Maddison DR. 2011. *Mesquite: a modular system for evolutionary analysis. Version 2.75.* Available via http://mesquiteproject.org.

Marjanović D, Laurin M. 2007. Fossils, molecules, divergence times, and the origin of lissamphibians. *Systematic Biology* **56**: 369–388.

Martins EP, Diniz-Filho JAF, Housworth EA. 2002. Adaptative constraints and the phylogenetic comparative method: a computer simulation test. *Evolution* **56**: 1–13.

Mayr G. 2005. The Paleogene fossil record of birds in Europe. *Biological Reviews* **80**: 515–542.

Mayr G. 2009. Paleogene Fossil Birds. Berlin: Springer.

Mooers AØ, Vamosi SM, Schulter D. 1999. Using phylogenetics to test macroevolutionary hypotheses of trait evolution in cranes (Gruinae). *The American Naturalist* **154**: 249–259.

Mourer-Chauviré C, Senut B, Pickford M, Mein P. 1996. The oldest representative of the genus *Struthio* (Aves: Struthionidae), *Struthio coppensi* n. sp., from the Lower Miocene of Namibia. *Comptes-Rendus de l'Académie des Sciences* **322**: 325–332.

Newman M. 2001. A new picture of life's history on Earth. *Proceedings of the National Academy of Sciences* **98**: 5955–5956.

Oakley TH, Gu Z, Abouheif E, Patel NH, Liu WH. 2005. Comparative methods for the analysis of gene-expression evolution: an example using yeast functional genomic data. *Molecular Biology and Evolution* **22**: 40–50.

Paton T, Haddrath O, Baker AJ. 2002. Complete mitochondrial DNA genome sequences show that modern birds are not descended from transitional shorebirds. *Proceedings of the Royal Society of London B: Biological Sciences* **269**: 839–846.

Phillips MJ, Gibb GC, Crimp EA, Penny D. **2010**. Tinamous and Moa Flock Together: Mitochondrial Genome Sequence Analysis Reveals Independent Losses of Flight among Ratites. *Systematic Biology* **59**: 90–107.

Prothero DR. 2004. Bringing Fossils to Life. An Introduction to Paleobiology (2nd edition). Boston: McGraw Hill.

Rodríguez-Trelles F, Tarrío R, Ayala FJ. 2002. A methodological bias toward overestimation of molecular evolutionary time scales. *Proceedings of the National Academy of Sciences* **99**: 8112–8115.

Rohlf FJ, Chang WS, Sokal RR, Kim J. 1990. Accuracy of estimated phylogenies: effects of tree topology and evolutionary model. *Evolution* **44**: 1671–1684.

Scotese CR. 2001. *Paleomap Project.* Available via http://www.scotese.com.

Shaul S, Graur D. 2002. Playing chicken (*Gallus gallus*): methodological inconsistencies of molecular divergence date estimates due to secondary calibration points. *Gene* **300**: 59-61

Veevers JJ, McElhinny MW. 1976. The separation of Australia from other continents.

Earth-Science Reviews **12**: 139–143.

Veevers J, Powell C, Roots S. 1991. Review of seafloor spreading around Australia. Synthesis of the patterns of spreading. *Australian Journal of Earth Sciences* **38**: 373–389.

Woodburne MO, Case JA. 1996. Dispersal, vicariance, and the Late Cretaceous to early Tertiary land mammal biogeography from South America to Australia. *Journal of Mammalian Evolution* **3**: 121–161.

Zar JH. 1984. Biostatistical Analysis (2nd edition). Englewood Cliffs, NJ: Prentice-Hall.

Zusi RL. 1984. A functional and evolutionary analysis of rhynchokinesis in birds. *Smithsonian Contributions to Zoology* **395**: 1–40.

Supporting information

Additional Supporting Information may be found in the online version of this article:

Data S1 NEXUS file containing all data on ratite species, along with the phylogeny that was used to test the evolutionary model of the characters.

Data S2 NEXUS file containing all data on ratite genera, along with the phylogeny that was used to test the evolutionary model of the characters.

Data S3 Detailed results of the CoMET analyses. Sheet one summarizes the results; sheet two has detailed logs of all analyses.

Data deposited at Dryad: doi: 10.5061/dryad.cr0qh5gc

Annexe II – Geometric and metabolic constraints on bone vascular supply in diapsids

Jorge Cubo, Jéromine Baudin, Lucas J. Legendre,

Alexandra Quilhac et Vivian de Buffrénil

Publication originale *in*: *Biological Journal of the Linnean Society* (sous presse, 2014)

Abstract
Periosteal, endosteal, and intracortical blood vessels bring oxygen and nutrients to and evacuate the metabolic byproducts from osteocytes. This vascular network is in communication with bone cells through a network of canaliculi containing osteocyte cytoplasmic processes. The geometric and physiologic contraints involved in the relationships between osteocytes (including canaliculi) and blood vessels in bones remain poorly documented in a comparative point of view. First we test the hypothesis (1) that osteocytes in endotherms may have higher energetic expenditure and may produce more metabolic byproducts than in ectotherms. For this, we test and find evidence for the prediction derived from this hypothesis that the maximum absolute thickness of avascular bone tissue is significantly higher in lepidosaurs than in birds. We also test two alternative hypotheses explaining the variation of bone vascular density in diapsids: (2a) As body mass increases, the relative effectiveness of vascular supply of the periosteum decreases because its surface increases proportionally to the second power of bone length, whereas bone mass to be supplied increases proportionally to the third power. Accordingly, we predict and find evidence that bone vascular density is directly related to bone size in both lepidosaurs and birds. The alternative hypothesis (2b) suggesting that bone vascular density, like mass-specific resting metabolic rate, may decrease as body mass increases has been refuted by these last results. Knowledge of the cytologic relationship between osteocytes and blood vessels in diapsids is poor. Here we also present preliminary results of a comparative cytologic study on such relationship.

Keywords: birds – bone vascularization – lepidosaurs – metabolism – size

Introduction

Osteocytes obtain nutriments and oxygen and evacuate their metabolic byproducts through cytoplasmic expansions located inside canaliculi and linked to vascular networks (Mishra, 2009). These vascular networks are housed within bone cortices (Brookes, 1971; Francillon-Vieillot *et al.*, 1990) and in the inner (endosteal) and outer (periosteal) connective tissues associated with the bones (Simpson, 1985). The geometric constraints that control the structure of the vascular networks and their final relationships with local and systemic metabolic processes have been very poorly studied at a comparative level (Mishra, 2009). We analyze here the impact of the scaling of metabolic rate on two bone histological features: the thickness of peripheral layer of avascular bone tissue and the density of bone vascular supply. Previous studies have shown that femoral cortices of small adult lepidosaurs and birds are avascular or almost avascular (Cubo *et al.*, 2005; de Buffrénil, Houssaye & Böhme, 2008), so that osteocytes perform metabolic exchanges exclusively with the inner and outer connective tissues. In birds, the relative thickness of the outer layer of avascular bone tissue scales to bone size with negative allometry (Ponton *et al.*, 2004). The maximum thickness of avascular bone in lepidosaurs and birds could be explained by a main hypothesis: (1) Osteocytes in endotherms have higher energetic expenditure and produce more metabolic byproducts than in ectotherms, which suggests that when bone cortical vascularization is absent endotherms need to have thinner layers of avascular bone, if transport of metabolites via canaliculi is under similar constraints in the different taxa. We thus expect significantly higher thickness of avascular bone tissue in lepidosaurs than in birds. Moreover, we analyzed the scaling of bone vascular density in the bones that actually display vascular canals. Two antagonist factors could possibly explain the variation of this feature: Considering that mass-specific resting metabolic rate (oxygen consumption, in ml/h, per body mass, grams) decreases as body mass

increases, we expect that the metabolic demands of osteocytes do likewise, in which case bone vascular density should decrease as body mass increases (hypothesis 2b). Conversely, as bone size increases, the vascular supply of the periosteum decreases in relative effectiveness because its surface increases proportionally to the second power of bone length, whereas bone mass (to be supplied) increases proportionally to the third power. So we expect that bone vascular density increases as body mass increases to compensate the smaller relative effectiveness of vascular supply of the periosteum (hypothesis 2a). It is well documented that osteocytes communicate with each other through the lacunocanalicular system (Mishra, 2009), but knowledge on the cytologic relationship between osteocytes and blood vessels (intracortical, endosteal and periosteal) in diapsids is poor. Here we present also preliminary results of a comparative cytologic study on such relationship.

Material and methods

The analysis of the effect of the scaling of metabolic rate on the histological features was performed using a sample of femora of 46 species of lepidosaurs and 30 species of birds. Only adult animals were used and all the sections were made in a transverse plane located at mid-diaphysis to work in a strict frame of homology (Legendre *et al.*, in press). The thin sections belong to preexisting collections at the Pierre & Marie Curie University, Paris (sample of birds) and the Muséum National d'Histoire Naturelle of Paris (sample of lepidosaurs). We quantified a number of cross-sectional geometric and histological features using ImageJ (Schneider, Rasband & Eliceiri, 2012): bone cross-sectional area (the area encircled by the periosteum, including the medullary cavity); bone cortical area : black plus grey in Fig. 1B : bone cross-sectional area (including vascular canals) minus medullary cavity area; bone vascular area (in black in Fig. 1B : the area occupied by vascular cavities); total

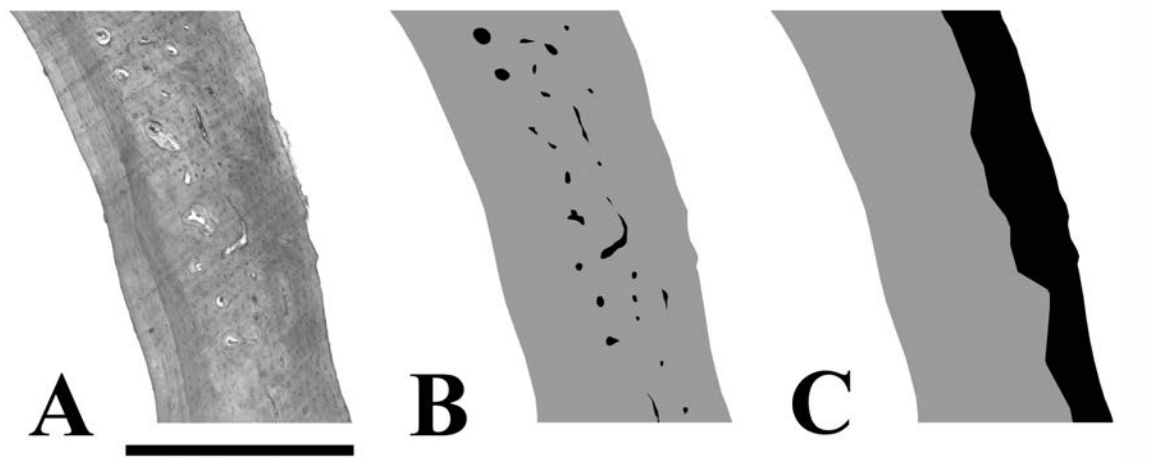

Figure 1. Fraction of a diaphyseal femoral transverse section of *Corvus corone* (Aves, Neognathae) showing the histological features quantified in this study. A. Histological section. B. Gray: bone cortex; black: vascular cavities. C. Gray: bone cortex minus the outer avascular layer; black: outer avascular layer.

number of vascular canals in a bone section; and the mean thickness of the outer layer of avascular bone tissue (in black in Fig. 1C) measured as the radius of a circle of area equal to bone cross sectional area minus the radius of a circle of area equal to the area encircled by the outermost vascular canals (*i.e.* the area containing all intracortical vascular canals). When vascular canals were absent, we measured the mean thickness of the whole cortex. Bone vascular density was computed as total number of vascular canals / bone cortical area. Moreover we analyzed bone vascular area / bone cortical area. In birds, when only a few (less than ten) blood vessels were present in a bone section, the bone was considered to be avascular because they probably were blood vessels running from the periosteum to the endosteum (nutrient canals), and so did not form a vascular network inside the bone cortex. All variables but the ratios were log transformed in order to spread the points more uniformly in the graphs to improve the interpretability. We analyzed only transverse sections but, considering that hydraulic resistance increases as the distance from osteocytes to blood vessel increases (Mishra, 2009), the key functional constraint is the distance from osteocytes to blood vessels (either intracortical or periosteal) in a given plane of section. In other words, a given osteocyte can in principle obtain nutrients from blood vessels located at different

positions in the 3D space, but in a given plane of section, the distance from an osteocyte to a blood vessel must be lower than the threshold above which the transport of oxygen and nutriments is no longer possible because of hydraulic resistance. In this context, because the critical biological constraint is the absolute distance from cells to blood vessels, we analyzed absolute (instead of relative to bone size) values of the thickness of the outer layer of avascular bone tissue and of the bone vascular density.

All statistical analyses were performed using phylogenetic comparative methods (*sensu* Harvey & Pagel, 1991). Phylogenetic relationships within the sample of birds used in this study (Fig. 2) were compiled from Barker, Barrowclough & Groth (2002), and Livezey & Zusi (2007). The phylogenetic tree of the sample of lepidosaurs used in this study (Fig. 3) was compiled from Ast (2001) and Conrad (2008). Branch lengths were estimated using Pyron (2010) for birds and Conrad (2008) for lepidosaurs. Regressions were performed using phylogenetic generalized least squares (Grafen, 1989). Pagel's lambda was compiled simultaneously with each regression via maximum-likelihood using the function pgls from R package 'caper' (Orme *et al.*, 2012), thus ensuring an accurate estimation of phylogenetic signal for each couple of variables (Revell, 2010): lambda = 0 means no phylogenetic signal; lambda = 1 means high phylogenetic signal (traits evolve following a Brownian motion model). The mean value for a given clade (*i.e.*, lepidosaurs, birds) was obtained as the value for the root node computed using squared-change parsimony optimization (Maddison, 1991) in the PDAP module (Midford, Garland & Maddison, 2011) of Mesquite (Maddison & Maddison, 2011). The corresponding confidence intervals were also computed using the PDAP module of Mesquite.

The cytologic analysis of the relationship between osteocytes and blood vessels was

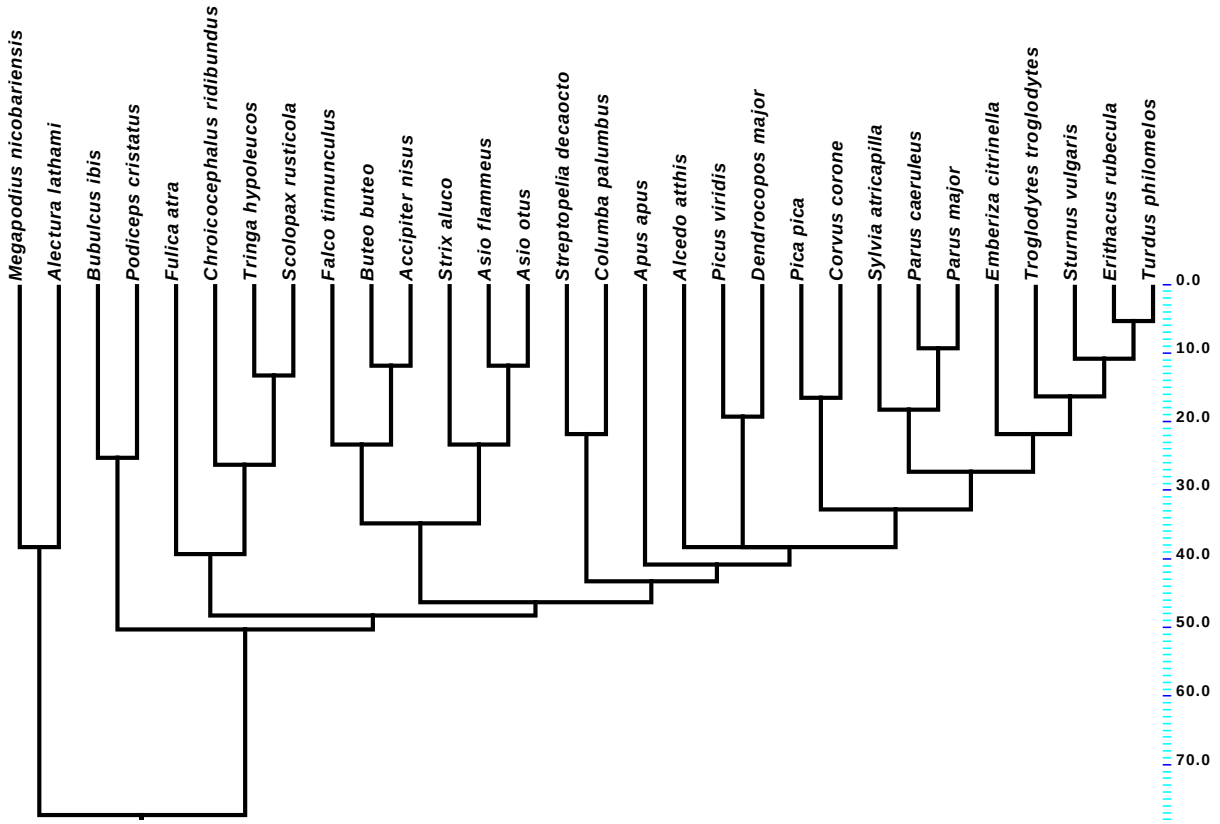

Figure 2. Phylogenetic relationships among the sample of birds used in this study. Higher order relationships were taken from Livezey & Zusi (2007). Relationships among passeriforms were compiled from Barker *et al.* (2002). Branch lengths were taken from Pyron (2010).

performed using four subadult *Varanus exanthematicus* and four subadult *Anas platyrhynchos* (Fig. 4). They all originate from breeding. After euthanasia, femora were fixed in a mixture containing 2.5% glutatraldehyde, 2 % paraformaldehyde in 0.1 M cacodylate buffer. The samples were demineralised using 5% EDTA added in the fixative. The demineralised samples were post fixed with 1% osmium tetroxide in the cacodylate buffer, dehydrated, and subsequently embedded in Epon. Semi-thin (1 μm) sections were stained with toluidine blue (pH 4) and examined using light microscopy. Thin (0.05 μm) sections were double-stained with uranyl acetate and lead citrate. The grids were viewed in a Zeiss Leo transmission electron microscope with an operating voltage of 80 kV.

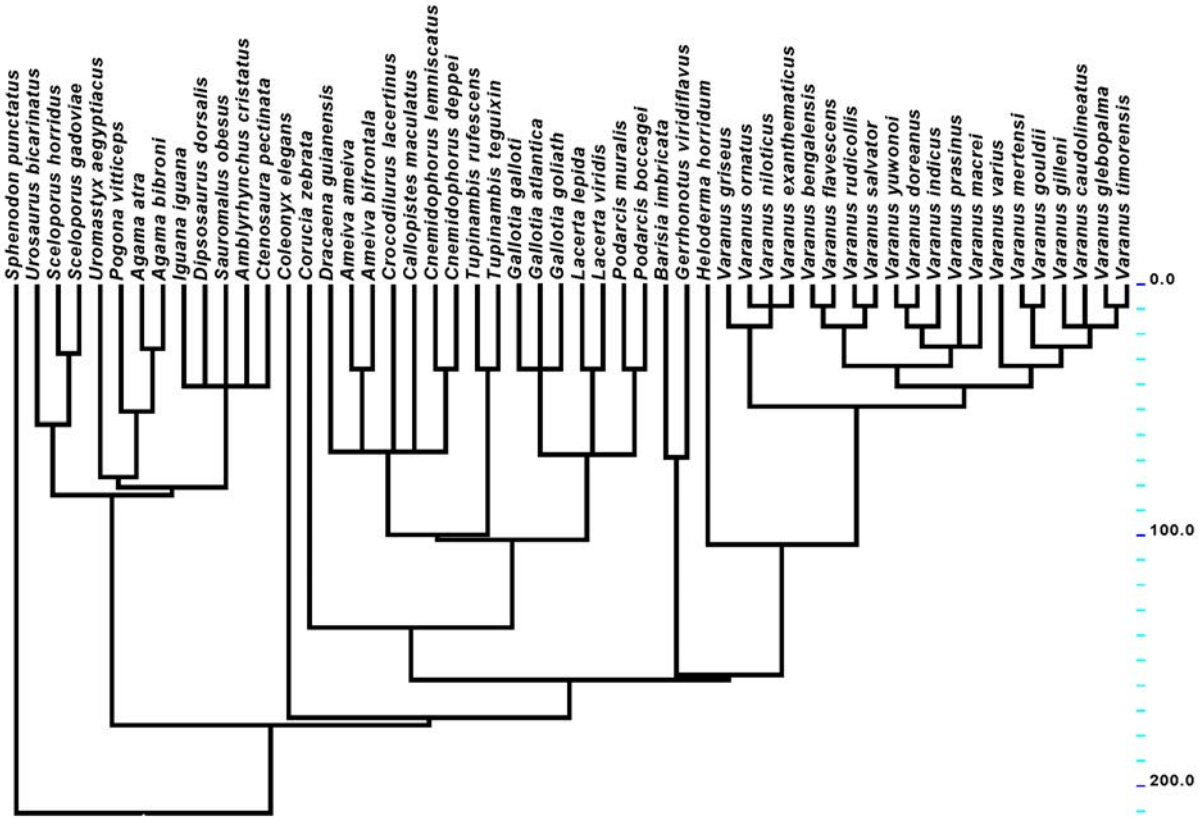

FIGURE 3. Phylogenetic relationships among the sample of lepidosaurs used in this study. Higher order relationships and branch lengths were taken from Conrad (2008). Relationships among *Varanus* species were compiled from Ast (2001).

Results

Thickness of avascular bone tissue

In birds, the mean thickness of the outer layer of avascular bone tissue is 0.072 mm, with lower and upper 95% confidence intervals of, respectively, 0.034 and 0.109 mm. Variation ranges from 0.033 mm in *Podiceps cristatus* to 0.122 mm in *Dendrocopos major*. In birds this layer was always present. In some species, the entire cortex is avascular: *Emberiza citrinella, Erithacus rubecula, Sylvia atricapilla, Parus caeruleus, Apus apus, Troglodytes troglodytes* and *Parus major* (table 1).

Table 1. Dataset corresponding to the sample of birds.

Species	Bone cross-sectional area (mm^2)	Thickness outer layer avascular bone (mm)	Bone vascular density ($1/mm^2$)	Bone vascular area / Bone cortical area
Accipiter nisus	15.148	0.092	83.544	0.020
Alcedo atthis	1.916	0.079	69.069	0.006
Alectura lathami	80.828	0.043	89.291	0.080
Apus apus	1.450	0.102	0.000	0.000
Asio flammeus	13.703	0.050	81.832	0.022
Asio otus	9.038	0.099	124.238	0.028
Bubulcus ibis	17.500	0.051	149.603	0.035
Buteo buteo	31.349	0.102	71.583	0.026
Chroicocephalus ridibundus	16.243	0.057	79.141	0.023
Columba palumbus	12.000	0.055	110.776	0.031
Corvus corone	13.335	0.092	65.909	0.023
Dendrocopos major	4.095	0.122	33.247	0.004
Emberiza citrinella	1.275	0.114	0.000	0.000
Erithacus rubecula	1.112	0.116	0.000	0.000
Falco tinnunculus	8.379	0.089	98.127	0.030
Fulica atra	16.388	0.094	79.106	0.022
Megapodius nicobariensis	25.668	0.121	69.318	0.036
Parus caeruleus	0.859	0.086	0.000	0.000
Parus major	1.626	0.092	0.000	0.000
Pica pica	6.733	0.090	70.151	0.025
Picus viridis	6.274	0.067	48.317	0.008
Podiceps cristatus	16.620	0.033	122.169	0.065
Scolopax rusticola	12.755	0.102	81.699	0.015
Streptopelia decaocto	7.126	0.044	82.321	0.016
Strix aluco	21.400	0.069	93.447	0.020
Sturnus vulgaris	4.954	0.088	21.465	0.003
Sylvia atricapilla	1.080	0.049	0.000	0.000
Tringa hypoleucos	2.210	0.046	82.636	0.017
Troglodytes troglodytes	0.808	0.096	0.000	0.000
Turdus philomelos	4.377	0.079	26.600	0.004

In lepidosaurs, vascular canals, when present, appear throughout bone cortex, from depth to periphery, so no outer layer of avascular bone tissue was defined. Instead, we analyzed the thickness of the cortex in a subsample of lepidosaurs containing exclusively species with avascular femora (see table 2). We obtained a mean thickness of the cortex in lepidosaurs with avascular femora of 0.790 mm with lower and upper 95% confidence intervals of, respectively, 0.381 and 1.199 mm. The range of variation is: 0.058 mm in *Coleonyx elegans* and 1.455 mm in *Amblyrhychus cristatus.*

Table 2. Dataset corresponding to the sample of lepidosaurs.

Species	Bone cross sectional area (mm^2)	Thickness outer layer avascular bone (mm)	Bone vascular density ($1/mm^2$)	Bone vascular area / Bone cortical area
Agama atra	2.490	0.422	0.000	0.000
Agama bibroni	2.320	0.380	0.000	0.000
Amblyrhynchus cristatus	29.158	1.455	0.000	0.000
Ameiva ameiva	2.050	0.265	0.000	0.000
Ameiva bifrontala	2.490	0.350	0.000	0.000
Barisia imbricata	0.561	0.231	0.000	0.000
Callopistes maculatus	3.750	0.480	0.000	0.000
Cnemidophorus deppei	0.480	0.120	0.000	0.000
Cnemidophorus lemniscatus	1.040	0.230	0.000	0.000
Coleonyx elegans	0.208	0.059	0.000	0.000
Corucia zebrata	10.290	0.000	0.130	0.007
Crocodilurus lacertinus	5.030	0.760	0.000	0.000
Ctenosaura pectinata	23.022	0.702	0.000	0.000
Dipsosaurus dorsalis	1.609	0.242	0.000	0.000
Dracaena guianensis	17.950	0.000	6.760	0.369
Gallotia atlantica	0.875	0.221	0.000	0.000
Gallotia galloti	0.919	0.279	0.000	0.000
Gallotia goliath	18.390	0.940	0.000	0.000
Gerrhonotus viridiflavus	2.730	0.363	0.000	0.000
Heloderma horridum	13.219	1.018	0.000	0.000
Iguana iguana	17.843	0.800	0.000	0.000
Lacerta lepida	5.970	0.770	0.000	0.000
Lacerta viridis	1.509	0.391	0.000	0.000
Podarcis boccagei	0.319	0.188	0.000	0.000
Podarcis muralis	0.360	0.195	0.000	0.000
Pogona vitticeps	5.013	0.507	0.000	0.000
Sauromalus obesus	5.655	0.495	0.000	0.000
Sceloporus gadoviae	0.446	0.138	0.000	0.000
Sceloporus horridus	0.511	0.104	0.000	0.000
Sphenodon punctatus	10.281	1.057	0.055	0.003
Tupinambis rufescens	13.135	0.000	29.915	2.855
Tupinambis teguixin	15.327	0.000	11.177	0.188
Uromastyx aegyptiacus	10.791	0.655	0.000	0.000
Urosaurus bicarinatus	0.326	0.129	0.000	0.000
Varanus bengalensis	18.290	0.000	13.850	0.650
Varanus caudolineatus	0.640	0.220	0.000	0.000
Varanus doreanus	31.407	0.000	11.163	0.387
Varanus exanthematicus	24.233	0.000	17.953	2.410
Varanus flavescens	16.465	0.000	7.155	0.130
Varanus gilleni	1.415	0.372	0.000	0.000
Varanus glebopalma	7.115	0.475	0.000	0.000
Varanus gouldii	13.535	0.000	7.410	0.530
Varanus griseus	10.220	0.000	33.330	0.620
Varanus indicus	14.590	0.000	5.790	0.060
Varanus macrei	6.483	0.680	0.000	0.000
Varanus mertensi	25.510	0.000	11.050	0.250
Varanus niloticus	34.542	0.000	28.424	2.111
Varanus ornatus	18.255	0.000	12.785	0.385
Varanus prasinus	6.637	0.610	0.000	0.000
Varanus rudicollis	18.973	0.000	43.803	1.595

We also regressed the log thickness of the outer layer of avascular bone tissue with log bone cross-sectional area in birds and did not find a significant relationship between these variables. The regression of log thickness of the outer layer of avascular bone tissue with log bone radius in birds is not significant either (Pagel's Lambda: 0.000; adjusted R^2: 0.04; *p*-value: 0.146; Fig. 5).

Bone vascular density

Bone vascular density (computed as number of vascular canals / bone cortical area) is positively related to log bone cross-sectional area in both lepidosaurs (Pagel's Lambda: 0.225; R^2: 0.112; *p*-value: 0.007) and birds (Pagel's Lambda: 1.000; R^2: 0.2629; *p*-value: 0.002). The ratio of bone vascular area / bone cortical area is also positively related to log bone cross-sectional area in in both lepidosaurs (Pagel's Lambda: 0.000; R^2: 0.1703; *p*-value: 0.001) and birds (Pagel's Lambda: 1.000; R^2: 0.2398; *p*-value: 0.003). Finally, bone vascular density is also related to log snout-vent maximal length in *Varanus* (Pagel's Lambda: 0.000; R^2: 0.2102; *p*-value: 0.024; Fig. 6). In *Varanus,* femora with a bone cross-sectional area of more than 8 mm^2 are vascularized. In the whole clade Lepidosauria, no femur smaller than 8 mm^2 is vascularized. However, many species with femora of bone cross-sectional area bigger than 8 mm^2 are avascular: *Uromastyx aegyptiacus* (10.7905 mm^2), *Heloderma horridum* (13.2185 mm^2), *Iguana iguana* (17.8433 mm^2), *Gallotia goliath* (18.3900 mm^2), *Ctenosaura pectinata* (23.0215 mm^2), and *Amblyrhynchus cristatus* (29.158 mm^2).

Cytologic analysis of the relationship between osteocytes and blood vessels

Anas platyrhynchos. The well-vascularized femoral periosteal bone tissue contains a

rich osteocyte network (Fig. 4A, B). Osteocytes are numerous around vascular canals. Their canaliculi clearly point towards blood vessels (Fig. 4B). In the periosteum, some osteoblasts are in close contact with capillary blood vessels (Fig. 4A). TEM images confirm the presence of a tight relationship between osteocytes and blood vessels (Fig. 4E). These osteocytes show a prominent nucleus and endoplasmic reticulum in the cytosol (Fig. 4E). The contact is established between the plasmic membrane of the blood vessel endothelial cell and the plasmic membrane of the osteocyte processes. Multiple canalicular projections protrude from the osteocyte body in all directions.

Varanus exanthematicus. The bone cortex is typically composed of a parallel-fibered bone tissue and displays vascular canals that are evenly distributed. The osteocytes situated in the periphery of the bone cortex show long canaliculi directed towards the periosteum (Fig. 4C) whereas those situated around vascular canals in the cortex show canaliculi directed towards the wall of these blood vessels (Fig. 4D).

Discussion

A series of hypotheses concerning the variation of bone vascularization in lepidosaurs and birds have been put forth in the introduction. We will successively discuss them. But before we will briefly discuss the results obtained in the cytologic analysis aimed at exploring the relationships between the osteocytes and the blood vessels.

Both animal models analyzed in this study (*Varanus exanthematicus* and *Anas platyrhynchos*) show a cortical network of canaliculi preferentially oriented towards the vascular canals (either intracortical or periosteal), which supply in nutrients and oxygen the

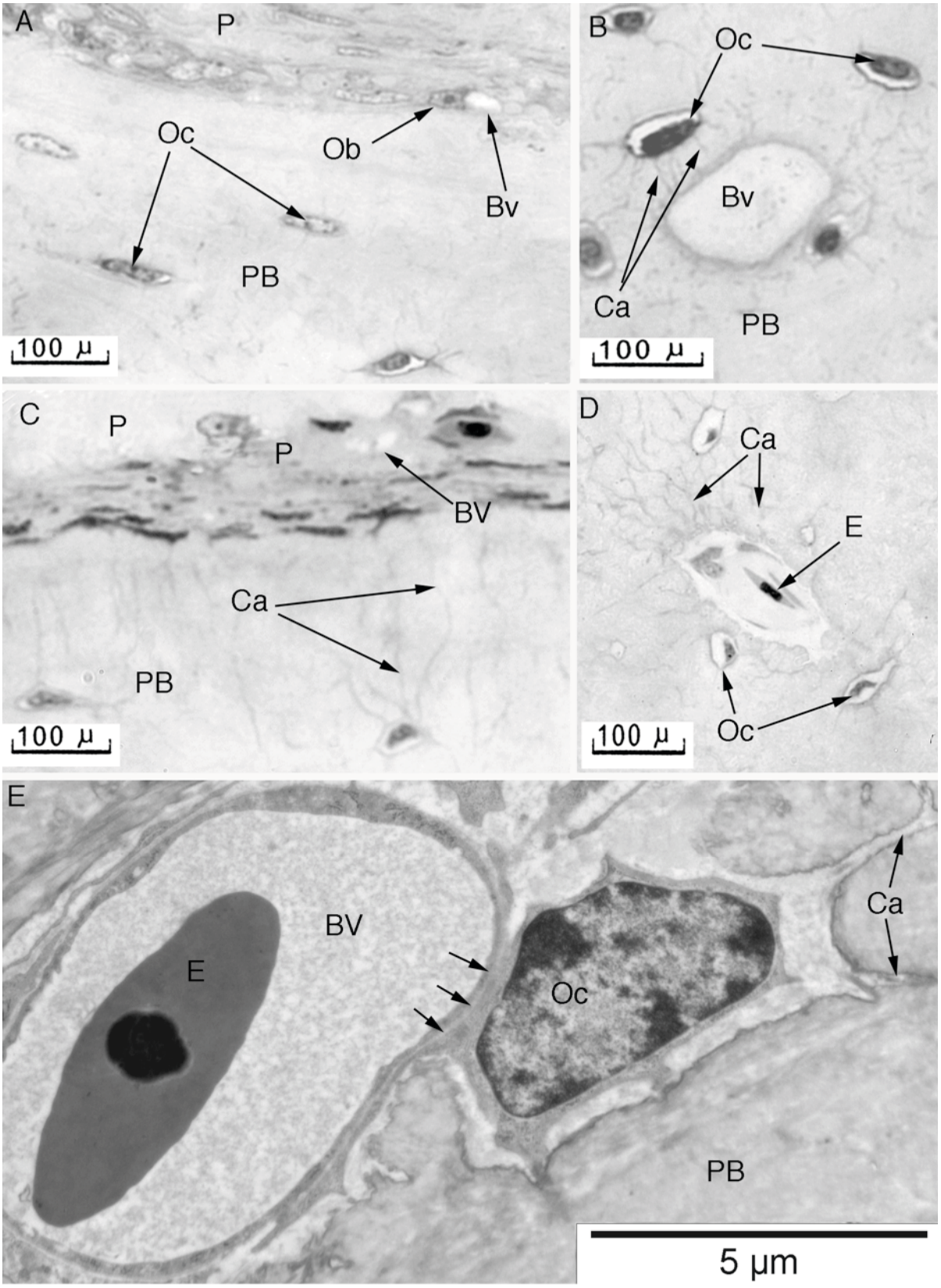
A
P
Oc
Ob
Bv
PB
100 µ
B
Oc
Bv
Ca
PB
100 µ
C
P
P
BV
Ca
PB
100 µ
D
Ca
E
Oc
100 µ
E
BV
E
Oc
Ca
PB
5 µm

Figure 4. Femoral semi-thin (A – D) and ultra-thin (E) mid-shaft cross sections of *Anas platyrhynchos* (A, B, E) and *Varanus exanthematicus* (C-D). A, In the periosteum (P), an osteoblast (Ob) is in close contact with a blood vessel (Bv). Osteocytes (Oc) are numerous in the periosteal bone (PB) and a rich canaliculi network is present. B, Canaliculi (Ca) are clearly directed towards the blood vessel located in the periosteal bone. C, Long canaliculi communicate with the periosteum where a blood vessel is visible. D, Osteocytes surrounding a blood vessel containing an erythrocyte (E). A rich canaliculi network is observed. E, Transmission electron microscopy micrograph showing a tight contact (black arrows) between the body cell of an osteocyte and the wall of a blood vessel where an erythrocyte is visible. The osteocyte shows long processes in the canaliculi throughout the bone matrix.

bone cells (Currey, 2002 ; Bonewald, 2011; Kennedy & Schaffler, 2012). Considering that hydraulic resistance increases as distance from blood vessel increases, there may be a threshold above which the transport may not be possible. Mishra (2009) concluded that osteon diameter is determined by this threshold. Here we hypothesize that the thickness of avascular bone tissue depends on the metabolic demands of bone cells; therefore this thickness is likely to be higher in lepidosaurs than in birds. The 95% confidence intervals for birds and lepidosaurs do not overlap: the lower limit of the lizard confidence interval (0.381 mm) is more than three times higher than the upper limit of the bird confidence interval (0.109 mm). On the other hand, the mean avascular thickness is more than ten times thicker in lepidosaurs (0.790 mm) than in birds (0.072 mm). These results are strong evidence for hypothesis 1, according to which we expect a higher thickness of avascular bone tissue in lepidosaurs than in birds because osteocytes of the latter have higher energetic expenditure and produce more metabolic byproducts than those of the former. Our result of a maximum thickness of the avascular layer (*i.e.* the farthest distance of an osteocyte from a blood vessel located on the periosteum) of 0.122 mm in birds is astonishingly congruent with those published by Mishra (2009), according to which mammalian osteon diameter is of 0.250 mm (which would represent the double of the farthest distance – *i.e.* 0.125 mm – between an osteocyte and the osteonal vascular canal). Values obtained here for lepidosaurs with avascular bone are extremely high to transport nutrients and oxygen from connective tissues (endosteum and periosteum) to bone cells placed at the center of the cortex. Mean thickness of the cortex in

lepidosaurs with avascular femora is 0.790 mm and the higher value, found in *Amblyrhynchus*

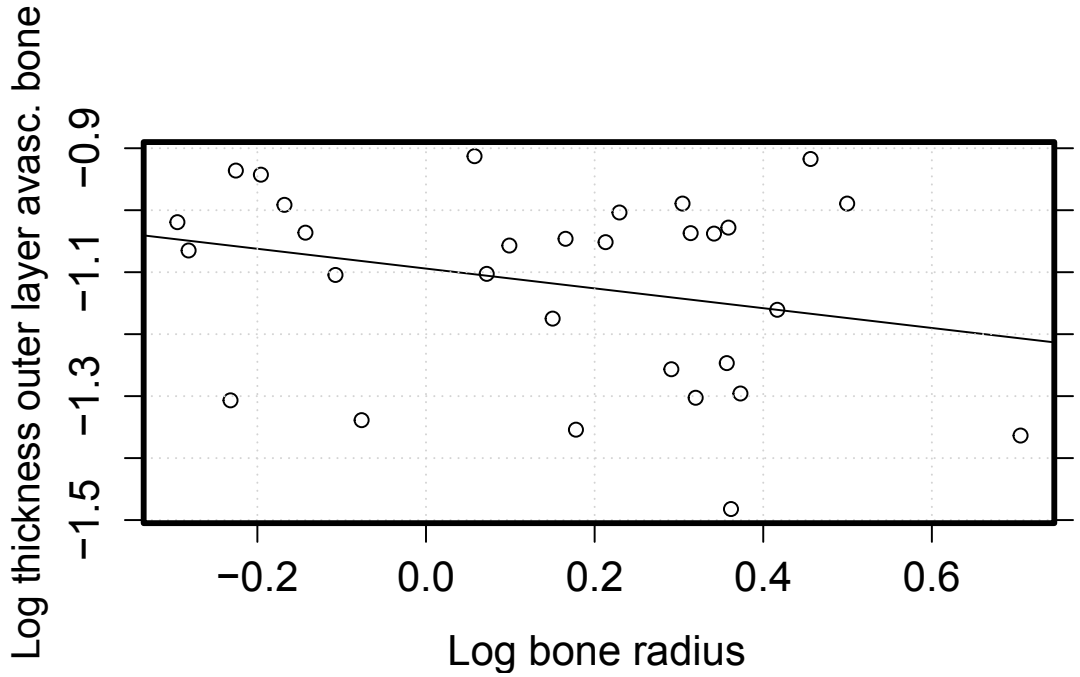

Figure 5. PGLS regression of the log thickness of the outer layer of avascular bone tissue with log bone radius in birds (R^2: 0.041; *p*-value: 0.146).

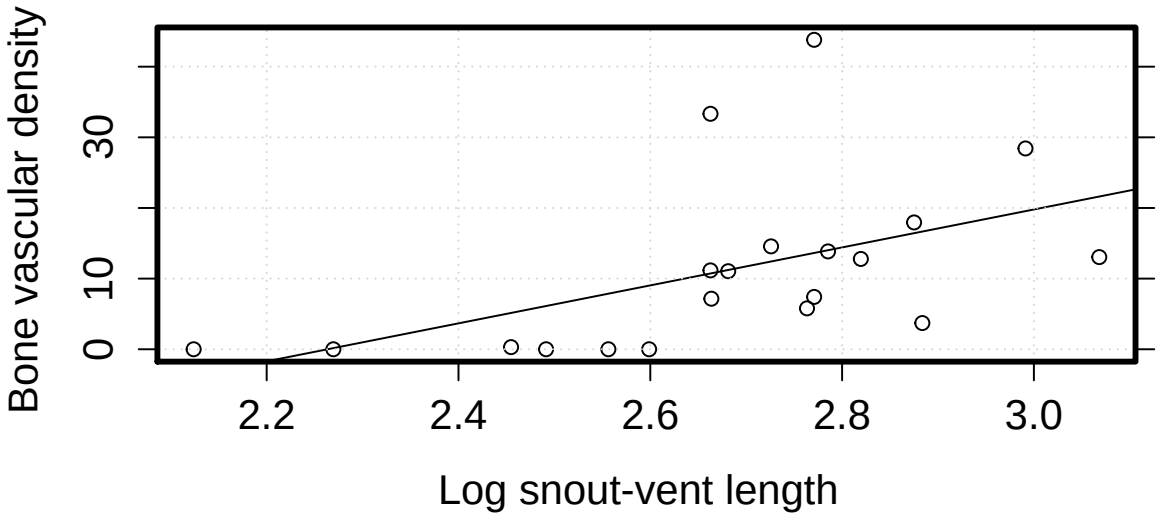

Figure 6. PGLS regression of the log bone vascular density with log snout-vent maximal length in *Varanus* (R^2: 0.210; *p*-value: 0.024).

---

cristatus, is 1.455 mm (*i.e.* the distance from endosteal or the periosteal blood vessels and osteocytes located in the middle of the bone cortex is 0.727 mm). These values are higher

than those previously cited by Mishra (2009) for the avascular bones of amphibians (distance between osteocytes and periosteal and endosteal blood vessels of 0.150 mm). This result is surprising because, for a body mass smaller than roughly 100 g, the standard metabolic rate (mL O_2 h^{-1}) of amphibians is smaller than that of "reptiles" (White, Phillips & Seymour, 2006).

Within birds, Ponton *et al.* (2004) showed that the ratio of the thickness of the outer layer of avascular bone tissue to bone cortical thickness scales with negative allometry relative to bone radius. This would mean that the bigger a bone, the thinner, relative to cortical thickness, its peripheral avascular layer. Here we have found that the absolute thickness of the outer layer of avascular bone tissue is independent from both bone cross sectional area and bone radius in birds. So we conclude that the negative allometry found by Ponton *et al.* (2004) reflects the fact that they analyzed relative values of outer avascular layer thickness. In other words, for a constant thickness of avascular bone, its relative thickness may decrease with increasing bone size. When analyzing absolute values (as has been done here), the thickness of the outer layer of avascular bone tissue is independent of bone size and so it may also be independent from body size.

Different factors have been evoked in the literature to explain the variation of bone vascularization in tetrapods. Our results allow a deeper knowledge on the determinism of bone vascularization in diapsids, as discussed below.

Phylogeny. Cubo *et al.* (2005) showed that the ratio bone vascular area / bone cortical area is explained by phyogeny at the nodes sauropsids, diapsids, archosaurs, lepidosaurs and birds, but not in testudines. Results obtained in this study for the sample of birds (Pagel's

Lambda = 1.000 suggesting a high phylogenetic signal) agree with those of Cubo *et al.* (2005) and those by Legendre *et al.* (in press). However, results obtained for lepidosaurs (Pagel's Lambda = 0.000 suggesting no phylogenetic signal) do not agree with those obtained by Cubo *et al* (2005), probably because these last authors used a smaller sample size. De Buffrénil *et al* (2008) concluded that phylogeny does not explain the variation of the ratio of bone vascular area to bone cortical area in *Varanus.* Our results agree with their conclusion: we obtained a Pagel's lambda of 0.000 in the regression of bone vascular area / bone cortical area to snout-vent maximal length (both with and without log transformation) in *Varanus,* suggesting no phylogenetic signal in the variation of this feature.

Bone cross-sectional area and body size. Bone vascular density and the ratio of vascular canal area / bone cortical area are positively related to bone cross-sectional area in both lepidosaurs and birds. Results obtained here using PGLS regressions are congruent with those obtained by Cubo *et al* (2005) for sauropsids using phylogenetically independent contrasts. On the other hand, bone vascular density is related to snout-vent maximal length in *Varanus*. This last result is congruent with that obtained by de Buffrénil *et al.* (2008) using a statistical methodology that did not include phylogeny. All these results may be interpreted as evidence for hypothesis 2a suggesting that bone vascular density increases as bone and body size increase to compensate the smaller relative effectiveness of vascular supply of the periosteum because periosteal supply depends on periosteal area, and thus increase quadratically as compared to bone linear dimensions; conversely, bone volume or mass (to be supplied) increase faster, with the third power of bone linear dimensions. The endosteum is also a potential source of nutrients for bone cells. However, its relative contribution is smaller than that of the periosteum because the cement line separating endosteal from periosteal bone most likely disrupts the osteocyte network and prevents any communication between

endosteal and periosteal canaliculi, as suggested by the fact that canaliculi are cut by, and do not have any communication through, the cement lines of secondary osteons (Kerschnitzki *et al.* 2011).

Metabolic rate. Mass-specific resting metabolic rate decreases as body mass increases (Schmidt-Nielsen, 1997; Hulbert *et al.*, 2007). We expect that the metabolic demands of osteocytes do likewise, in which case bone vascular density and the ratio bone vascular area / bone cortical area may also decrease as body mass (tightly related to bone size) increases (our hypothesis 2b). We have found the opposite result, which refutes this hypothesis. However, a small effect of metabolic rate on bone vascularization may exist, as suggested by the following data: In *Varanus,* the threshold above which femora are vascularized is lower (bone cross-sectional area = 8 mm^2) than in other lepidosaurs, probably because the former have higher metabolic rates.

Bone growth rate. De Buffrénil *et al* (2008) concluded that bone growth rate is the main proximal factor explaining the variation of bone vascularization in *Varanus*, in agreement wih Amprino's rule (Amprino, 1947). This explanation may be correct for the whole clade of diapsids when primary bone in the inner part of the cortex is analyzed. However, when the whole cortex is analyzed (as it is the case in the present study), we must take into account the fact that bone growth rate decreases with age, so that some regions are formed at high rates (and show high vascular densities) whereas other, more peripheral (younger) regions show low or no vascularization of all. In birds, considering that the thickness of the outer avascular layer is independent from bone size and more or less constant, big species may retain at adulthood a bigger fraction of rapidly formed, densely vascularized, bone tissue than small species, which may retain exclusively the outer avascular layer.

In conclusion, bone vascular density, bone growth rate, bone cross-sectional area and mass-specific metabolic rate, are functionally linked and so they are constrained to co-evolve. These characters may constitute a case of the correlated progression concept (Kemp, 2007), the phylogeny being an explanatory (but not a causal) factor. On the other hand, the thickness of the outer layer of avascular bone tissue is significantly higher in lepidosaurs than in birds clearly showing a phylogenetic pattern which may be explained by different metabolic requirements of osteocytes in these clades. Future work on the effect of osteocyte size and density on the variation of both the thickness of the outer layer of avascular bone tissue and the bone vascular density in a more comprehensive sample of diapsids may allow additional tests of our hypotheses.

Acknowledgements

We thank very much reviewers Koen Stein and Michael D'Emic and associate editor Alexandra Houssaye for interesting suggestions that greatly improved the quality of the manuscript. This work was supported by the Spanish Gouvernement (grant CGL2011-23919 to JC), the Centre National de la Recherche Scientifique and the Université Pierre et Marie Curie (operating grant of UMR 7193 to JC, JB, AQ and LL) and by the Centre National de la Recherche Scientifique and the Muséum National d'Histoire Naturelle (operating grant of UMR 7207 to VdB).

Author contribution

JC and VdB conceived research. JC and LJL performed statistical analyses. JC wrote the paper. JB quantified histological data in birds and VdB in lepidosaurs. AQ performed the cytological study.

References

Amprino R. 1947. La structure du tissue osseux envisagée comme l'expression de différences dans la vitesse de l'accroissement. *Archives de Biologie* **58:** 315-330.

Ast JC. 2001. Mitochondrial DNA evidence and evolution in Varanoidea (Squamata). *Cladistics* **17:** 211-226.

Barker FK, Barrowclough GF, Groth JG. 2002. A phylogenetic hypothesis for passerine birds: taxonomic and biogeographic implications of an analysis of nuclear DNA sequence data. *Proceedings of the Royal Society B: Biological Sciences* **269:** 295-308.

Bonewald LF. **2011**. The amazing osteocyte. *Journal of Bone Mineral Research* **26**:229–238.

Brookes M. 1971. The blood supply of bone. London: Butterworths & Co.

de Buffrénil V, Houssaye A, Böhme W. 2008. Bone vascular supply in Monitor lizards (Squamata: Varanidae): influence of size, growth and phylogeny. *Journal of Morphology* **269:** 533-543.

Conrad JL. 2008. Phylogeny and systematics of Squamata (Reptilia) based on morphology. *Bulletin of the American Museum of Natural History* **310:** 1-182.

Cubo J, Ponton F, Laurin M, de Margerie E, Castanet J. 2005. Phylogenetic signal in bone microstructure of sauropsids. *Systematic Biology* **54:** 562-574.

Currey JD. 2002. *Bones* 2nd edition. Princeton University press: New Jersey, USA

Francillon-Vieillot, H, de Buffrénil V, Castanet J, Géraudie J, Meunier FJ, Sire JY, Zylberberg L, de Ricqlès A. **1990**. Microstructure and Mineralization of Vertebrate Skeletal Tissues. In: Carter JG, ed. *Skeletal Biomineralization: Patterns, Processes and Evolutionary Trends. Volume I.* New York, NY: Van Nostrand Reinhold, 471–530.

Grafen A. **1989**. The Phylogenetic Regression. *Philosophical Transactions of the Royal Society B: Biological Sciences* **326**: 119–157.

Harvey PH, Pagel MD. 1991. The comparative method in evolutionary biology. Oxford: Oxfor University Press.

Hulbert AJ, Pamplona R, Buffenstein R, Buttemer WA. 2007. Life and death: metabolic rate, membrane composition and life span of animals. *Physiological Reviews* **87**: 1175–1213.

Kemp TS. 2007. The concept of correlated progression as the basis of a model for the evolutionary origin of major new taxa. *Proceedings of the Royal Society B: Biological Sciences* **274**: 1667–1673.

Kennedy OD, Schaffler MB. **2012**.The roles of osteocyte signaling in bone. *Journal of American Academy of Orthopaedic Surgeons* **20**: 670–671.

Kerschnitzki M, Wagermaier W, Roschger P, Seto J, Shahar R, Duda GN, Mundlos S, Fratzl P. 2011. The organization of the osteocyte network mirrors the extracellular matrix orientation in bone. *Journal of Structural Biology* **173** : 303-311.

Livezey BC, Zusi RL. 2007. Higher-order phylogeny of modern birds (Theropoda, Aves: Neornithes) based on comparative anatomy. II. Analysis and discussion. *Zoological Journal of the Linnean Society* **149:** 1-95.

Maddison WP. 1991. Squared-change parsimony reconstructions of ancestral states for continuous-valued characters on a phylogenetic tree. *Systematic Zoology* **40:** 304–314.

Maddison WP, Maddison DR. 2011. *Mesquite: A modular system for evolutionary analysis. Version 2.75.* Available via http://mesquiteproject.org

Midford P, Garland TJ, Maddison WP. 2011. *PDAP Package for Mesquite. Version 1.16.* Available via http://mesquiteproject.org/pdap_mesquite/index.Html

Mishra S. 2009. Biomechanical aspects of bone microstructures in vertebrates: potential approach to palaeontological investigations. *Journal of Biosciences* **34:** 799-809.

Orme D, Freckleton R, Thomas G, Petzoldt T, Fritz S, Isaac N, Pearse W. **2012**. The caper package: comparative analysis of phylogenetics and evolution in R. R package version 0.5.2

Ponton F, Elzanowski A, Castanet J, Chinsamy A, de Margerie E, de Ricqlès A, Cubo J. 2004. Variation of the outer circumferential layer in the limb bones of birds. *Acta Ornithologica* **39:** 137-140.

Pyron RA. 2010. A likelihood method for assessing molecular divergence time estimates and the placement of fossil calibrations. *Systematic Biology* **59**: 185-194.

Revell LJ. **2010**. Phylogenetic signal and linear regression on species data. *Methods in Ecology and Evolution* **1**: 319–329.

Simpson AHRW. 1985. The blood supply of the periosteum. *Journal of Anatomy* **140**: 697-704.

Schmidt-Nielsen K. 1997. Animal physiology (5th edition). Cambridge: Cambridge University Press.

Schneider CA, Rasband WS, Eliceiri KW. 2012. NIH image to ImageJ: 25 years of image analysis. *Nature Methods* **9**: 671-675.

White CR, Phillips NF, Seymour RS. 2006. The scaling and temperature dependance of vertebrate metabolism. *Biology Letters* **2**: 125-127.

Résumé

Les archosaures sont un clade de vertébrés comprenant les oiseaux, les crocodiliens, ainsi que de nombreux groupes fossiles (notamment les ptérosaures et les dinosaures non-aviens). Ce groupe fait depuis plusieurs décennies l'objet d'un important débat parmi les paléontologues quant à l'évolution du thermométabolisme au sein de ses différentes lignées. L'hypothèse classique considère que seuls les oiseaux modernes sont endothermes (*i.e.* capables de produire leur propre chaleur corporelle), tandis que tous les autres archosaures sont ectothermes (*i.e.* totalement dépendants du milieu extérieur pour maintenir leur corps à une température élevée). L'histologie osseuse permet d'étudier et de modéliser plusieurs traits relatifs à la croissance osseuse et au thermométabolisme, par ailleurs impossibles à mesurer sur des spécimens fossiles ; c'est pourquoi nous avons utilisé des caractères mesurés sur des coupes histologiques d'os longs afin de tester cette hypothèse.

Les relations phylogénétiques entre espèces dans un échantillonnage peuvent avoir un impact très important sur la variation de caractères quantitatifs lors de la construction d'un modèle statistique. Afin de mieux caractériser cet impact pour le prendre en compte efficacement lors de nos analyses ultérieures, le premier volet de cette thèse a consisté en une étude approfondie de l'information phylogénétique présente dans la variation de nos caractères quantitatifs ostéohistologiques. Nous avons pu mettre en évidence la présence d'un signal phylogénétique très élevé dans plusieurs de ces caractères pour un échantillonnage d'amniotes et pour un autre, plus exhaustif, d'oiseaux paléognathes, ce qui justifie l'emploi de méthodes phylogénétiques comparatives pour la construction de notre modèle prédictif appliqué au thermométabolisme.

Après une étude préliminaire consacrée à l'élaboration d'un modèle prédictif du taux de croissance osseuse, qui est un indicateur indirect du thermométabolisme, nous avons construit un modèle global capable de prédire directement le taux métabolique au repos de nos spécimens fossiles en utilisant à la fois des caractères histologiques et la position phylogénétique de chaque spécimen comme variables indépendantes. Nos résultats montrent que la majorité des archosaures inclus dans notre échantillonnage, ainsi que de proches groupes-frères, étaient endothermes, avec pour certains d'entre eux des taux métaboliques comparables à ceux des oiseaux actuels. Cela implique que le dernier ancêtre commun des archosaures était probablement endotherme, et que les crocodiliens actuels sont donc devenus secondairement ectothermes, probablement en réponse aux contraintes du milieu aquatique auquel ils se sont adaptés. Plusieurs études antérieures sur la physiologie des crocodiliens et sur la description de l'histologie osseuse d'archosaures fossiles corroborent ce résultat. Des études plus spécifiques sur la lignée des pseudosuchiens (*i.e.* crocodiliens et groupes fossiles apparentés) devraient permettre de déterminer de manière plus précise à quel niveau de l'arbre phylogénétique s'est effectué le retour à un état ectotherme, ainsi que les contraintes adaptatives à l'origine de cette acquisition.

Mots-clés : archosaure – histologie osseuse – caractères quantitatifs – paléontologie des vertébrés – modèle prédictif – méthodes phylogénétiques comparatives

Abstract

Archosaurs are a clade of vertebrates that includes birds, crocodiles, and numerous fossil groups (including pterosaurs and non-avian dinosaurs). This clade has been a matter of debate among paleontologists for decades concerning the evolution of thermometabolism in its different lineages. The classical hypothesis considers that only modern birds are truly endotherms (*i.e.* able to produce their own body heat), whereas all other archosaurs are ectotherms (*i.e.* relying entirely on the external environment to maintain their body at a high temperature). Bone histology allows to study and to model several traits linked to bone growth rate and thermometabolism, otherwise impossible to estimate on fossil specimens; for this reason, we used characters measured on long bone histological sections in order to test this hypothesis.

Phylogenetic relationships between species in a sample can have a very strong impact on the variation of quantitative features when building a statistical predictive model. In order to describe this impact more accurately to take it into account in further analyzes, the first part of this thesis consisted in a comprehensive study of the phylogenetic information found in the variation of our osteohistological quantitative characters. We were able to identify a very high phylogenetic signal for several of these characters in a sample of amniotes, and in another, more exhaustive sample of palaeognathous birds. This is why we used phylogenetic comparative methods to build our predictive model applied to thermometabolism.

After a preliminary study during which we built a predictive model for bone growth rate, which is an indirect estimator of thermometabolism, we built a global model to predict the resting metabolic rate of our fossil specimens, using both histological features and phylogenetic information for each specimen as independant variables. Our results show that a majority of archosaurs in our sample, as well as some close outgroups, were endotherms, with metabolic rates sometimes comparable to those of modern birds. This implies that the last common ancestor of archosaurs was likely an endotherm, and that modern crocodiles became secondarily ectothermic, probably in response to the constraint of their aquatic environment. Several previous studies on crocodile physiology and descriptions of the bone histology of fossil archosaurs corroborate this result. More specific studies on pseudosuchians (*i.e.* crocodiles and close fossil outgroups) should allow to precisely identify the level of the phylogenetic tree at which the ectothermic state was acquired, as well as adaptive constraints behind this acquisition.

Keywords: archosaur – bone histology – quantitative features – vertebrate paleontology – predictive modeling – phylogenetic comparative methods